AUTHENTICATING TURBOCHARGER PERFORMANCE UTILIZING ASME PERFORMANCE TEST CODE CORRECTION METHODS

by

JACQUE SHULTZ

B.S., Kansas State University, 1998

A THESIS

Submitted in partial fulfillment of the
requirements for the degree

MASTER OF SCIENCE

Department of Mechanical and Nuclear Engineering
College of Engineering

KANSAS STATE UNIVERSITY
Manhattan, Kansas
2011

Approved by:

Major Professor
Dr. Kirby S. Chapman

Copyright

JACQUE SHULTZ

2011

Abstract

Continued regulatory pressure necessitates the use of precisely designed turbochargers to create the design trapped equivalence ratio within large-bore stationary engines used in the natural gas transmission industry. The upgraded turbochargers scavenge the exhaust gases from the cylinder, and create the air manifold pressure and backpressure on the engine necessary to achieve a specific trapped mass. This combination serves to achieve the emissions reduction required by regulatory agencies.

Many engine owner/operators request that an upgraded turbocharger be tested and verified prior to re-installation on engine. Verification of the mechanical integrity and airflow performance prior to engine installation is necessary to prevent field hardware iterations. Confirming the as-built turbocharger design specification prior to transporting to the field can decrease downtime and installation costs. There are however, technical challenges to overcome for comparing test-cell data to field conditions.

This thesis discusses the required corrections and testing methodology to verify turbocharger onsite performance from data collected in a precisely designed testing apparatus. As the litmus test of the testing system, test performance data is corrected to site conditions per the design air specification. Prior to field installation, the turbocharger is fitted with instrumentation to collect field operating data to authenticate the turbocharger testing system and correction methods. The correction method utilized herein is the ASME Performance Test Code 10 (PTC10) for Compressors and Exhausters version 1997.

Table of Contents

List of Figures

List of Tables

Acknowledgements

I would like to thank my wife Jennifer for her patience and support, and sons Jonas and Xavier for the external motivation to complete this work. I hope to make our futures as worthwhile as the patience you have afforded me.

To Dr. Kirby Chapman my professor, advisor, supervisor and esteemed mentor, whom I would like to thank for career changing opportunities. With Chapman there have been many distinct occasions for me to learn the depth of my drive and motivation. Kirby has helped to solidify learning and real world application for so many people, especially in the form of the National Gas Machinery Lab of Kansas State University. This is a center for industry outreach, and one source of the options I am fortuned.

To all staff currently and previously employed by the National Gas Machinery Lab whose efforts are magnanimous. The work, ideas, and innovations they have provided to the testing center are applauded and main reasons for the integrity of this center of expertise. I genuinely appreciate all of your efforts, especially those I have had the distinct honor of working with.

To Rich Vinton, with great admiration, for continued learning and controls application in the field of turbocompression and rotating equipment. His clear direction, experience, and strong advice have furthered my knowledge and abilities in so many ways.

To my technical committee for their participation and excellent guidance in this work.

Thank you.

Nomenclature

a	Representing calculation substitution
ACFM	Actual volumetric flow rate, $\dfrac{\text{ft}^3}{\text{min}}$
AF	Air to fuel ratio
b	Representing calculation or constant substitution
b_2	Impeller exit blade height
c	Speed of sound
C	Constant
$\bar{c}_p$	Isobaric specific heat (constant pressure), mole basis
c_p	Isobaric specific heat (constant pressure), mass basis
c_v	Isochoric specific heat (constant volume), mass basis
∂	Partial derivative
D	Diameter
D_2	Compressor impeller diameter at exit location
D_{pipe}	Internal pipe diameter
E_v	Fluid bulk modulus of elasticity
f	Frictional piping losses
g	Gravitational constant
h	Enthalpy
Δh	Enthalpy change

$h_{2,a}$	Actual enthalpy at exit condition
$k_{1...n}$	Constants for reduced saturation line
L_e	Equivalent pipe length
$\dot{m}$	Mass flow rate
Ma	Mach number of gas at point of interest
M_m	Machine Mach number
MW	Molecular weight
n	Polytropic exponent
N	Rotational shaft speed
p	Pressure of gas condition
p_{amb}	Ambient pressure / barometric pressure
p_{cr}	Critical pressure
$p_{dis.losses}$	Piping/system discharge losses upstream of turbo outlet pressure tap location
$p_{inlet.losses}$	Piping/system inlet losses downstream of turbo inlet pressure tap location
p_{pc}	Pseudo-reduced critical pressure
p_r	Reduced critical pressure
p_{sat}	Saturation pressure of water vapor in ambient air
p_{vapor}	Pressure of water vapor in ambient air
Δp_{pipe}	Piping pressure losses
$\dot{P}_a$	Gas power (actual compression power)

$\dot{P}_c$	Gas power (compression power)
PR	Compressor pressure ratio
$\dot{Q}_{cv}$	Heat transfer rate of control volume
$q_{n's}$	Dimensional model variables
rh	Relative humidity
Re	Reynolds number
Re_m	Machine Reynolds number
RA	Intermediate calculation in Wiesner Reynolds number correction method
RB	Intermediate calculation in Wiesner Reynolds number correction method
RC	Intermediate calculation in Wiesner Reynolds number correction method
R_g	Specific Gas Constant / R-value of the gas
$\overline{R}_u$	Universal Gas Constant: $1545 \dfrac{\text{ft lbf}}{\text{lbmol} \, ^\circ\text{R}}$
T	Temperature of gas condition
T_{cr}	Critical temperature
T_{pc}	Pseudo-reduced critical temperature
T_r	Reduced critical temperature
u	Thermodynamic internal energy
u_2	Impeller tip speed
v	Specific volume
V	Velocity

$\dot{V}$	Volumetric flow
$\dot{W}_{cv}$	Work rate of control volume
y_v	Mole fraction of water vapor
z	Elevation
Z	Gas compressibility

Greek Symbols

β_k	Reduced saturation pressure
ε	Material surface roughness
η	Isentropic or polytropic compressor efficiency
θ	Critical temperature ratio of steam
κ	Ratio of specific heats
μ	Absolute (dynamic) fluid viscosity
μ_c	Compressible work
ψ	Dimensionless head coefficient
υ	Kinematic viscosity
π	Pi – 3.14159
$\Pi_{1\cdots n}$	Terms of dimensionless coefficients
ϕ	Function of…
ρ	Fluid density
σ	Substitution in K-function saturation line calculation

φ	Dimensionless flow coefficient
Ω	Dimensionless power coefficient

Subscripts

1, 2	Condition 1, Condition 2
a	Actual condition
abs	Absolute condition of temperature or pressure
air	Referencing air in mixture
avg	Average of entrance to exit conditions
c	Polytropic or isentropic condition
corr	Corrected
cv	Control volume
dynamic	Dynamic temperature or pressure component of total condition
fuel	Referencing fuel in mixture
i	Component of a mixture
inlet	Inlet condition of state or process
mix	Gas mixture
n	Iteration counter
outlet	Outlet condition of state or process
p	Isobaric notation
p	Polytropic condition

s	Isentropic condition
sp	Site specified conditions
static (st)	Static condition of fluid stream
t	Total condition of fluid stream
te	Test conditions
tip	Compressor/impeller tip
v	Isochoric notation
vapor	Referencing water vapor in mixture

CHAPTER 1: Introduction

A turbocharger (turbo) is a unique machine in the group of turbomachines utilizing a turbine section to extract energy from a flowing gas stream, driving a rotating shaft common to a compressor section. This provides the shaft power needed to compress air with the attached centrifugal compressor. This turbomachine can be utilized to extract energy contained in the hot exhaust stream of a reciprocating engine and provide compressed inlet air at a higher than ambient density to the engine air intake manifold. The higher air intake pressure provides more air available for the combustion process in contrast to a naturally aspirated engine, thus increasing the engine energy density. Additionally, the compressed air provides a means of controlling the engine air fuel mixture (specific trapped mass) to assist in controlling emissions.

For a large-bore stationary engine as found on the natural gas transmission pipeline, a turbocharger is quite large, weighing from 1,000 to 6,000 lbs on average. In many applications two turbochargers are required per engine, one for each exhaust bank. This demands balanced operation between the two air-intake and exhaust manifolds of the engine. When a turbo is designed or upgraded, a specific compressor and turbine match is developed for the engine power and site location. This establishes the turbocharger design point(s) for the engine to operate at an expected optimal condition, to meet the site environmental air pollution requirements. Matching the turbocharger to the engine is imperative for success of a project. Turbo maintenance and upgrades can be quite expensive and time demanding. High profile engines have limited available downtime for maintenance. An upset to a schedule in a turbocharger rebuild or upgrade can have a very high indirect cost due to loss of production. A savings advantage exists for validating performance and detecting problems before incurring shipping, installation and field commissioning costs.

The inlet airflow through the turbocharger compressor can range between 1,000 ACFM and 24,000 ACFM, with turbine inlet temperatures upwards of 1,000°F. The weight, airflow and turbine inlet temperature requires a specifically designed infrastructure for validating performance. Such a test facility is a combination of measuring and supporting systems to operate a turbo in a test condition matching that on-engine. This provides the controlled ability to collect accurate mechanical and thermodynamic performance data while isolated from the engine, and to verify a turbo is field worthy prior to shipment and reinstallation on the engine.

The test center and engine design specification will rarely match ambient air conditions. A challenge exists to match test and site conditions for the turbocharger compressor. This requires an accurate methodology for comparing data between conditions. This thesis discusses the methodology of comparing test and site conditions and the importance thereof. The American Society of Mechanical Engineers has established the required methodology for testing and comparing conditions defined in ASME Performance Test Code 10 for Compressors and Exhausters (PTC10). This performance test code first established in 1949, is an industry standard. Through the years there have been two revisions (1965, 1997); the most recent revision released as PTC10-1997. The method of validating machine performance in the revised code has further leveled the playing field between the end user and manufacturers.

This thesis details a turbocharger performance test prior to shipment, and utilizes the methodology required to validate the test data with field data collected from the turbocharger operating on engine. CHAPTER 2: Literature Review, explores the background thermodynamics, and correction methodology. This provides important details and the basis of the performance test code. CHAPTER 3: Test Apparatus, details the specifically designed test cell of the National Gas Machinery Lab at Kansas State University. This test cell was established

to collect accurate performance data from an operating turbocharger independent of the engine. CHAPTER 4: Turbocharger Specification, details the air specification and design point for optimal turbocharger operation on engine. Performance data collected from a turbocharger utilized in this thesis is detailed in CHAPTER 5: Test Cell Data. Instrumentation is fitted to the turbo prior to engine installation to collect field operating data. CHAPTER 6: Field Data, details the challenges of normalizing months of field collected data from the turbo on engine. A comparison of the test cell and field data is summarized in CHAPTER 7: Correlating Test and Field Data. This chapter details the power of dimensional analysis as applied to the turbocharger to link the test and engine site locations to certify the performance test and authenticate the test cell.

CHAPTER 2: Literature Review

2.1 Turbomachine

Turbomachinery is a group of machines that create or extract work by increasing or decreasing the enthalpy of a constant flowing working fluid. The root word 'turbo' is from the Latin word 'turbinis' meaning circular movement, describing the central rotating shaft of a turbomachine *(Dixon, 1998)*. The energy of the working fluid is dynamically converted to or from kinetic energy via a bladed rotor section attached to the central shaft. Centrifugal compressors are one form of turbomachine utilizing rotating energy to increase the enthalpy of a working fluid. Conversely a turbine extracts rotating energy from a working fluid thus decreasing enthalpy. The turbine and compressor sections can be termed radial or axial referencing the flow direction compared to the central shaft. For a turbine this terminology references the inlet flow to the turbine section; the airflow for an axial inflow turbine is parallel to the central shaft. Regarding the compressor, this term references the outlet flow defining a centrifugal compressor as radial or perpendicular to the central shaft. The work herein discusses a turbocharger with an axial inflow turbine and radial discharge compressor or centrifugal compressor.

2.1.1 How a Turbocharger Works

A turbocharger utilizes the high temperature exhaust of a reciprocating engine to convert the exhaust gas flow into rotational energy. The rotational energy is provided via a turbine extracting energy from the exhaust gas, and transmitted directly to the shaft connected compressor. A centrifugal compressor delivers pressurized airflow to the engine for the air and fuel mixture for combustion. In many cases a turbocharger is a free spinning turbomachine with lubricated bearings supporting the central shaft.

Figure 2.1 shows a cutaway of a Globe Turbocharger Specialties model 1215 for a large-bore engine. Both compressor and turbine sections provide inlet and outlet flow paths for the free passage of the working fluid. After passing through the axial turbine, exhaust gas collects in the turbine case before exiting. For the compressor, the impeller rotation provides negative pressure drawing air into the inducer or inlet section of the compressor impeller. As the air exits the impeller blades of the compressor, it passes through a vaned or vaneless diffuser before collecting in the compressor discharge scroll and exiting the compressor outlet. The diffuser section is a region before the discharge scroll for reducing the fluid velocity and thereby recovering pressure of the working fluid *(Dixon, 1998)*.

Figure 2.1: Cutaway of a Turbocharger for a Large-Bore Engine

(Globe Turbocharger Specialties Inc., 2010)
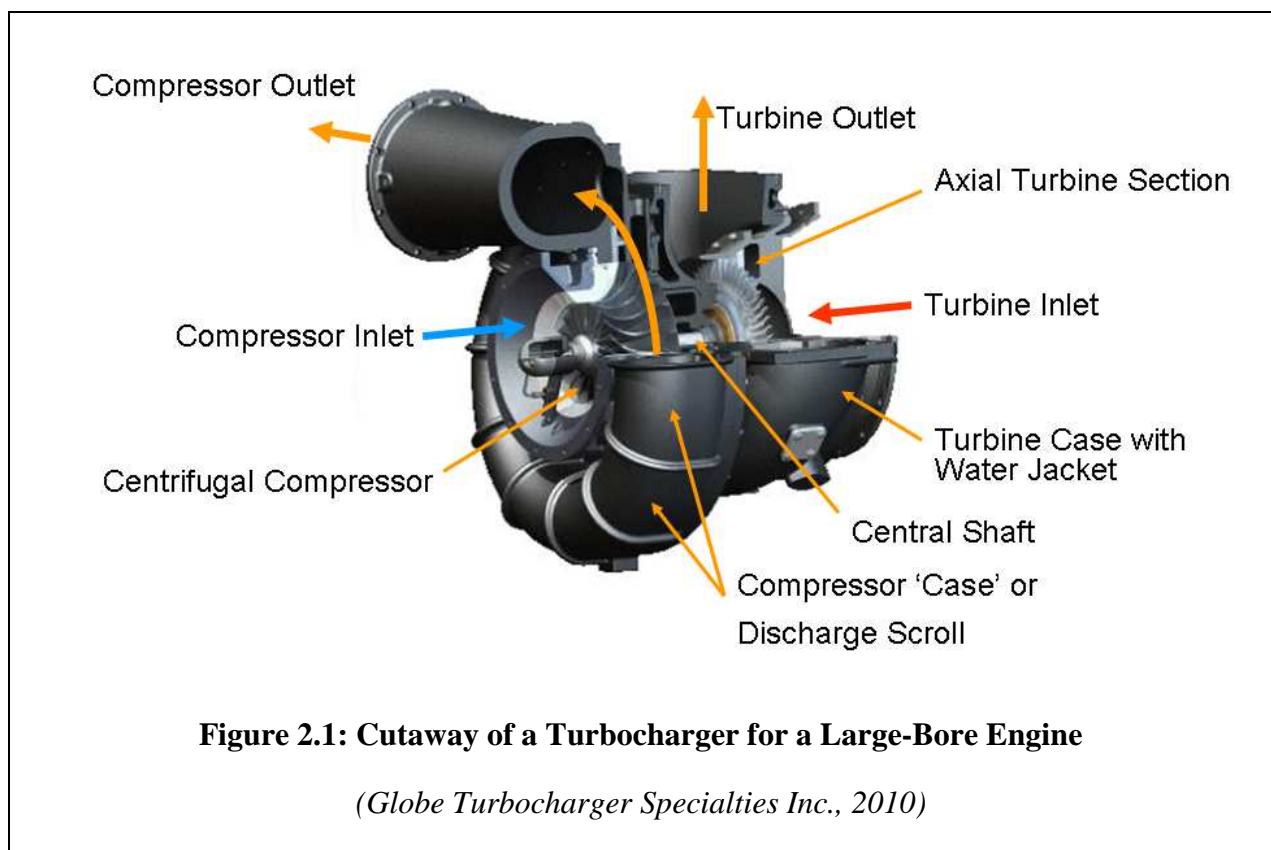
In the case of reciprocating engines, turbine inlet temperatures are higher than outlet temperatures as depicted with the differing colored inlet and outlet flow arrows in the figure. The

compressor adds energy to the compressible working fluid, increasing the temperature in the process and depicted with the colors of the inlet and outlet flow arrows as well. A pair of oil lubricated journal bearings house the central shaft. Because of the high temperatures of the exhaust gases, the turbine section has a surrounding water jacket to remove heat from the turbine case and prevent cracking of the casing material. To minimize heat transfer from the turbine case to the compressor case, there is an insulating section between the cases and surrounding the bearing housing.

The compressor discharge temperature is a function of the compressor efficiency and pressure rise. For discharge pressures of a turbocharger in the range of 10 psig, the estimated temperature rise is 115°F above inlet temperature. Depending on the engine design and combustion fuel, the exhaust gas temperatures to the turbine inlet can be as high as 1,200°F. The temperature extremes cause the central shaft to grow axially. To minimize leakage of the working fluid and minimize shaft frictional losses, the central shaft is sealed at the compressor end with a free spinning labyrinth seal.

2.1.2 Centrifugal Compressor

Centrifugal compressors are volumetric machines that intake a given inlet volume flow for a given operating speed and compressible work, independent of the inlet fluid density. This defines the shape of the operating map or compressor map as compared to other compressor technologies as seen in Figure 2.2. A screw compressor and reciprocating compressor have an almost fixed or linear intake volume for all pressures in the performance map, nearly vertical volume versus pressure lines.
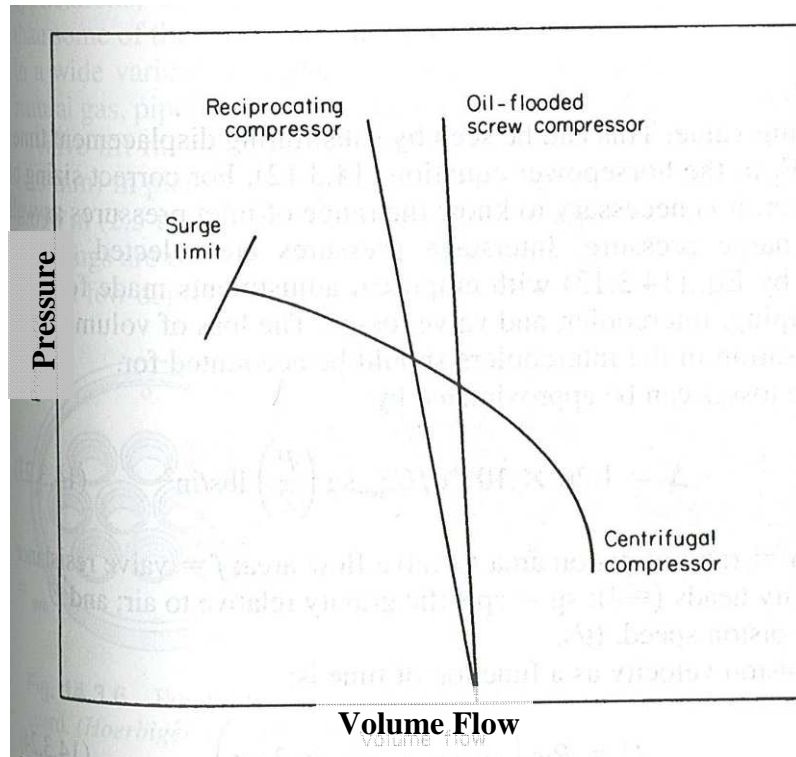
Figure 2.2: Comparison Compressor Map of Available Technologies

(Avallone, 2007)

The volumetric intake capacity of the centrifugal compressor is close coupled to the compressor work of the working fluid. If speed were an operating variable of the map in Figure 2.2, there would be numerous parallel compressor operating curves as detailed in Figure 2.3. Though Figure 2.2 details pressure versus volume flow, the basic operation of a centrifugal compressor is compressible work (head) versus inlet volumetric flow (capacity) as detailed in the compressor map in Figure 2.3.

This base compressor map is utilized for compressor selection and defines the various operating speed curves in relation to the maximum compressor speed *(Ehlers, 1994)*. With speed as a variable, the number of head and flow combinations of the compressor are virtually infinite within the bounds of the performance map and ability of the turbine to provide power to the compressor. This presents a challenge when comparing different inlet temperature and pressure conditions. Matching conditions for a given operating point in the compressor map (Figure 2.3) is achieved through the use of similarity laws, detailed in Section 2.9.
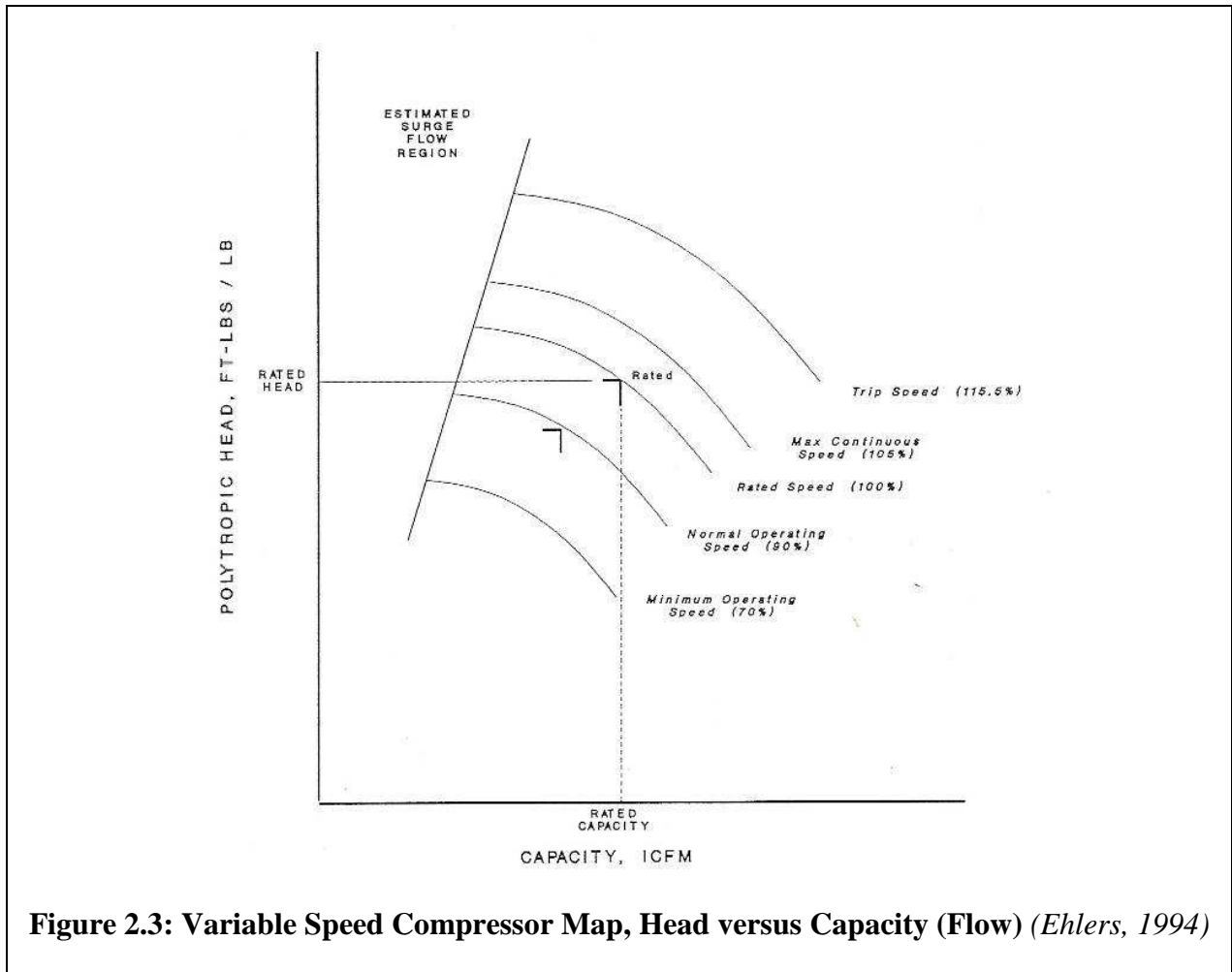
Figure 2.3: Variable Speed Compressor Map, Head versus Capacity (Flow) *(Ehlers, 1994)*

2.1.3 Turbocharger Use on Engine

The application of a turbocharger to an engine serves two purposes, increase energy density of the engine and help to control engine emissions *(Avallone, 2007)*. Figure 2.4 provides a schematic of a four stroke engine with turbocharger. The turbine uses engine exhaust manifold pressure and temperature to provide the required energy to drive the compressor, creating a backpressure or restriction on the engine. The compressor pressurizes the engine intake air manifold for scavenging exhaust products from the cylinder and increases the amount of air in the engine cylinder per fresh air/fuel charge, or specific trapped mass.

Figure 2.4: Schematic of Turbocharged Engine *(Avallone, 2007)*
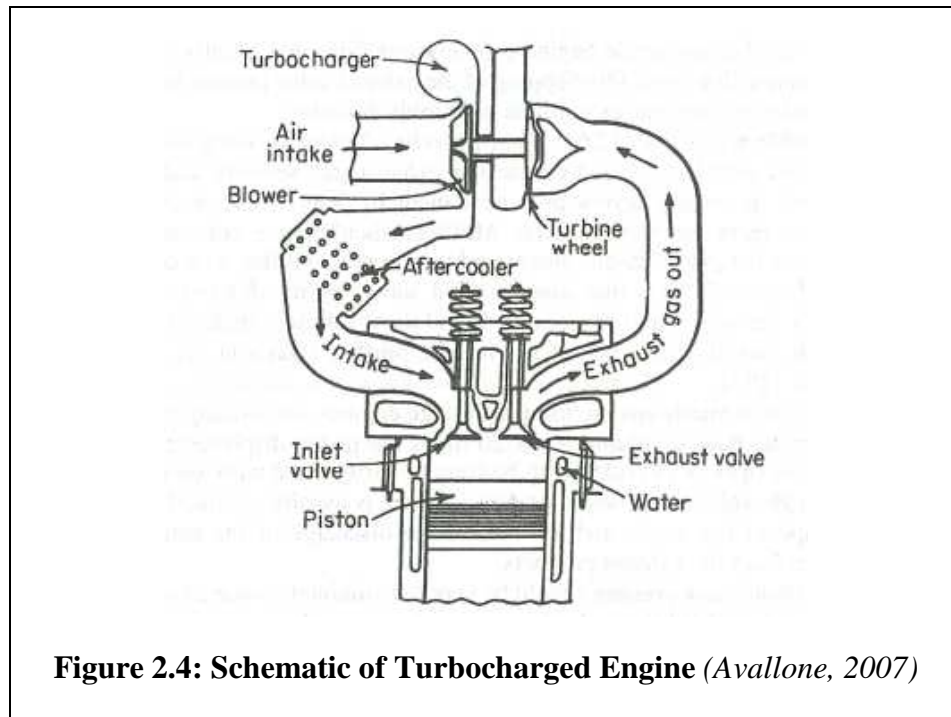
The second purpose but more primary purpose in recent years for turbocharging an engine is to control and minimize Hazardous Air Pollutants (HAPs) released to the atmosphere, one of which is the NOx group, NO and NO_2. Ozone (O_3) is the primary ingredient of photochemical smog creating the air pollution events associated with large cities and suburban areas *(Sillman, 2010)*. Ozone affects human health and is associated with respiratory problems. Controlling or reducing

the formation of ozone is a primary concern in air pollution control. Ozone occurs naturally in small amounts in the atmosphere; however the human formation of the pollutants NOx and Volatile Organic Compounds (VOCs) causes nearly ten times the natural formation of ozone. Reducing NOx formation from combustion products reduces air pollution and ozone creation.

The formation of the NOx group in a spark engine is highly dependent on the air to fuel ratio (*AF*) for combustion. As detailed in Figure 2.5, controlling the air to fuel ratio is one method of controlling the NOx products formed during combustion with the variables of brake specific fuel consumption (BSFC) and air to fuel ratio. The air to fuel ratio is defined as:

$$AF = \frac{\dot{m}_{air}}{\dot{m}_{fuel}} \tag{2.1}$$

According to Zheng et al. *(2004)*, an excessively lean fuel mixture (high air fuel ratio) could produce substantially lower NOx emissions to a lower limit of flame stability in the cylinder. As detailed (see Figure 2.5) there is a small region for effectively controlling the air to fuel ratio and reducing emissions. Applying the correct turbocharger turbine and compressor match for an engine is imperative. To control the air to fuel ratio with a turbocharger requires matching the turbocharger air delivery and turbine work to the local ambient conditions of the engine installation, and available energy from the exhaust gas. As will be seen in CHAPTER 6, ambient conditions vary throughout the day and as volumetric machines this challenges the engine and turbocharger match to achieve the required air to fuel ratio.

Figure 2.5: Specific Fuel Consumption and Emissions versus Air to Fuel Ratio
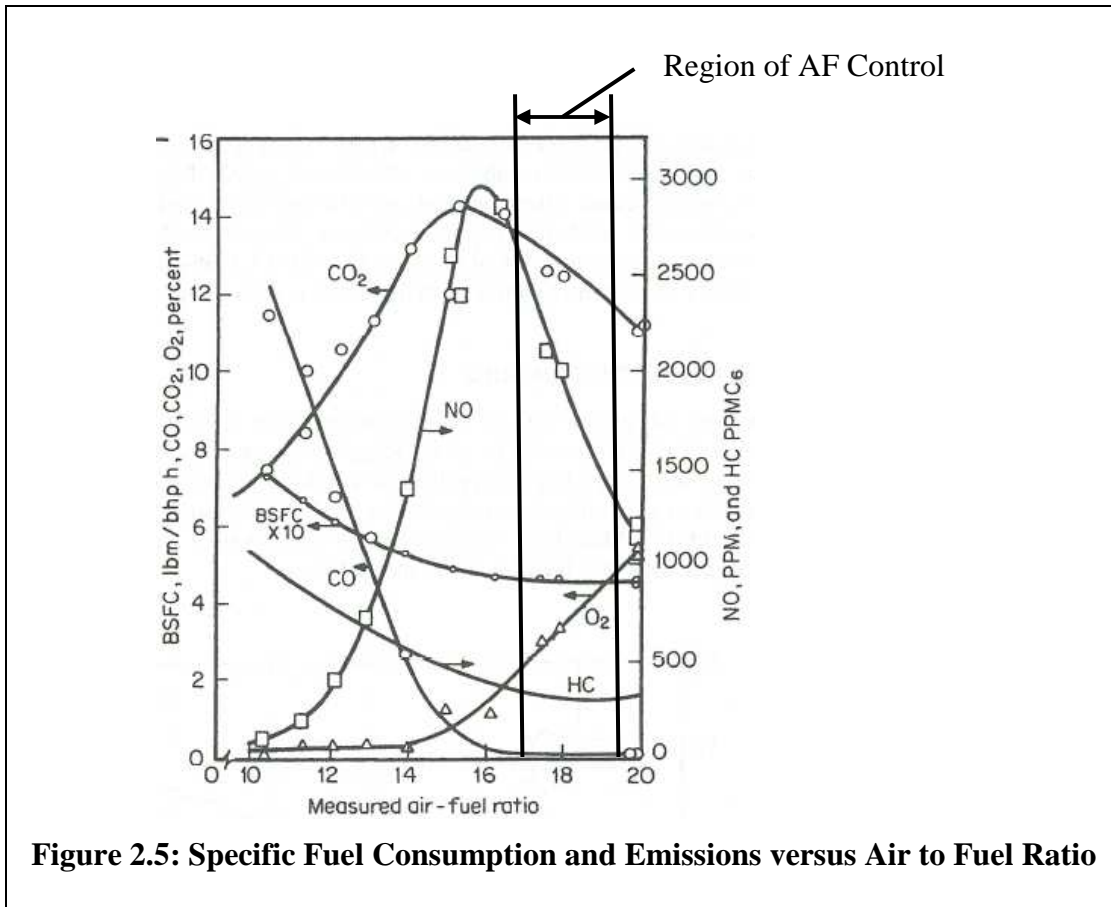
2.2 Motivation to Evaluate Established Performance Correction Models

Open any book on turbomachinery, (gas turbines, turbines, axial compressors, centrifugal compressors, fans, etc.) and there will be a section to detail correcting flow and pressure performance data between two operating conditions, for example test and specified conditions. Most references provide a basic guidance of the correction equations however; the equations between differing sources may be presented quite differently. This leaves the reader to question where the work originated and why different sources have different equations for the same topic. Through this work, a few of the correction models are evaluated in detail to establish origination, and itemize some of the differences between correction sets.

This research compares a turbocharger performance test in a well established testing system and field collected data. The comparison model is the ASME Performance Test Code 10 for Compressors and Exhausters established by a working committee under the American Society of Mechanical Engineers. Performance Test Code 10 (PTC10) provides methods of testing and evaluating performance of turbomachinery where the performance of a compressor or turbine can be detailed independently. Conveniently the code applies to both the turbine and compressor section of a turbocharger. Because of the difficulty of measuring the turbine inlet flow of the turbocharger on engine, this work concentrates on the compressor performance where methods are established to collect accurate operating flow, pressure and temperature measurements. Though in reality this is a coupled interaction, the turbine is here considered an energy provider to the centrifugal compressor providing a fresh air charge to the engine.

This work details the background thermodynamics and fluid mechanics, and their application to evaluate the centrifugal compressor performance and operation of a turbocharger. Most of the details presented here provide the background and application of the ASME PTC10 method. Specific instances in this literature review referencing PTC10 will detail the code and section, for example to detail paragraph 5.5.5 of PTC10, the reference is listed as: [PTC10-par. 5.5.5]. This work is not to reproduce the established method nor limit the scope of, rather to focus on specific instances of the performance code imperative for an accurate performance evaluation of a centrifugal compressor. This work details the power of dimensional analysis to a centrifugal compressor and its overall importance to the subject.

2.3 Volumetric Flow

Centrifugal compressor flow is defined in terms of inlet volumetric flow. The unit for volumetric flow is commonly cubic feet per minute (ft^3/min), and referred to the inlet condition as ICFM. This requires a designer to consider the inlet volume flow and the minimum and maximum site conditions (barometric pressure, temperature, relative humidity, and inlet losses) defining the inlet density, and resulting delivered mass flow to the engine. The conservation of mass relates the inlet density, inlet volume flow rate and mass flow rate *(Munson, 2002)* as follows:

$$\dot{V}_{inlet} = \frac{\dot{m}_{inlet}}{\rho_{inlet}} \tag{2.2}$$

A standard volumetric flow designation of SCFM (standard ft^3/min) is a mass flow definition in the effort of industry to rationalize volume flow for fans and compressors. SCFM is always accompanied by the barometric pressure, temperature and relative humidity utilized in the designation. Most industries maintain a reference barometric pressure at sea level, 14.696 psia, however many different industries define the temperature and relative humidity condition to what best suits their use. Many texts utilize an ambient temperature of 59°F, some use 68°F, while others use 80°F as standard reference temperatures. There is also a deviation in the relative humidity designation between industries, of which 0%, 36% and 65% are typically found. Therefore an SCFM designation must be accompanied with the ambient reference condition to define the 'S' in the volumetric unit.

2.4 Compression Process

Working with compressible fluids (gases) must consider the effects of compressibility when the density change is greater than 5% *(Daugherty, 1977)*. The compression work process is the path

between two pressure and volume conditions of a working fluid as detailed in Figure 2.6. The importance lies in evaluating the thermodynamic process adequately to define the gas compression work correctly *(Moran, 1995).* The thermodynamic compression work creates an enthalpy rise and a pressure rise in the working fluid. The two methodologies that best represent compression work are the polytropic process and the isentropic process *(Ikoku, 1984).* Each compression process considers the pressure-volume relation along the compression path of the gas between the inlet and outlet conditions.

Figure 2.6: Pressure Volume Diagram of Compressible Fluid
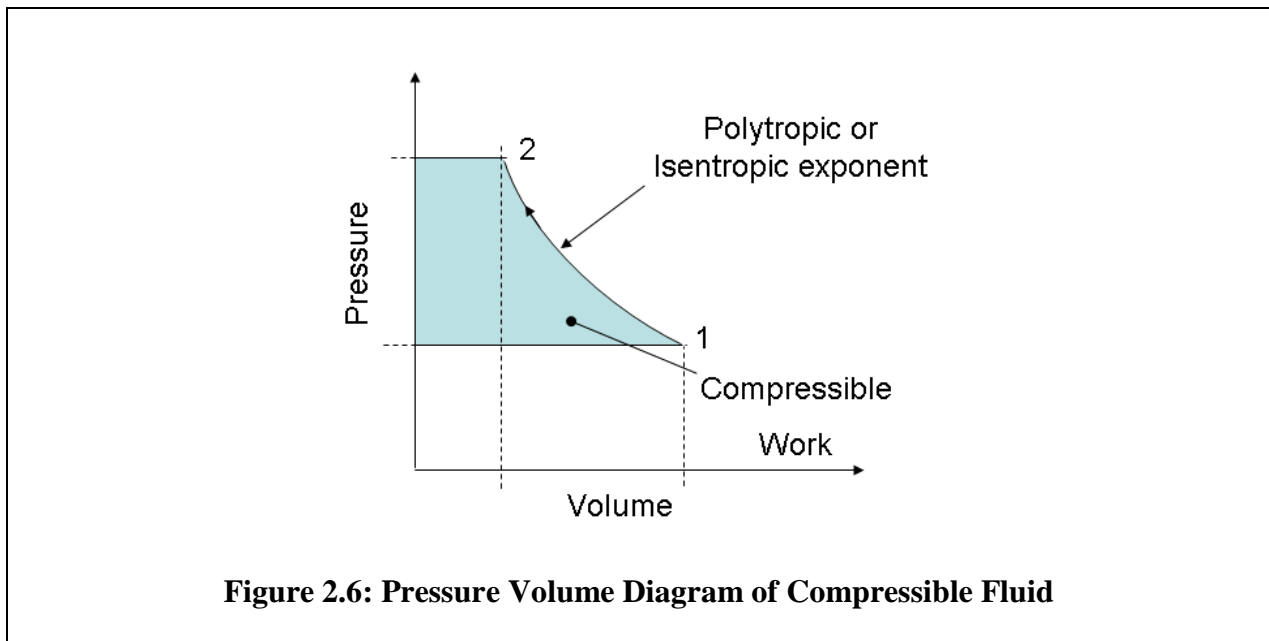
2.4.1 Compressible Work

The overall pressure rise and inlet gas condition is utilized to evaluate the compression work between the inlet and outlet of the compressor. The compressor work is the conversion of kinetic energy into gas power described with units of energy per unit mass of the working fluid; in Imperial units this is commonly: ft·lbf/lbm. This is also termed as compressible head or simply head. Compressible head accounts for the gas compression between pressure states as either a polytropic or isentropic process. Both compression processes are detailed in this section.

In thermodynamic analysis, the internal energy and pressure-volume terms appear as a sum; the term enthalpy created to reference this combination *(Shapiro, 1953)*. Enthalpy is a function of temperature, pressure and volume of a gas and defines the working fluid at the start and end states of the compression process. The compression work definition is established from the enthalpy relation. The control volume of the compression process noting the pressure, temperature, gas velocity, heat transfer, and elevation of the working fluid is detailed in Figure 2.7.

Figure 2.7: Control Volume of Compression Process
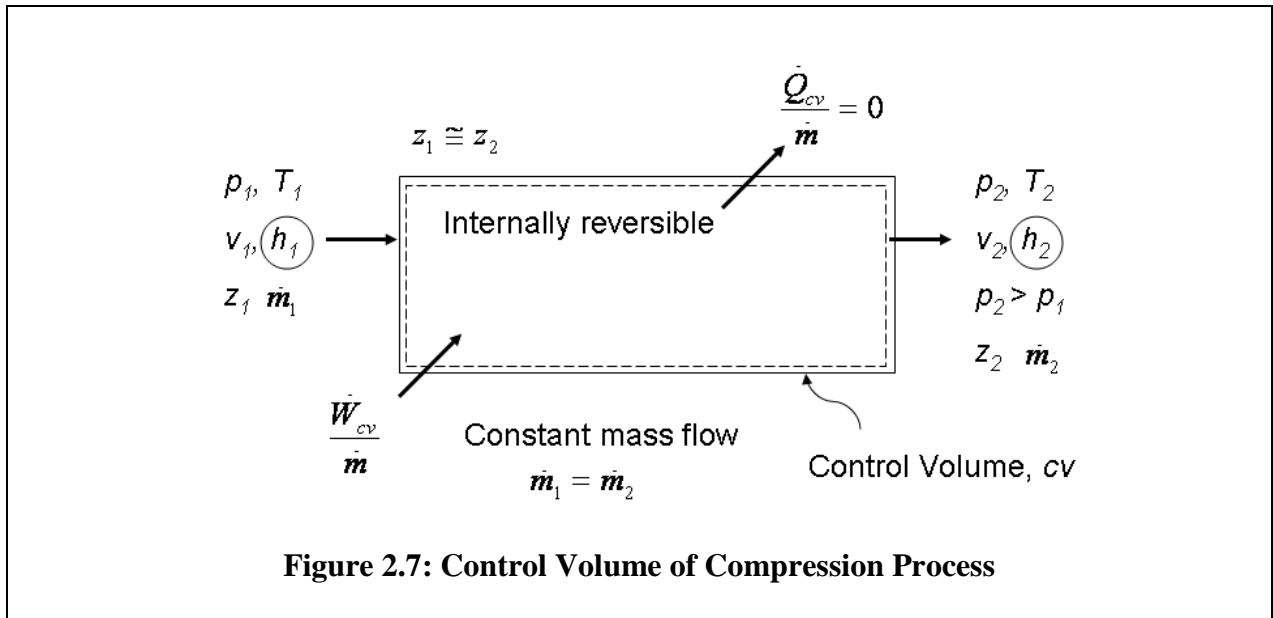
Consider the first law of thermodynamics in the following form as an energy rate balance for the control volume in Figure 2.7:

$$\frac{\dot{W}_{cv}}{\dot{m}} = \frac{\dot{Q}_{cv}}{\dot{m}} + (h_2 - h_1) + \left(\frac{V_2^2 - V_1^2}{2}\right) + g(z_2 - z_1)$$

(2.3)

For a constant entropy process (reversible process, frictionless, adiabatic), $\frac{\dot{Q}_{cv}}{\dot{m}} = 0$, this reduces to the following form of the energy rate balance from above:

$$\frac{\dot{W}_{cv}}{\dot{m}} = (h_2 - h_1) + \left(\frac{V_2^2 - V_1^2}{2}\right) + g(z_2 - z_1) \qquad (2.4)$$

With compressible gas as the working fluid, and minimal elevation change between the inlet and discharge connections, the effects of gravity on the working fluid in the control volume become zero. Additionally, there is a minor velocity change between inlet and discharge rendering this kinetic energy component negligible for the analysis *(Moran, 1995)*. Removing the effects of potential energy, $g(z_2 - z_1)$ and kinetic energy, $\left(\frac{V_2^2 - V_1^2}{2}\right)$, from the energy rate balance forms the compressor specific work defined from the ideal enthalpy change as follows:

$$\frac{\dot{W}_{cv,c}}{\dot{m}} = (h_2 - h_1) \qquad (2.5)$$

Considering the actual enthalpy at inlet and outlet states defines the actual gas compression power in the form of:

$$\dot{W}_{cv,a} = \dot{m}(h_{2,a} - h_1) \qquad (2.6)$$

The next sections detail compressor work in the form of a polytropic and isentropic process. For these processes, the derivations will be expanded to form the equations of compression work. The models of compression work are reversible processes and differ by the exponent in the ideal gas relation, $pV^n = \text{constant}$.

2.4.2 Polytropic Compression Process

For a polytropic process, the pressure-volume relationship of the compressible gas follows the polytropic equation of state of the form:

$$\left(pV^{n}\right)_{1} = \left(pV^{n}\right)_{2} = \text{constant} \tag{2.7}$$

where the polytropic exponent, *n*, is a function of the compression process or compression equipment *(Lindeburg, 2001)*. With the pressure and volume relation of a centrifugal compressor, or turbomachinery in general, a specific polytropic exponent is utilized for each operating point on the performance curves of the compressor map (see Figure 2.3). The polytropic exponent is calculated by rearranging the polytropic equation of state (Eq. 2.7), defined here as:

$$n = \frac{\ln\left(\dfrac{p_2}{p_1}\right)}{\ln\left(\dfrac{v_1}{v_2}\right)} = \frac{\ln\left(\dfrac{p_2}{p_1}\right)}{\ln\left(\dfrac{p_2}{T_2}\dfrac{T_1}{p_1}\right)} \tag{2.8}$$

Rearranging the compressible work Equation (2.5) to define the work between inlet and outlet states of the polytropic Equation (2.7) forms the following integration to determine the compressible work shaded area of Figure 2.6:

$$\Delta h_{p,c} = \mu_{p,c} = \frac{\dot{W}_{cv}}{\dot{m}} = \int vdp = C^{1/n} \int \frac{dp}{p^{1/n}} \tag{2.9}$$

$$\mu_{p,c} = \frac{n}{n-1}\left(p_2 v_2 - p_1 v_1\right) \tag{2.10}$$

The pressure, temperature, and density thermodynamic relation of matter is termed the equation of state *(von Mises, 2004)*. The equation of state of an ideal gas is:

$$\rho = \frac{1}{v} = \frac{p}{R_g T} \tag{2.11}$$

Rearranging Equation (2.11) with respect to the inlet and outlet conditions of the control volume (Figure 2.7) defines the following:

$$p_2 v_2 = R_g T_2 \quad \text{and} \quad p_1 v_1 = R_g T_1 \tag{2.12}$$

Rearranging the compressible equation of state (Eq. 2.7) with respect to temperature defines:

$$T_2 = T_1 \left(\frac{p_2}{p_1} \right)^{\frac{n-1}{n}} \tag{2.13}$$

From Equation (2.12), the compressible work Equation (2.10) is rearranged into the following:

$$\mu_{p,c} = \left(\frac{n}{n-1} \right) \left[R_g T_2 - R_g T_1 \right] = \left(\frac{n}{n-1} \right) R_g \left[T_2 - T_1 \right] \tag{2.14}$$

Adding the compressible relation of temperature (Eq. 2.13) defines the polytropic head as:

$$Head_{polytropic} = \mu_{p,c} = \frac{\dot{W}_{cv}}{\dot{m}} = \left(\frac{n}{n-1} \right) R_g T_1 \left[\left(\frac{p_2}{p_1} \right)^{\frac{n-1}{n}} - 1 \right] \tag{2.15}$$

2.4.3 Isentropic Compression Process

The term adiabatic refers to a thermodynamic system taking place without heat gain or loss to the surroundings of the control volume. A reversible process without heat transfer of the working fluid with the surroundings is a constant entropy or isentropic process. Industrial terminology commonly refers to this type of process as isentropic, reversible adiabatic, or adiabatic *(Lindeburg, 2001)*. Given the process definition, all terms acceptably apply. In an adiabatic

process, the pressure-volume relation of the compressible gas is defined by the following equation of state as:

$$\left(pV^{\kappa}\right)_1 = \left(pV^{\kappa}\right)_2 = \text{constant} \tag{2.16}$$

where the exponent κ is the ratio of specific heats and intrinsically a function of the gas mixture. Considering Equation (2.16) and the change in pressure-volume between the start and end states of the compression process defines the equation for isentropic compressible work or isentropic head. From the work addition to the control volume in Figure 2.7, the enthalpy change is defined from Equation (2.5), repeated for reference:

$$\frac{\dot{W}_{cv,c}}{\dot{m}} = \left(h_2 - h_1\right) \tag{2.17}$$

The thermodynamic definition of enthalpy is as follows considering the internal energy and pressure-volume relation:

$$h = u + pv \tag{2.18}$$

Substitution of the ideal gas law (Eq. 2.11) in place of the pv term yields:

$$h = u + R_g T \tag{2.19}$$

The partial derivative with respect to temperature of the enthalpy definition is:

$$\frac{\partial}{\partial T}\left(h = u + R_g T\right) \tag{2.20}$$

This defines the isobaric and isochoric heat capacities as follows, respectively:

$$\left(\frac{\partial h}{\partial T}\right)_p = c_p \quad , \quad \left(\frac{\partial u}{\partial T}\right)_v = c_v \tag{2.21}$$

The isobaric term is the specific heat at constant pressure; the isochoric term is the specific heat at constant volume. The partial derivative of enthalpy with respect to temperature (Eq. 2.20) can be rewritten in terms of the heat capacities of Equation (2.21) as follows:

$$c_p = c_v + R_g \tag{2.22}$$

A term used extensively in gas compression and gas dynamics is the ratio of specific heats. This is a ratio of enthalpy and internal energy of the gas to form the following:

$$\kappa = \frac{c_p}{c_v} \tag{2.23}$$

Rearranging Equations (2.22) and (2.23) defines the isobaric heat capacity in terms of the ratio of specific heats and specific gas constant as follows:

$$c_p = \frac{\kappa}{\kappa - 1} R_g \tag{2.24}$$

Relating to the ideal enthalpy difference between the start and end states of the compression process defines the isentropic compressor work from Equations (2.21) and (2.24) as the integration with respect to temperature change:

$$\mu_{s,c} = (h_2 - h_1) = c_p \int_{T_1}^{T_2} dT = \frac{\kappa}{\kappa - 1} R_g (T_2 - T_1) \tag{2.25}$$

Considering a frictionless ideal compressor, the discharge temperature is calculated from the compressible equation of state (Eq. 2.16) as follows:

$$T_2 = T_1 \left(\frac{p_2}{p_1} \right)^{\frac{\kappa-1}{\kappa}} \tag{2.26}$$

Substituting into Equation (2.26) the compression work for pressure in place of temperature defines the isentropic compressor work equation:

$$Head_{isentropic} = \mu_{s,c} = \frac{\dot{W}_{cv}}{\dot{m}} = \left(\frac{\kappa}{\kappa-1} \right) R_g T_1 \left[\left(\frac{p_2}{p_1} \right)^{\frac{\kappa-1}{\kappa}} - 1 \right] \tag{2.27}$$

Notably this definition is similar to the polytropic compressor work defined in Equation (2.15). Replacing the exponent n of the polytropic head equation defines the isentropic head. The two compression process models were derived from different starting points and result in similar final equations, differing by the exponent referring to the appropriate compression process.

2.4.4 Conclusion of Compressible Work Discussion

With appropriate gas properties, the polytropic head or isentropic head of the delivered gas is accurately calculated. The actual compression process is between a polytropic and isentropic process, thus considering either of these models presents an accurate description of the compression process. For single-stage compressors, industry typically utilizes the isentropic process relation for evaluation *(Gresh, 2001)*. The International Organization for Standardization (ISO) has defined suitable applications for polytropic and isentropic processes regarding the evaluation of centrifugal compressors in the Turbocompressor Performance Test Code standard ISO 5389. According to this standard, an isentropic process can be considered as the compression process model for single-stage compressors with low pressure ratios and when the compressed fluid exhibits no change in compressibility. This standard further defines the

application of a polytropic process as best suited for moderate to high pressure ratios, multistage compressors, and applications where the compressed fluid acts as a real gas during the compression process; hence the compressibility is less than 1.0, *(ISO 5389, 2005)*. Ideal gas and real gas considerations in PTC10 are defined through the adherence of the gas compressibility within specified limits of compressor pressure ratio [PTC10-Table 3.3]. Gas compressibility will be covered in further detail in Section 2.7.6.

2.4.5 Compression Power

The power for an ideal compressor to compress the inlet volume flow to the required compressible work is termed the gas power. The gas power is calculated via a polytropic process or isentropic process. Rearranging the Equation (2.5) considering the polytropic head in Equation (2.15), and inlet mass flow (Equation 2.2) defines the gas power as:

Polytropic Gas Power:

$$\dot{P}_{p,c} = \dot{W}_{p,c} = \left(\rho\dot{V}\right)_{inlet} \mu_{p,c} \tag{2.28}$$

Isentropic Gas Power:

$$\dot{P}_{s,c} = \dot{W}_{s,c} = \left(\rho\dot{V}\right)_{inlet} \mu_{s,c} \tag{2.29}$$

Considering the compression efficiency with the gas power details the actual gas power:

Actual Polytropic Gas Power:

$$\dot{P}_{p,a} = \dot{W}_{p,a} = \left(\rho\dot{V}\right)_{inlet} \frac{\mu_{p,c}}{\eta_p} \tag{2.30}$$

Actual Isentropic Gas Power:

$$\dot{P}_{s,a} = \dot{W}_{s,a} = \left(\rho\dot{V}\right)_{inlet}\frac{\mu_{s,c}}{\eta_s} \qquad (2.31)$$

2.4.6 Compressor Polytropic and Isentropic Efficiency

There is an ideal compression process and the actual compression process of the operating machine. The compression efficiency is established thermodynamically to evaluate a machines ability to create head and volumetric flow. Both the isentropic and polytropic compression models have an efficiency relation respective of the process. The efficiency calculation of both compression models utilizes total or stagnation temperature and pressure of the working fluid, referencing absolute conditions of the respective measurements. The isentropic efficiency is defined as follows:

$$\eta_s = \frac{\left[\left(\frac{p_{t,abs,2}}{p_{t,abs,1}}\right)^{\frac{\kappa-1}{\kappa}} - 1\right]}{\left[\left(\frac{T_{t,abs,2,a}}{T_{t,abs,1}}\right) - 1\right]} \qquad (2.32)$$

The polytropic efficiency is defined through the ratio of the polytropic exponent and the isentropic exponent as:

$$\eta_p = \frac{\left(\frac{n}{n-1}\right)}{\left(\frac{\kappa}{\kappa-1}\right)} \qquad (2.33)$$

2.5 Turbocharger Measurement Locations

According to research performed by Chapman and Mohsen *(2000)* monitoring performance of the turbocharger operating on-engine is an important asset to the overall emissions strategy of the owner/operator. When instrumentation is applied correctly, engine air delivery and efficiency can be monitored to evaluate the general health of the turbocharger. There is a significant challenge to collecting accurate field data. In a dedicated test cell, the piping layout to and from the compressor and turbine can be designed to establish swirl free fluid streams to obtain accurate pressure and temperature measurements to detail the machine performance. On engine, the turbocharger piping depends on the air and exhaust manifolds per design by the original equipment manufacturer and specific installation. The manifolds may vary dramatically between installations; thus standardizing instrument locations in the field piping would be an impossible task.

The performance parameters to monitor for important operating information of a turbochargers health and air supply to the engine are *(Chapman, 2000)*:

- Turbine inlet/outlet pressure and temperature

- Compressor inlet/outlet pressure and temperature

- Compressor delivered airflow

- Ambient conditions collected in the vicinity of the installation (barometric pressure, temperature, relative humidity)

These performance measurements are best suited at the flange locations on-board the turbocharger to minimize piping effects, however proper care and calibration of the instrumentation is required. The flow profiles at the flange locations are unsteady and highly turbulent. Following a suitable calibration of the instruments applied at these locations with a well established testing system, the measurements can detail the operating turbocharger performance on-engine. Figure 2.8 and Figure 2.9 detail the installation locations determined through the research by Chapman and Mohsen.

Figure 2.8: Compressor Performance Measurement Locations *(Chapman, 2000)*

| Turbine Inlet Temperature and Pressure | Turbine Outlet Temperature |

Figure 2.9: Turbine Performance Measurement Locations *(Chapman, 2000)*
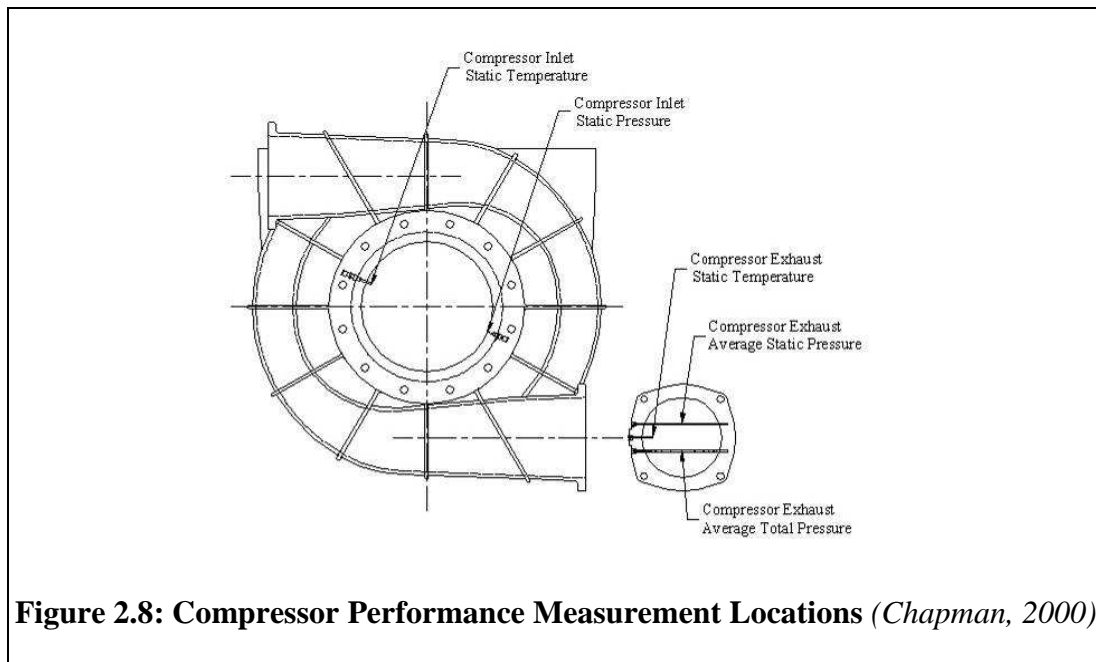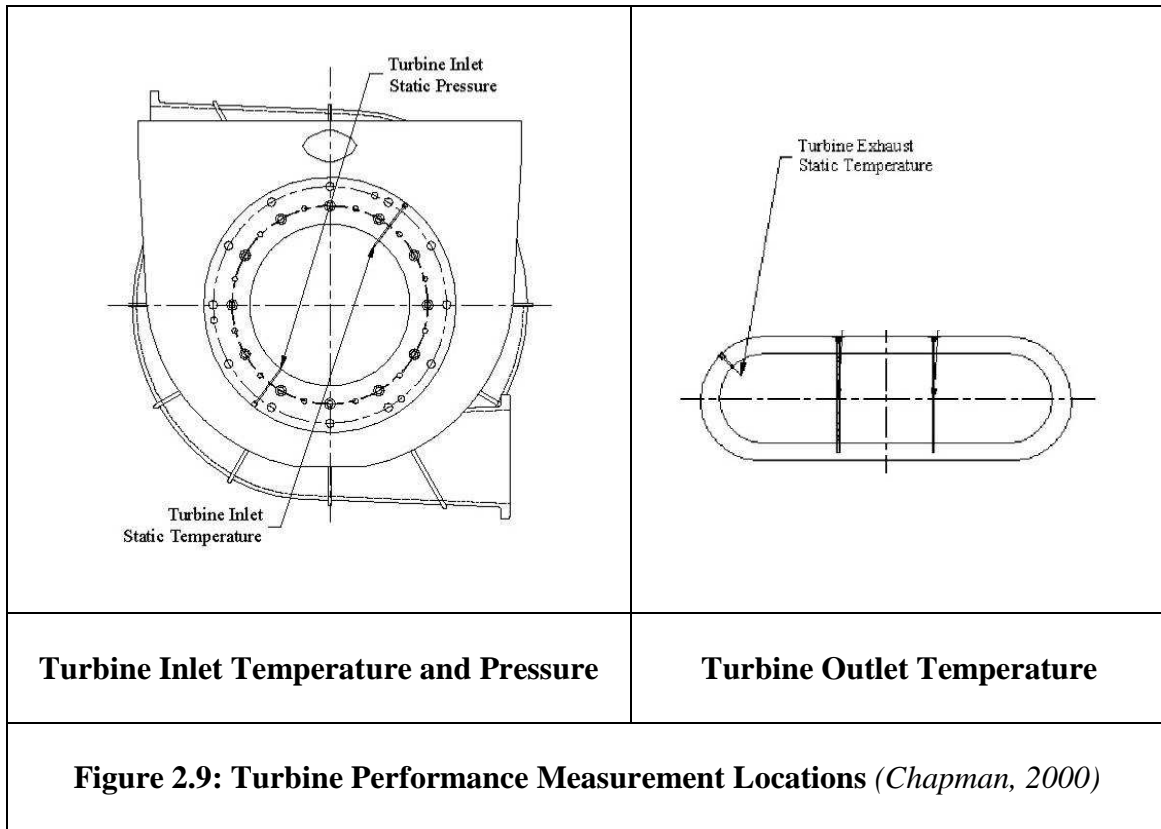
2.6 Piping Pressure Losses

The compression pressure ratio between the inlet and discharge conditions at the respective compressor flanges is a key component of compressible work. If pressure tap locations are significantly away from the compressor inlet and outlet locations, losses incurred through filter media, pipe connections, etc. shall be considered in the pressure ratio to accurately evaluate the overall pressure rise of the compressor. The pressure ratio equation below includes the losses for the inlet and discharge connection considerations.

$$PR = \frac{p_2}{p_1} = \frac{p_2 + p_{dis.losses}}{p_{amb} - p_{inlet.losses}} \tag{2.34}$$

To account for piping losses, a differential pressure measuring device could be installed, or the pressure difference can be calculated from well established equations. In the case of Equation

(2.34) for pipe connections, the losses can be determined by suitable friction factor and pressure loss evaluation for the flowing fluid.

Relative roughness, ε, is a factor measured as the average size of surface imperfections in the piping material. The relative roughness for carbon steel piping is 0.0002 ft *(Lindeburg, 2001)*. The surface roughness coefficient is defined by the relative roughness and the inner diameter of the piping as follows:

$$\text{Surface Roughness Coefficient} = \frac{\varepsilon}{D} \tag{2.35}$$

The Reynolds number of the flowing fluid is a ratio of inertial to viscous forces. This is used to compare the dynamic fluid flow condition between differing piping conditions to ensure the frictional forces of the flowing boundaries are compared *(Munson, 2002)*:

$$Re = \frac{\rho V D}{\mu} \tag{2.36}$$

For circular piping, the Reynolds number can be defined in terms of the mass flow and reference geometry in place of the velocity component in Equation (2.36) as follows:

$$Re = \frac{4\dot{m}}{\pi \mu D} \tag{2.37}$$
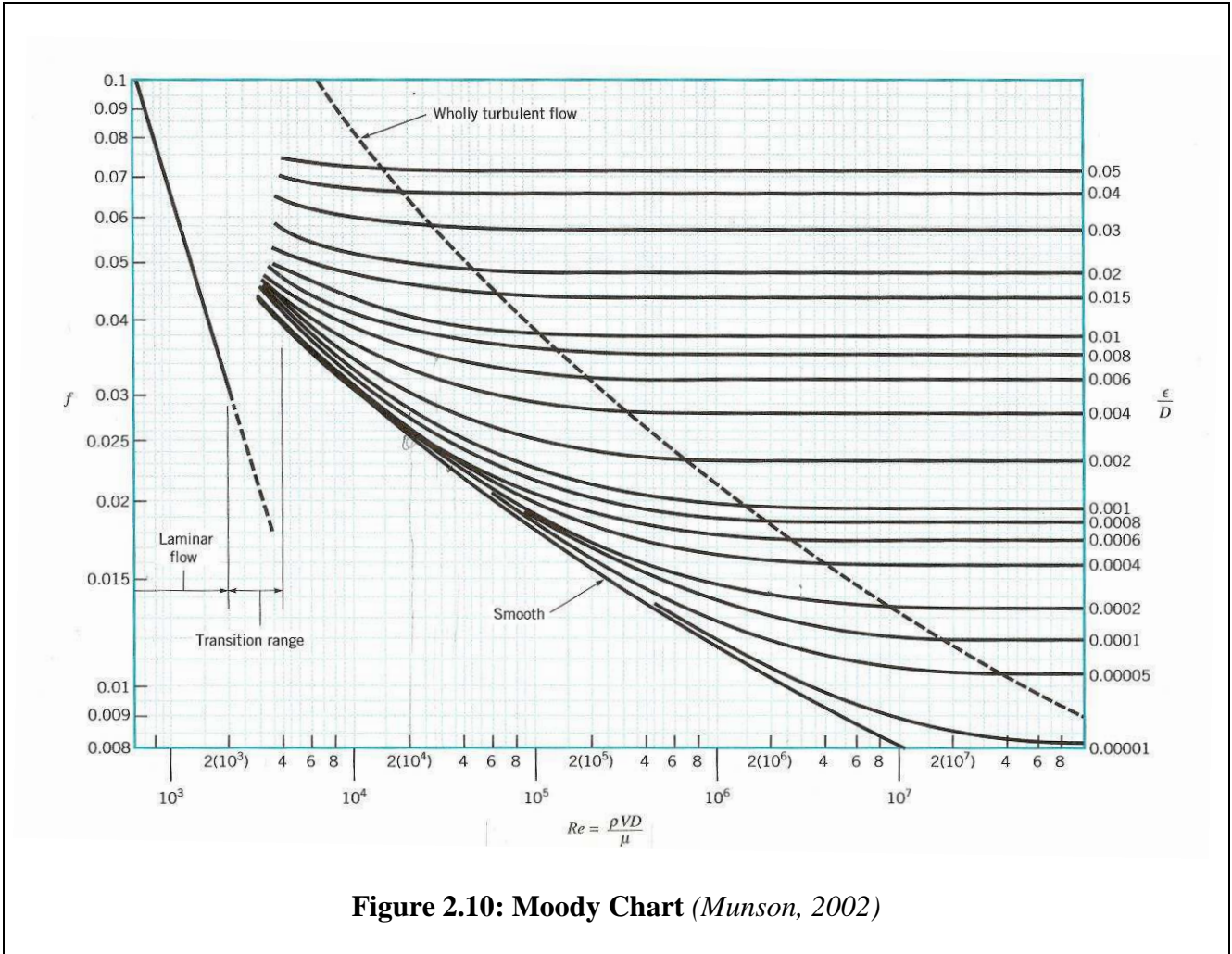
Figure 2.10: Moody Chart *(Munson, 2002)*

As detailed by the Moody chart (Figure 2.10), the friction factor, *f*, of a flowing fluid through a pipe or conduit depends on the surface roughness coefficient, and the Reynolds number of the flowing fluid. The friction factor is required for use in pressure drop calculations with the Darcy Equation (2.42) (Table 2.1).

There has been significant effort to detail the Moody chart in the form of functional equations to establish friction factor without the requirement of reviewing the chart in Figure 2.10. The equations in Table 2.1 determine friction factor as a function of the surface roughness coefficient, and Reynolds number. With the exception of Churchill (Eq. 2.41) and Chen (Eq. 2.39), the equations are for Reynolds numbers greater than 3,500, or above the transition range in

Figure 2.10. Each equation was compared against the Moody chart, finding the accuracy of Churchill suitable for the analysis for two reasons: larger Reynolds number range and accuracy with Moody chart when compared against the Chen and Swamee-Jain equations (Eq's. 2.39 and 2.40). The Colebrook equation (Eq. 2.38) was not evaluated due to iteration requirements of the friction factor, f.

Table 2.1: Friction Factor and Pipe Pressure Loss

Name	Equation	Eq. No.
Colebrook	$$\frac{1}{\sqrt{f}} = -2.0\log\left[\left(\frac{\varepsilon/D}{3.7}\right) + \frac{2.51}{Re\sqrt{f}}\right] \quad, Re \geq 3500$$ *(Munson, 2002)*	(2.38)
Chen (1979)	$$\frac{1}{\sqrt{f}} = -2.0\log\left[\left(\frac{\varepsilon/D}{3.7065}\right) - \frac{5.0452}{Re}\log\left(\frac{1}{2.8257}\left(\frac{\varepsilon}{D}\right)^{1.1088} + \frac{5.8506}{Re^{0.8981}}\right)\right]$$ $Re \geq 1$	(2.39)
Swamee-Jain (1976)	$$f = \frac{0.25}{\left[\log\left[\left(\frac{\varepsilon/D}{3.7}\right) + \frac{5.74}{Re^{0.9}}\right]\right]^2} \quad, Re \geq 3500$$	(2.40)
Churchill (1977)	$$f = 8.0\left[\left(\frac{8}{Re}\right)^{12} + \frac{1}{\left(a^{16} + b^{16}\right)^{1.5}}\right]^{\frac{1}{12}} \quad, Re \geq 1$$ $$a = 2.457\ln\left[\left(\frac{\varepsilon/D}{3.7}\right) + \left(\frac{7}{Re}\right)^{0.9}\right] \quad b = \frac{37530}{Re}$$	(2.41)
Darcy	$$\Delta p_{pipe} = \frac{\rho f L_e V^2}{2D_{pipe}g}$$ *(Munson, 2002)*	(2.42)

2.7 Thermodynamic and Fluid Properties

The mixture of the working fluid is integral to both the polytropic (Eq's. 2.15 and 2.27) and isentropic compression processes in the specific gas constant, R_g. With ambient air as the working fluid of a turbocharger, the two components to consider in the specific gas mixture are dry air and water vapor. These components define the molecular weight of the gas mixture, MW_{mix}. The molecular weight of the mixture details the specific gas constant from the universal gas constant, $\overline{R}_u$. The specific gas constant of the inlet air considering the molecular weight is defined as:

$$R_g = \frac{\overline{R}_u}{MW_{mix}} \tag{2.43}$$

The specific gas constant is required to accurately calculate the gas density, ratio of specific heats and compressible work. The ambient condition and mixture will change throughout the course of a day and therefore are required to detail the gas condition for any compressor operating point in question. The following sections detail the water vapor, isobaric specific heat, and ratio of specific heats.

2.7.1 Mole Fraction and Molecular Weight

The molecular weight of the mixture requires the fraction of each component of the mixture; or the mole fraction. The mole fraction of water vapor is calculated from the actual water vapor, barometric pressure and saturated vapor pressure as follows:

$$y_v = \frac{p_{vapor}}{p_{amb} - p_{sat}} \tag{2.44}$$

The water vapor of the mixture is determined from the relative humidity and the saturated vapor pressure as follows:

$$p_{vapor} = rh \ p_{sat}$$ (2.45)

With the mole fraction of the water vapor, the molecular weight of the mixture is calculated as follows:

$$MW_{mix} = \sum_i y_{v,i} MW_i = (1 - y_v) MW_{air} + y_v MW_{vapor}$$ (2.46)

2.7.2 Saturated Vapor Pressure of Air

The water vapor of the inlet gas changes due to ambient conditions. The amount of water vapor in the inlet air can be determined from the psychrometric chart or via the saturated vapor from thermodynamic tables for steam. However, these methods require examining the chart or tables for each operating data point of the compressor operation. To determine the saturated vapor pressure without the use of the psychrometric chart or steam table, an algorithm can be used, provided the accuracy of the calculation method is reasonable.

To determine the saturated vapor pressure of the intake airflow, the steam tables are evaluated utilizing the relation in Figure 2.11. This is the K-function saturation line established in the ASME Steam Tables *(ASME, 1993)*.

Constants for the reduced saturation pressure:

$$k_1 = -7.691234564 \quad k_2 = -26.08023696$$
$$k_3 = -168.1706546 \quad k_4 = 64.23285504$$
$$k_5 = -118.9646225 \quad k_6 = 4.16711732$$
$$k_7 = 20.975067600 \quad k_8 = 10^9$$
$$k_9 = 6.0$$

$$\theta = \frac{Temp(K)}{647.27K} \quad \& \quad \sigma = 1 - \theta \qquad \text{(2.47) \& (2.48)}$$

$$\beta_k = \left[\frac{1}{\theta} \cdot \frac{k_1\sigma^1 + k_2\sigma^2 + k_3\sigma^3 + k_4\sigma^4 + k_5\sigma^5}{1 + k_6\sigma + k_7\sigma^2} \right] - \left[\frac{\sigma}{k_8\sigma^2 + k_9} \right] \qquad \text{(2.49)}$$

Critical pressure: $\qquad\qquad p_{cr} = 3208.235 \, \text{psia}$

Saturated vapor pressure: $\qquad p_{sat}(\text{psia}) = p_{cr} \cdot e^{\beta_k} \qquad\qquad \text{(2.50)}$

Figure 2.11: K-Function Saturated Vapor Pressure of Water

The K-function is suitable from 32.018°F to the critical temperature of 705.47°F, well outside of the requirements to detail water vapor of the inlet ambient air, 32°F-120°F. This function provides a method to calculate the saturated vapor pressure for the operating inlet temperature. As compared against the steam tables, this function presents an accuracy of +0.003%, -0.004% for the temperature range of ambient air. Additional methods at slightly reduced accuracy are detailed for reference in Appendix A: Saturated Vapor Pressure Methods.

2.7.3 Isobaric Heat Capacity

The gas mixture at a given state typically requires reviewing data tables for each gas component of the mixture. As detailed in Equation 2.20, enthalpy changes with respect to temperature can be detailed as the isobaric heat capacity, c_p. The specific heat of dry air and water vapor of the mixture, $c_{p,mix}$, will be calculated separately for each component on a molar basis, $\overline{c}_{p,i}$. The specific heat of the mixture on a mass basis is calculated from the component molar specific heats and the molecular weight as follows:

$$c_{p,mix} = \sum_i \frac{\overline{c}_{p,i}}{y_{v,i} MW_i} \tag{2.51}$$

The specific heat of dry air and water vapor on a molar basis is calculated by the following polynomial equation *(Moran, 1995)*:

$$\overline{c}_{p,i} = \left(\alpha + \beta T + \gamma T^2 + \delta T^3 + \varepsilon T^4\right)\overline{R}_u \tag{2.52}$$

The constants of this polynomial and the molecular weights of air and water vapor are defined in Table 2.2.

Table 2.2: Constants for Specific Heat Polynomial for Dry Air and Water Vapor

Gas	Molecular Weight	α	$\beta \times 10^{-3}$	$\gamma \times 10^{-6}$	$\delta \times 10^{-9}$	$\varepsilon \times 10^{-12}$
Air	28.97 lb/lbmol	3.653	-0.7428	1.017	-0.328	0.02632
Water Vapor	18.0153 lb/lbmol	4.070	-0.616	1.281	-0.508	0.0769

2.7.4 Ratio of Specific Heats

In many cases the water vapor contribution to the mixture is neglected which can be a source of error in the calculations. With the definition of the specific gas constant and isobaric specific heat of the mixture, the ratio of specific heats of the mixture is determined with substitution of Equation 2.22 as follows:

$$\kappa = \frac{c_{p,mix}}{c_{v,mix}} = \frac{c_{p,mix}}{c_{p,mix} - R_g} \tag{2.53}$$

At times, the isobaric specific heat is considered a constant value of the gas at the inlet gas temperature. There is a significant compressor work and temperature change between beginning and end states of the compression process. Because the ratio of specific heats, κ, and specific heat at constant pressure, $c_{p,mix}$, are a function of temperature, increased accuracy from the change of these values during compression is calculated as follows:

$$\kappa_{avg} = \frac{\kappa_{inlet} + \kappa_{outlet}}{2} \tag{2.54}$$

According to Lüdtke *(2004)*, the polytropic exponent and the isentropic exponent should be calculated between beginning and end states for accuracy of the compression process. Performance Test Code 10 considers this change with respect to the isentropic exponent; however this is not a consideration of the polytropic exponent.

2.7.5 Viscosity of Air and Water Vapor

The absolute viscosity of the inlet airflow is required for the Reynolds number. Considering the gas mixture, the absolute viscosity is calculated as follows *(Miller, 1996), (Ikoku, 1984)*:

$$\mu_{mix} = \frac{\sum y_i \mu_i \sqrt{MW_i}}{\sum y_i \sqrt{MW_i}} = \frac{(1-y_v)\mu_{air}\sqrt{MW_{air}} + y_v\mu_{vapor}\sqrt{MW_{vapor}}}{(1-y_v)\sqrt{MW_{air}} + y_v\sqrt{MW_{vapor}}} \tag{2.55}$$

The absolute viscosity of air is calculated as follows *(Tapley, 1990)*:

$$\mu_{air} = \left(-4.659\times10^{-6}T(°F)^2 + 0.006834\,T(°F) + 3.297\right)\times10^{-7}\,\frac{\text{lbf sec}}{\text{ft}^2} \tag{2.56}$$

The absolute viscosity of water vapor is calculated as follows *(ASME Steam Tables, 1993)*:

$$\mu_{vapor} = \left(1.278\times10^{-6}T(°F)^2 + 0.003306\,T(°F) + 1.799\right)\times10^{-7}\,\frac{\text{lbf sec}}{\text{ft}^2} \tag{2.57}$$

2.7.6 Gas Compressibility

Gases either follow the ideal gas law or the real gas law, depending on the compressibility for the pressure and temperature condition of the gas. The critical pressure and critical temperature of a gas mixture is evaluated as a pseudo-critical condition. The pseudo-critical pressure and temperatures are comprised of the individual components of the gas.

Pseudo-critical Pressure:

$$p_{pc} = \sum_i y_i p_{cr,i} \tag{2.58}$$

Pseudo-critical Temperature:

$$T_{pc} = \sum_i y_i T_{cr,i} \tag{2.59}$$

The reduced pressure and temperature of the gas mixture are then determined by the following:

Reduced Pressure:

$$p_r = \frac{p}{p_{pc}}$$
(2.60)

Reduced Temperature:

$$T_r = \frac{T}{T_{pc}}$$
(2.61)

To verify use of the ideal gas equations for a compressibility of Z=1.0, the reduced temperature and pressure are utilized in Figure 2.12 to determine the gas compressibility.
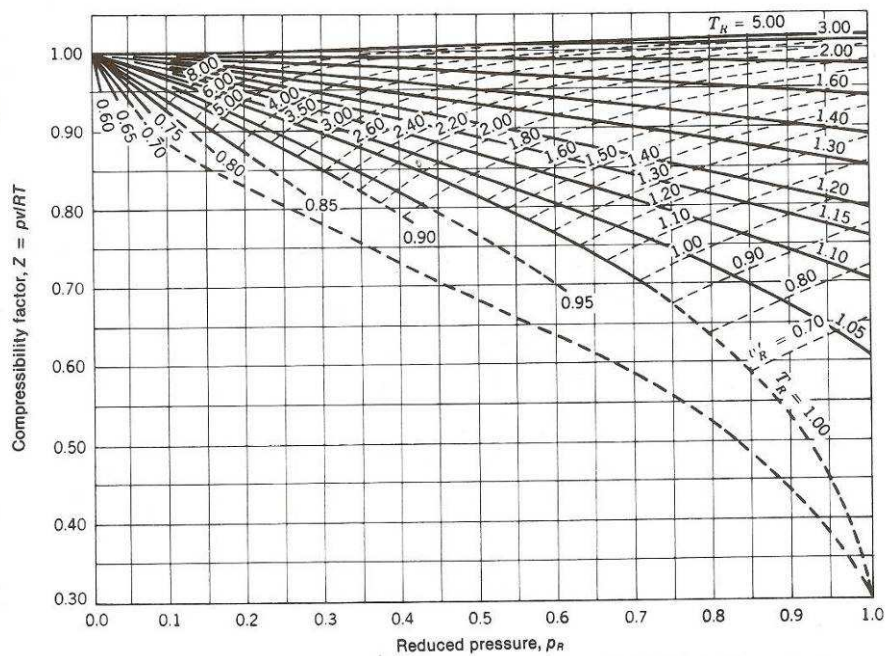
Figure 2.12: Compressibility Chart for Reduced Pressure *(Moran, 1995)*

2.7.7 Total Conditions

Temperature and pressure measurements in the piping system of the turbine and compressor flow paths are static measurements, defined as: T_{static} or p_{static} for the respective measuring location. The working fluid is in motion at the measuring locations, containing both a static and dynamic (velocity) component of the temperature and pressure measurements. If the working fluid were brought to zero velocity and the temperature and pressure measured, a static measurement would be the total or stagnation measurement of the gas condition. To account for the dynamic component of the working fluid in motion, the total condition is calculated from the following equations [PTC10-Eq's. 5.4.4 and 5.4.6].

$$p_{t,abs} = p_{static,abs} + \left(\frac{\rho_t V^2}{2}\right)_{dynamic} \tag{2.62}$$

$$T_{t,abs} = T_{static,abs} + \left(\frac{V^2}{2c_{p,mix}}\right)_{dynamic} \tag{2.63}$$

$$\rho_t = \frac{p_{t,abs}}{R_g T_{t,abs}} \tag{2.64}$$

$$Error = \rho_{t,n} - \rho_{t,n-1} \leq 10^{-5} \tag{2.65}$$

The total pressure and total density of the working fluid are interdependent making this an iterative calculation. This is performed with a seed value in the form of static density, and then iterated to a suitable accuracy for the total pressure and density of the fluid stream. An error between iterations for density or pressure as detailed in Equation (2.65) provides a suitable accuracy required for performance considerations. The importance herein is the comparison of

the total conditions of the working fluid independent of the fluid piping and fluid velocity where measurements are collected. The total conditions of the working fluid are required to accurately detail compressor work and efficiency.

2.8 Dimensional Analysis and Similitude

A useful method of comparing conditions for numerous engineering models is through the method of dimensional analysis and similitude. Imagine a physical system (or physical model) under study with at least five variables contributing to the system, each of which requires experimentation to determine their contribution. This requires a separate experiment for each variable, maintaining the remaining variables constant.

Following the individual experimentation, all data from all experiments would require organization to detail the overall contribution to the model. Therefore a system of five variables requires five experiments at a minimum and the data between all experiments is segmented. If the number of variables were to increase, the model testing and evaluation can quickly get out of hand. Moreover, some variables are interdependent. The viscosity and density of a gas are temperature dependent; holding temperature constant maintains these important gas conditions constant as well.

If the experimenter were to evaluate not the individual contribution but the coupled interaction of the variables relating to the model, experimentation is focused to collecting more useful information much easier. This is performed through dimensional analysis. Dimensional analysis is a method of deducing important information of a model given a description by a dimensionally correct, dimensionless equation of the specific important variables of the model *(Langhaar, 1951)*.

The purpose of dimensional analysis is to provide a means of relating the physical analysis to useful dimensionless packets of information containing the interaction of the variables of a model. The method is generally used in fluid mechanics in the exploration of aerodynamics. Although not obvious, one well known example of this method is the Moody chart (Figure 2.10). The Moody chart relates the dimensionless friction loss of flow with respect to the surface roughness coefficient, and the Reynolds number of the fluid and piping. The application of dimensional analysis is found in the study of problems of stress and strain, fluid mechanics, heat transfer, electromagnetics and physics *(Langhaar, 1951)*. Additionally, this method can be used in differential equations in the study of transients as found with natural frequency analysis, and gas dynamics to mention a few. The full power of this method is realized once applied and provides a quick method of comparing models without lengthy or tedious calculations.

Though there have been many researchers in this field including the well known works of Lord Rayleigh, Edgar Buckingham, and Percy Bridgman, the method is commonly referred to as the Buckingham PI theorem or simply PI theorem *(Taylor, 1974), (Munson, 2002)*. Through the analysis, the resulting relations are generally referenced as PI terms, noted with the Greek letter Π. This comes from the paper by Edgar Buckingham *(1914)* detailing the method which presented the dimensionless products as Π terms.

To explore this topic we must also define the concept of similitude to consider the geometry, and dynamic and kinematic conditions required for model testing. The following section details similitude and the use of dimensional analysis. These concepts develop the fundamental methodology for evaluating compressor or turbine performance.

2.8.1 Units of Measure

Units of measure can be expressed in terms of established standards and presented numerically to detail the physical relationship between quantities such as time, length, temperature, mass, velocity, acceleration, density, etc. Units of measure of length are expressed through established standards as meters, feet, yards, inches, miles, etc. Area is expressed in terms of length squared, detailing that a quantity applies to two length dimensions in relation to each other. Area is expressed in terms of meters², feet², yards², inches², miles², etc². The basic unit or fundamental dimension of area is therefore length squared (L^2); the units of measure provide a physical comparison to a standard reference measure.

There are different measurement systems, each have relation to each other through standard universal reference units. The two most recognized measuring systems in general use today are: the British Gravitational (BG) System, and International System (SI) *(Munson, 2002)*. These measurement systems provide a means of establishing a numerical value in standard recognized units of measure.

The effort of evaluating models through dimensional analysis will provide the same overall results independent of the unit measuring system, provided the fundamental units and resulting equations are dimensionally homogenous. To be dimensionally homogenous, the unit relations must follow the same measuring system and basic units, for example: length in terms of feet, time in terms of seconds, etc. Mixing units (e.g. inches and feet) will result in non-homogeneous relations that are unit and variable dependent and therefore physically meaningless *(Douglas, 1985)*.

2.8.2 Fundamental Dimensions

Fundamental dimensions are the basic units of length, time, mass and force. In dimensional analysis two fundamental dimension systems derive the relations to the physical quantities: the 'force, length, time' (FLT) system, and the 'mass, length, time' (MLT) system.

Applying the fundamental dimensions to the equation of force, $F = ma$, for example provide the following dimensional groupings:

The FLT system:

$$(F)^F = \left(FL^{-1}T^2\right)^m \left(LT^{-2}\right)^a \tag{2.66}$$

The MLT system:

$$\left(MLT^{-2}\right)^F = \left(M\right)^m \left(LT^{-2}\right)^a \tag{2.67}$$

where the indices F, m and a are used to detail the terms of the force equation in the dimensional groupings. Both groupings are correct considering the fundamental dimensions. Due to simplicity for the dimensions of a centrifugal compressor, the fundamental dimensions herein utilize the MLT system. The following sections detail the use and explore the application to a centrifugal compressor.

2.8.3 Application of Dimensional Analysis to Centrifugal Compressor

As detailed by Buckingham's theorem *(Buckingham, 1914)* the number of PI terms, *r*, to form a complete description of the model depends on the number of variables to evaluate the model, *n*, and the number of fundamental dimensions, *m*. The number of PI terms that will form from this

are: $n - m = r$. The theorem states that for a number of related but independent variables, q_n's, of a model:

$$\phi(q_1, q_2, q_3, \ldots q_n) = 0 \qquad (2.68)$$

A solution of the dimensionless products of the q_n's exists as follows:

$$\phi(\Pi_1, \Pi_2, \Pi_3, \ldots \Pi_r) = 0 \qquad (2.69)$$

The application to a centrifugal compressor will provide a means to compare between the infinite combinations of inlet air temperature, pressure, relative humidity, volume flow, compressible head and speed to create an effective evaluation between differing operating conditions. The operating variables and fundamental dimensions of a centrifugal compressor are detailed in Table 2.3.

Table 2.3: Centrifugal Compressor Dimensional Variables

Quantity	Variable	Unit	Dimensions
Compressible Work	μ_c	$\dfrac{\text{ft lbf}}{\text{lbm}}$	$L^2 T^{-2}$
Inlet Volume Flow	$\dot{V}$	$\dfrac{\text{ft}^3}{\text{min}}$	$L^3 T^{-1}$
Shaft Rotating Speed	N	RPM	T^{-1}
Compressor Impeller Tip Diameter at Exit	D_2	ft	L
Gas Density	ρ	$\dfrac{\text{lbm}}{\text{ft}^3}$	ML^{-3}
Absolute Gas Viscosity	μ	$\dfrac{\text{lb sec}}{\text{ft}^2}$	$ML^{-1}T^{-1}$
Fluid Bulk Modulus of Elasticity	E_v	$\dfrac{\text{lbf}}{\text{ft}^2}$	$ML^{-1}T^{-2}$
Surface Roughness of the Internal Passages	ε	ft	L

Since compressible work is the energy per unit weight of the compressible fluid it is appropriate to define this quantity (μ_c) to include the effects of gravity in the unit dimensions [PTC10-Eq. 5.1-3], *(Douglas 1985)*. This establishes the dimensional groups interrelated to compressible work as:

$$\mu_c = \phi(\dot{V}^a, N^b, D^c, \rho^d, \mu^e, E_v^{\ f}, \varepsilon^h) \tag{2.70}$$

$$\mu_c = \dot{V}^a N^b D^c \rho^d \mu^e E_v^{\ f} \varepsilon^h \tag{2.71}$$

where the alphabetic indices in the above equation are place holders for the evaluation. Substituting the fundamental dimensions into this relation provides the following:

$$\mu_c = L^2 T^{-2} = (L^3 T^{-1})^a , (T^{-1})^b , (L)^c , (ML^{-3})^d , \left(ML^{-1}T^{-1}\right)^e , \left(ML^{-1}T^{-2}\right)^f , (L)^h \qquad (2.72)$$

Note there are seven variables (n) in the potential solution and three fundamental dimensions (m), defining four dimensionless groups (r) to detail the model. Resolving the indices in the above relation algebraically while maintaining compressible work and volume flow as a primary function of compression details the following relation:

$$\mu_c = \dot{V}^a N^{(2-a-e-2f)} D^{(2-3a-2e-2f-h)} \rho^{(-e-f)} \mu^e E_v{}^f \varepsilon^h \qquad (2.73)$$

Regrouping each of the indices details the dimensionless groups from the above relation as follows:

$$\frac{\mu_c}{N^2 D^2} = \phi(\Pi_1, \Pi_2, \Pi_3, \Pi_4) = \left(\frac{\dot{V}}{ND^3} ; \frac{\mu}{\rho ND^2} ; \frac{E_v}{\rho N^2 D^2} ; \frac{\varepsilon}{D} \right) \qquad (2.74)$$

Define the impeller tip speed (u_2) as a primary quantity of the impeller diameter at the exit (D_2) in Equation (2.75). The added π is a constant and defines the rotational tip speed of the impeller from the rotational velocity (N) and impeller diameter (D_2). The constant has no dimensions therefore maintaining dimensional homogeneity in the group.

$$u_2 = \left(\pi N D_2\right) \qquad (2.75)$$

with tip speed, this simplifies the groups as a function of compressible work as follows:

$$\left(\frac{\mu_c}{u_2^2}\right)^{\psi} = \left[\left(\frac{\dot{V}}{u_2 D_2^2}\right)^{\varphi} ; \left(\frac{\mu}{\rho u_2 D_2}\right)^{1/Re} ; \left(\frac{E_v}{\rho u_2^2}\right)^{1/Ma^2} ; \left(\frac{\varepsilon}{D_2}\right)\right] \qquad (2.76)$$

The variable indices (ψ, φ, Re, Ma) in the resulting group (Eq. 2.76) detail the variables that will be utilized to represent each PI term. This statement defines the following important relations:

- Head is a function of the impeller tip speed squared; the head coefficient, ψ.

- Volume flow is a function of the tip speed and impeller exit diameter squared; the flow coefficient, φ.

- The flow, head, and tip speed are coupled through the flow and head coefficient. Plotting the head coefficient versus flow coefficient therefore defines a dimensionless compressor map normalized with respect to impeller tip speed. This is the compressor signature of operation, all operating and specified conditions can be evaluated from this map.

The following also form a relation with the head coefficient:

- Inverse Reynolds number, $1/Re$.

- Inverse Mach number squared, $1/Ma^2$, or the inverse Cauchy number.

- Surface roughness coefficient, ε/D_2.

The speed of sound, c, is defined from the bulk modulus and fluid density and can be rearranged into the more common form found in gas dynamics as:

$$c = \sqrt{\frac{E_v}{\rho}} = \sqrt{\kappa R_g T(g)} \qquad (2.77)$$

When working with compressible fluids, either the Cauchy number or the Mach number may be used *(Munson, 2002)*. Although both are acceptable, when working with gas dynamics the Mach is the more common parameter.

Since all operating parameters of the compressor are defined in the dimensionless groups, the above relations define the correction methodology for centrifugal compressors. Following the dimensional relations to maintain dimensional homogeneity, each dimensionless parameter can be modified adding numerical constants. This is one alteration typically found in turbomachinery books and references.

2.8.4 Similitude

The concept of similitude provides a method of comparison between fundamentally similar physical systems by following an appropriate matching of the dimensionless parameters. This forms a characteristic match of the models. There are three considerations or similarity laws to maintain when matching conditions between models of comparison: geometry, fluid dynamics, and kinematics.

A geometric match between models is the highest concern of comparison through dimensionless parameters. Schlichting details the geometric consideration as providing mechanically similar flows *(Schlichting, 2000)*. The dimensionless quantities are in relation to a specific impeller geometry; the impeller shape and blade height which are fixed. If vanes are present in the discharge diffuser the vane angle must be fixed as well when matching differing operating conditions.

Matching fluid dynamics considers maintaining the fluid effects of the models. This compares the Reynolds and Mach numbers between models to ensure the applied fluid forces are maintained for the deformation of the working fluid through the compressor. This also defines the density ratio (specific volume ratio) considerations between inlet and outlet conditions of PTC10. This is provided to maintain consistency between test and specified conditions [PTC10-Table 3.2].

Finally, to match the kinematics between models, the rotational velocity of the compressor must be maintained to fulfill the final similarity law. Because of the dependence of compressible head on the tip speed, the rotational velocity plays a significant role in matching between model conditions. By matching geometry and either dynamics or kinematics, the third is automatically matched through the fundamentals of similarity, and ensures similitude and validation of the models *(Munson, 2002)*.

2.9 Application of Similitude to Centrifugal Compression

For the case of a centrifugal compressor, the primary considerations for matching conditions between models are geometry and kinematics. The inertial forces of the fluid are much larger than the viscous forces, establishing large Reynolds numbers for a compressor. This plays a lesser effect on the model comparison. According to Taylor *(1974)* model flexibility is key; insistence on utilizing the Mach number and Reynolds number matching can paralyze the observer in detailing similitude in this application. Therefore, the machine Mach and Reynolds numbers are secondary coefficients of similitude of the compressor model. Research in this area has established technical guidance for considering the Reynolds number and Mach number in models, and detailed in Sections 2.9.5 and 2.9.6.

For any operating point of interest of the compressor, a set of dimensionless parameters exists to define the operating point. Secondly, considering the head and flow conditions as primary operation of the compressor, the following definition (Equation 2.78) is therefore valid to compare any two operating points between differing inlet density conditions (ambient conditions) or different compressible fluids. This is termed as test and specified conditions and the flow and head coefficient match is as follows:

$$\varphi_{sp} = \varphi_{te} \quad \& \quad \psi_{sp} = \psi_{te} \tag{2.78}$$

This definition is the fundamental relation required to establish performance comparison between any two operating conditions of the compressor. Additionally, the Reynolds number and Mach number must be considered to complete the concept of similitude. The following sections detail the head and flow coefficients as found in various texts, and detail the Mach number and Reynolds number relations required to complete the analysis.

2.9.1 Flow Coefficient

Considering a centrifugal compressor the dimensionless parameter for flow is [PTC10-Eq. 5.5.7]:

$$\varphi = \frac{\dot{m}}{\rho} \frac{1}{2\pi N D_2^{\,3}} = \frac{\dot{V}}{2\pi N D_2^{\,3}} = \frac{\dot{V}}{2\,u_2 D_2^{\,2}} \tag{2.79}$$

The flow coefficient is defined in multiple sources with multiple constants, confusing the usage. Each comparison is valid if data is collapsed and expanded via the same dimensionless parameter. Table 2.4 details different flow coefficients found from sources referenced herein.

This table details the importance of knowing the flow coefficient utilized to guard against error in collapsed or dimensionless data.

Table 2.4: Comparison of Compressor Flow Coefficients

Equation No.	Variant Constant, a	Flow Coefficient $\dfrac{1}{a}\left(\dfrac{\dot{V}}{u_2 D_2{}^2}\right)$	Dimensionless?	Reference Source
(2.80)	2	$\dfrac{\dot{V}}{2u_2 D_2{}^2}$	Yes	*(PTC10)*
(2.81)	$\dfrac{\pi}{4}$	$\dfrac{\dot{V}}{\dfrac{\pi}{4}D_2{}^2 u_2}$	Yes	*(ISO 5389)*
(2.82)	N/A	$\dfrac{\dot{m}\sqrt{c_{p.mix}T_{1,abs}}}{p_1 D_2{}^2}$	Yes	*(Bathie, 1995)*
(2.83)	$\dfrac{1}{\pi}$	$\dfrac{\dot{V}}{ND_2{}^3}$	Yes	*(Japikse, 1997)* *(Dixon, 1998)*

In the above table, Equation (2.81) is commonly found in European texts, and references the flow of the compressor in comparison to a similarly sized hole for the term $\left(\dfrac{\pi}{4}D_2{}^2\right)^{-1}$. Equation (2.82) includes the isobaric heat capacity and excludes impeller rotational velocity. Error may be introduced with this relation if the heat capacity or inlet temperature were considered constant, or if speed were different in the analysis. As found during formation of the dimensionless relations, Equation (2.83) references the fundamental flow coefficient in Equation (2.74).

2.9.2 Head Coefficient

Similar to the flow coefficient, the head coefficient is defined slightly different by various sources. The parameter for dimensionless head is [PTC10-Eq's. 5.1-3 and 5.1T-4]:

$$\psi = \frac{\mu_c}{u_2{}^2} \qquad (2.84)$$

Table 2.5 details head coefficients from sources referenced herein, comparing the applied constant to the coefficient used in the text.

Table 2.5: Compressor Head Coefficient Comparison

Equation No.	Variant Constant, a	Head Coefficient $\frac{1}{a}\left(\frac{\Delta h}{u_2{}^2}\right)$	Dimensionless?	Reference Source
(2.85)	1	$\dfrac{\mu_c}{u_2{}^2}$	Yes	*(PTC10)* *(Japikse, 1997)*
(2.86)	$\dfrac{1}{2}$	$\dfrac{\frac{\mu_c}{u_2{}^2}}{2}$	Yes	*(ISO 5389)*
(2.87)	$\dfrac{1}{\pi^2}$	$\dfrac{(\Delta p / \rho)}{N^2 D_2{}^2}$	Yes	*(Japikse, 1997)*
(2.88)	$\dfrac{1}{\pi^2}$	$\dfrac{\mu_c}{N^2 D_2{}^2}$	Yes	*(Japikse, 1997)* *(Dixon, 1998)*

In this table, Equation (2.86) is the ratio of head and the impeller tip speed in a form similar to the ratio of head to kinetic energy from the energy rate Equation (2.4). Though the velocity

difference between inlet and outlet conditions is considered negligible, this equation follows the same form due to the importance of tip speed to compressible head. Equation (2.87) defines a pseudo-head with the term $\Delta p / \rho$. This equation does not utilize the equation of state for gases (Eq's. 2.7 and 2.16) and may introduce error with differing gas conditions. As found during formation of the dimensionless relations, Equation (2.88) references the fundamental head coefficient in Equation (2.74).

2.9.3 Power Coefficient

The dimensional analysis in Section 2.8.3 can be utilized to form the power coefficient for the compressor as the head and flow coefficients were formed. This can also be completed by utilizing the flow and head coefficient (Eq's. 2.79 and 2.84), and the gas power in Equation (2.28) or (2.29) as follows.

$$\dot{P}_{p,c} = \left(\rho \dot{V} \right)_{inlet} \mu_{p.c} = \left(\rho_{inlet} \right) \left(2 \varphi u_2 D_2{}^2 \right) \left(\psi_p u_2{}^2 \right) \tag{2.89}$$

Forming the polytropic power coefficient as follows:

$$\Omega_{p,c} = \frac{\dot{P}_{p,c}}{2 \rho_{inlet} D_2{}^2 u_2{}^3} \tag{2.90}$$

Similar to the flow and head coefficients, the dimensionless power can be utilized to compare the gas power signature of the compressor at varying specified density and speed conditions. The actual gas power can therefore be established as follows:

$$\Omega_{p,a} = \frac{\Omega_p}{\eta_p} = \frac{\dot{P}_{p,c}}{2 \rho_{inlet} D_2{}^2 u_2{}^3 \eta_p} \tag{2.91}$$

2.9.4 Dimensionless Compressor Map

Plotting the dimensionless characteristics of a model presents a method of comparing numerous details and aspects for evaluating data *(Taylor, 1974)*. As defined above, the head coefficient is a function of flow coefficient. The isentropic or polytropic efficiency is a function of the flow coefficient as well. Due to the interdependence of speed, diameter, head and flow, a dimensionless map can be detailed. Plotting the head coefficient and efficiency versus flow coefficient for the compressor model and impeller geometry, develops a characteristic curve or signature of operation for a specific compressor model *(Lüdtke, 2004)*.

2.9.5 Machine Mach Number

As resolved in the dimensionless groups (Eq. 2.76) the Mach number defines an important parameter to the compressor performance evaluation. In place of the Mach number, a machine specific Mach number will be defined as the ratio of the tip speed of the impeller, u_2, to the inlet speed of sound, c_1, of the working fluid as follows:

$$M_m = \frac{u_2}{c_1}$$ (2.92)

This is a reference Mach number suitable for evaluation of compressor consistency between model conditions. The name could be suitably termed tip speed Mach number. The importance lies in the dependency of compressor head and pressure ratio on the impeller tip speed, i.e. the Mach number *(Lüdtke, 2004)*. Rearranging Equation (2.27) to define the pressure ratio in terms of the head coefficient and machine Mach number defines the following important relation:

$$\frac{p_2}{p_1} = \left[\psi_{s,c} \, M_m^{\,2} (\kappa - 1) + 1 \right]^{\left(\frac{\kappa}{\kappa - 1} \right)}$$ (2.93)

The importance of this equation is the head coefficient is a function of the tip speed, and the pressure ratio is a function of the Mach number. This defines the importance of the machine Mach number in the correction procedure and the establishment of speed limits. Following the guidance of PTC10 requires the difference in machine Mach number between test and specified conditions, $\left(M_{m.t} - M_{m.sp}\right)$ to be within the boundaries plotted in Figure 2.13 to ensure a suitable comparison between conditions.
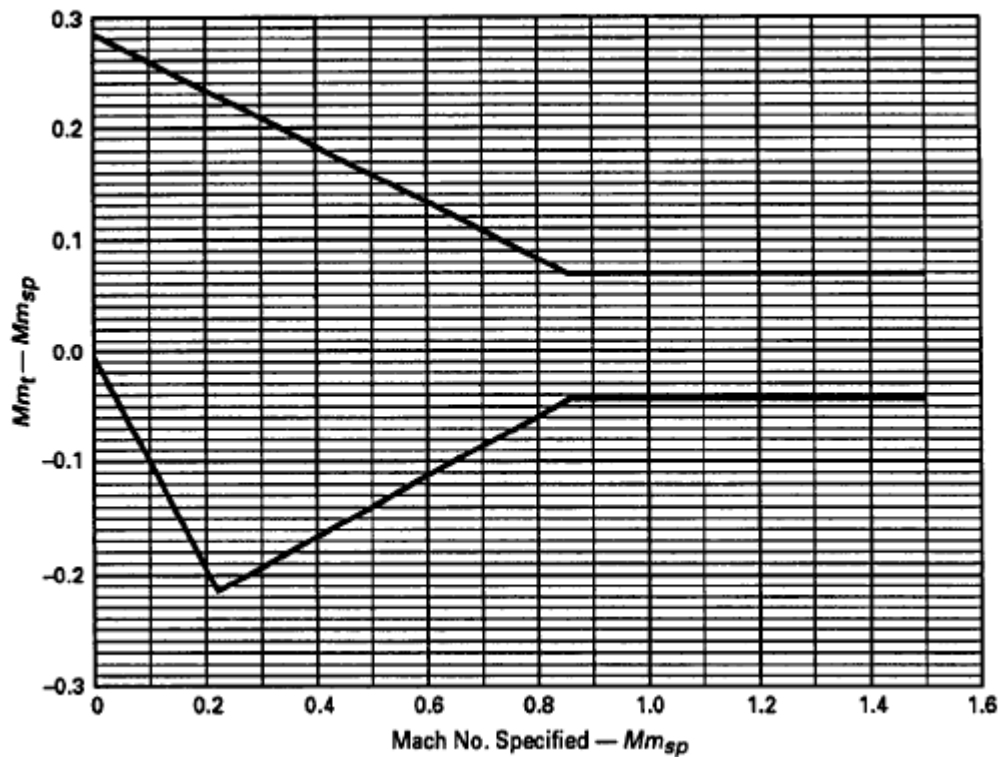
Figure 2.13: Allowable Machine Mach Number Departure *(ASME PTC10-Fig.3.3)*

2.9.6 Machine Reynolds Number

As with the machine Mach number, the Reynolds number is modified to suit the dynamics of the compressor to represent the fluid friction in the flow passages of the compressor diffuser section *(Lüdtke, 2004)*. From the dimensionless groups defined in Equation (2.76), the Reynolds number is modified to accommodate blade height of the impeller at the exit (b_2) to the diffuser, viscosity in terms of the inlet condition, and velocity in terms of the tip speed of the impeller. This defines the machine Reynolds number as:

$$Re_m = \frac{\rho_1 u_2 b_2}{\mu_1} \qquad (2.94)$$

Following the guidance of PTC10 requires adherence within the boundaries plotted in Figure 2.14 to ensure a suitable comparison between test and specified conditions. This also ensures the machine Reynolds number between test and specified conditions is within a suitable range for correcting efficiency and the head coefficient.

GENERAL NOTE: 90,000 is cutoff

Figure 2.14: Allowable Machine Reynolds Number Departure *(ASME PTC10-Fig.3.5)*
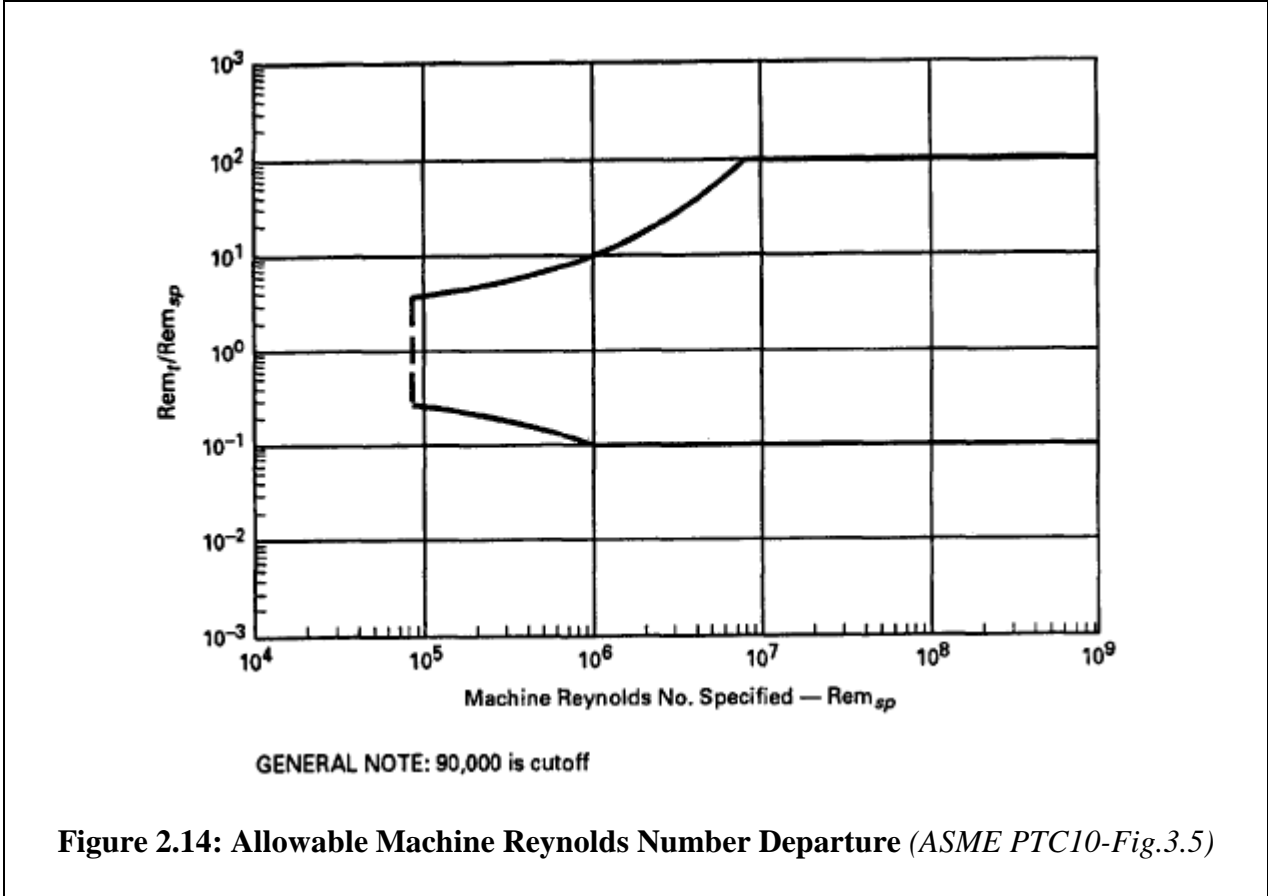
2.9.7 Reynolds Number Correction for Centrifugal Compressors

The two notable variables of the machine Reynolds number are tip speed and kinematic viscosity

($\upsilon = \mu / \rho$), or the absolute viscosity and density. The tip speed must be within the bounds of the

machine Mach number limits (Figure 2.13). It is not feasible or cost effective to maintain the

machine Reynolds number during performance testing *(Simon, 1983)*. Wiesner *(1979)*

established a method for correcting for the effects of Reynolds number on the head and flow

coefficients, and efficiency. This method has been simplified for use in PTC10 and corrects the

head coefficient and efficiency only, as detailed in Equations (2.95 thru 2.101) [PTC10-Eq's.

5.6.1-5.6.5]:

$$RC = \frac{0.988}{Re_m^{\,0.243}} \tag{2.95}$$

$$RA = 0.066 + 0.934 \left[\frac{\upsilon_{sp} b_2}{Re_m} \right]^{RC} \tag{2.96}$$

where:
$$\upsilon_{sp} = 4.80 \cdot 10^6 \, \frac{\text{ft}^2}{\text{sec}} \tag{2.97}$$

$$RB = \frac{\log\left(\varepsilon_{sp} + \dfrac{13.67}{Re_m} \right)}{\log\left(\varepsilon_{te} + \dfrac{13.67}{Re_m} \right)} \tag{2.98}$$

where:
$$\varepsilon_{sp} = 0.000125 \, \text{in} \tag{2.99}$$

When the Reynolds number ratio, $Re_{m,te} / Re_{m,sp}$, is within the bounds of Figure 2.14, the efficiency and head coefficient can be corrected for the effects of Reynolds number on the working fluid. The polytropic efficiency correction is as follows:

$$\eta_{p,sp} = 1 + \left(\eta_{p,te} - 1 \right) \left(\frac{RA_{sp}}{RA_{te}} \right) \left(\frac{RB_{sp}}{RB_{te}} \right) \tag{2.100}$$

The Reynolds number correction coefficient, $Re_{m,corr}$, then defines the correction to the polytropic head coefficient as:

$$Re_{m,corr} = \frac{\eta_{p,sp}}{\eta_{p,te}} = \frac{\psi_{p,sp}}{\psi_{p,te}} \tag{2.101}$$

This correction applies to either polytropic or isentropic efficiency, and polytropic or isentropic head with the corresponding substitution in Equations (2.100) and (2.101).

Although there are a number of additional works from numerous authors in this area, it is beyond the scope of this work to detail each of the Reynolds number correction methods available for use today. Interestingly most works in this area root from the Colebrook equation as the basis of theory and derivation, therefore they agree in principle and not in the finer details of the application *(Wiesner, 1979)*. Interestingly the Reynolds number correction model for ISO 5389 utilizes a method developed by Strub et al. *(1987)*. Therefore, the Reynolds number correction methods in the widely referenced compressor performance test codes in the United States and Europe (PTC10 and ISO 5389, respectively) vary significantly requiring a thorough review of the open literature, and suitable evaluation of either method prior to use.

2.9.8 Density Ratio

The density ratio between inlet and outlet conditions enables a comparison of compression between the test and specified gases. PTC10 establishes that the normalized density ratio of test to specified conditions equals one, with a tolerance of ±4%. The following equation details the calculation of the specific volume ratio and density ratio for test and specified conditions [PTC10-Eq. 5.5.5]:

$$r_v = \frac{\left(\dfrac{v_i}{v_d}\right)_{sp}}{\left(\dfrac{v_i}{v_d}\right)_t} = \frac{\left(\dfrac{\rho_d}{v_i}\right)_{sp}}{\left(\dfrac{\rho_d}{v_i}\right)_t} \tag{2.102}$$

$$\text{Tolerance}: 96\% \leq r_v \leq 104\%$$

2.10 Concluding Remarks

The above literature review leads to the following observations:

- Matching the specified condition of the turbocharger is imperative to verify the design before installation. The importance of this is to verify the compressor and turbine efficiency which can have a significant effect on fuel consumption due to their coupling to exhaust gas backpressure and air delivery to the intake manifold.

- A suitable testing apparatus to accurately detail the information required to define performance of the turbomachine will utilize significant live computations at time of test. The calculations to detail the operation must be performed at time of test to ensure an accurate verification process.

- The required thermodynamic conditions of the inlet air are defined by the temperature, pressure, and molecular weight detailed through the relative humidity.

- The polytropic and isentropic compression processes are comparable and differ by a compression exponent representing a machine explicit or gas explicit exponent. The use of the polytropic equations may significantly limit the use of dimensional analysis because the specific inlet and outlet gas conditions are collapsed in the compressible work data. Re-expanding this data into pressure conditions requires the specific polytropic exponent of an operating point. However, collapsed isentropic head can be re-expanded easily to nearly any condition in the compressor map because the isentropic exponent is defined by the gas mixture of interest.

- The use of dimensional analysis provides a method of collapsing and re-expanding collected data to any condition required for evaluation. This method could be applied at time of test to verify that all data for a given turbocharger follows a dimensionless characteristic curve or signature providing a method of quality assurance at time of test. This method may detail any operating point in the compressor map.

- The effects of the speed variable may be significantly reduced in the Mach and Reynolds number analysis by testing at the required speed to demonstrate the required head. There appears to be a significant variation that could be applied to a corrected data set given the limits of the PTC10 models when the test and specified gas is the same, as in the use of air for this study.

CHAPTER 3: Test Apparatus

Operating a turbocharger for a large-bore engine offsite requires a specific infrastructure to supply the required power to the turbocharger for mechanical testing and collecting accurate data of the performance envelope. With the command of often times certifying performance prior to field installation, the importance of this task is great. A test cell was designed at the National Gas Machinery Lab (NGML) of Kansas State University for this specific reason.

3.1 Test Cell Design Requirements

There are a number of systems required to support a turbocharger under test and collect accurate data. The following list details the systems required:

- Carefully designed piping system and mass flow measuring devices.

- Properly installed and calibrated instrumentation and data collection system.

- Reliable control systems for generating turbine exhaust gas and controlling compressor discharge pressure.

- Auxiliary systems for heat rejection and bearing lubrication.

- Heavy duty support system for turbocharger under test, and collecting robust vibration data.

ASME has developed several Performance Test Codes (PTC's) to define best practices for design configuration and measuring instrumentation to maximize accuracy for performance measurements of compressors and exhausters. The design of the test cell utilized the following ASME guidelines to detail the configuration and provide guidance:

- PTC10 on Compressor and Exhausters

- PTC19.5 on Fluid Meters and Flow Measurement

3.2 Exhaust Gas Power System

This section discusses important details of the design as it pertains to the turbocharger testing required herein. The test cell was designed to deliver a variable flow rate of 3 lb/sec to 30 lb/sec of compressed air at up to 36 inHgG at 1,000°F exhaust gas temperature to the turbine inlet of a turbocharger. This provides the power necessary to completely performance map a compressor and turbine of turbochargers with moderately high turbine inlet pressures. Figure 3.1 details the system layout of the designed test cell.

A gas turbine engine driving an axial compressor provides the pressurized air stream for the exhaust gas to the turbocharger turbine. The axial compressor was a modified compressor core section of an Allison T56 (501D) gas turbine engine. The combustion and turbine section of the engine were replaced with an aft bearing and discharge air collector as the rear housing. A coupled 2,400 HP gas turbine engine (GE-T64B) provided the shaft power for the axial compressor.

The air leaving the compressor discharge collector enters a piping section to measure the mass air supply to the turbocharger turbine inlet. An inline combustion burner utilizing natural gas heated the compressed air from the axial compressor to a maximum of 1,000°F, establishing the independent exhaust gas stream of the test cell. The fuel mass flow rate was measured with an orifice run to obtain the air fuel ratio and the resulting specific heat and ratio of specific heats for turbocharger turbine calculations.
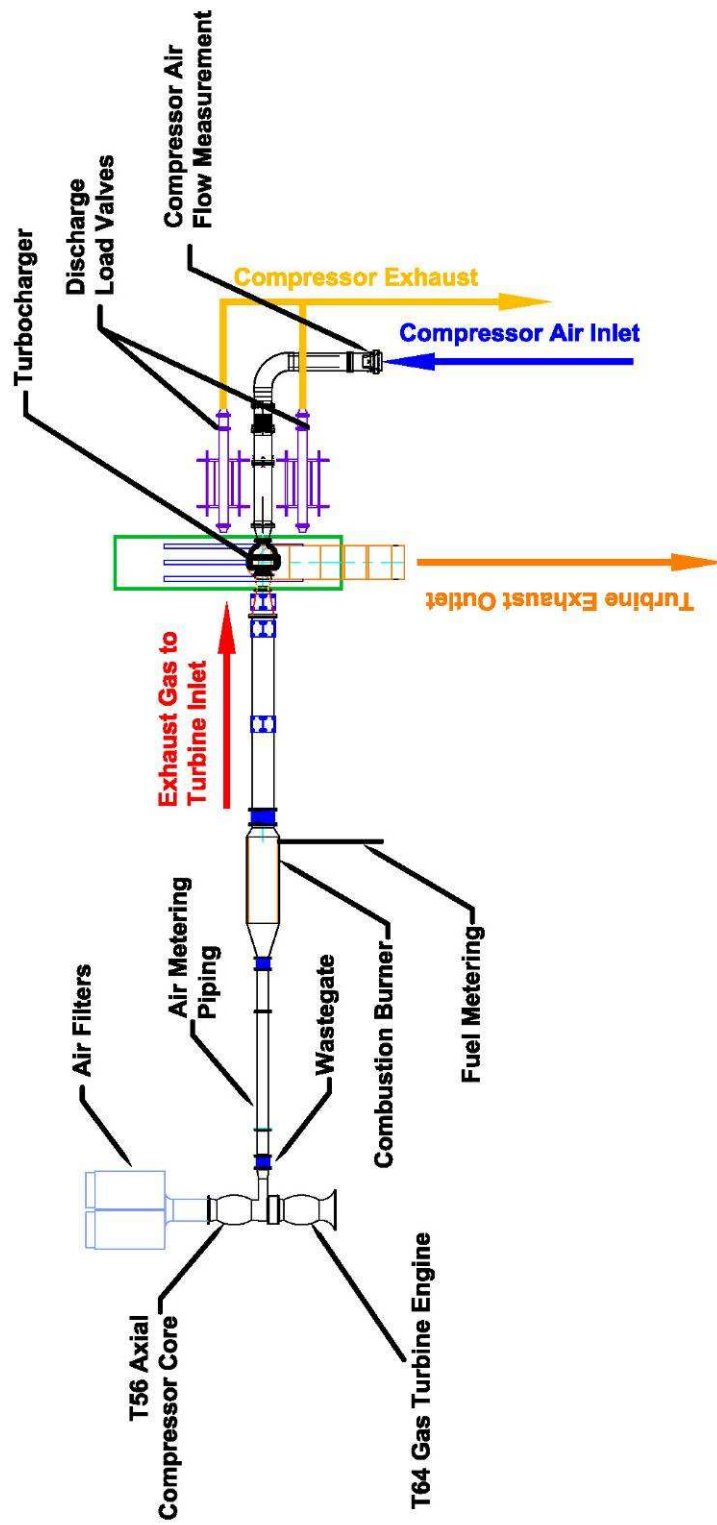
Figure 3.1: Turbocharger Test Cell Layout

3.3 Compressor Air System

The airflow drawn into the turbocharger was measured with a high accuracy ASME long radius flow nozzle. An ambient measuring station details the local weather conditions of the testing center. Instrumentation in the piping preceding the compressor inlet measures the temperature, pressure, and airflow to the compressor. To control the compressor pressure rise, two discharge headers are fitted with precision valves to simulate the restriction an engine would provide. The discharge headers are instrumented to measure the pressure and temperature rise of the compressor discharge air.

3.4 Instrumentation and Performance Data

Instrument and measurement accuracy is important for determining machine performance. Per the guidance of PTC10 to ensure the condition of the compressible gas is accurately measured, temperature and pressure are measured for the turbine and compressor inlet and outlet flow streams with four instruments for each location. This is detailed in the process and instrumentation diagram (P&ID) of Figure 3.2. There is one exception to this statement, due to piping diameter considerations there are only two pressure transmitters installed in each of the discharge headers preceding load valve 1 and 2 as detailed in the P&ID.

The compressor discharge and turbine inlet headers were fitted with insulation to minimize heat loss to the surroundings, and maintain accuracy of the high-temperature measurements. All instruments are connected to a programmable logic controller (PLC) to continually monitor the turbocharger under test. In addition to monitoring temperatures and pressures of the turbine and compressor conditions, the PLC monitors bearing and jacket water conditions for stability and safety.
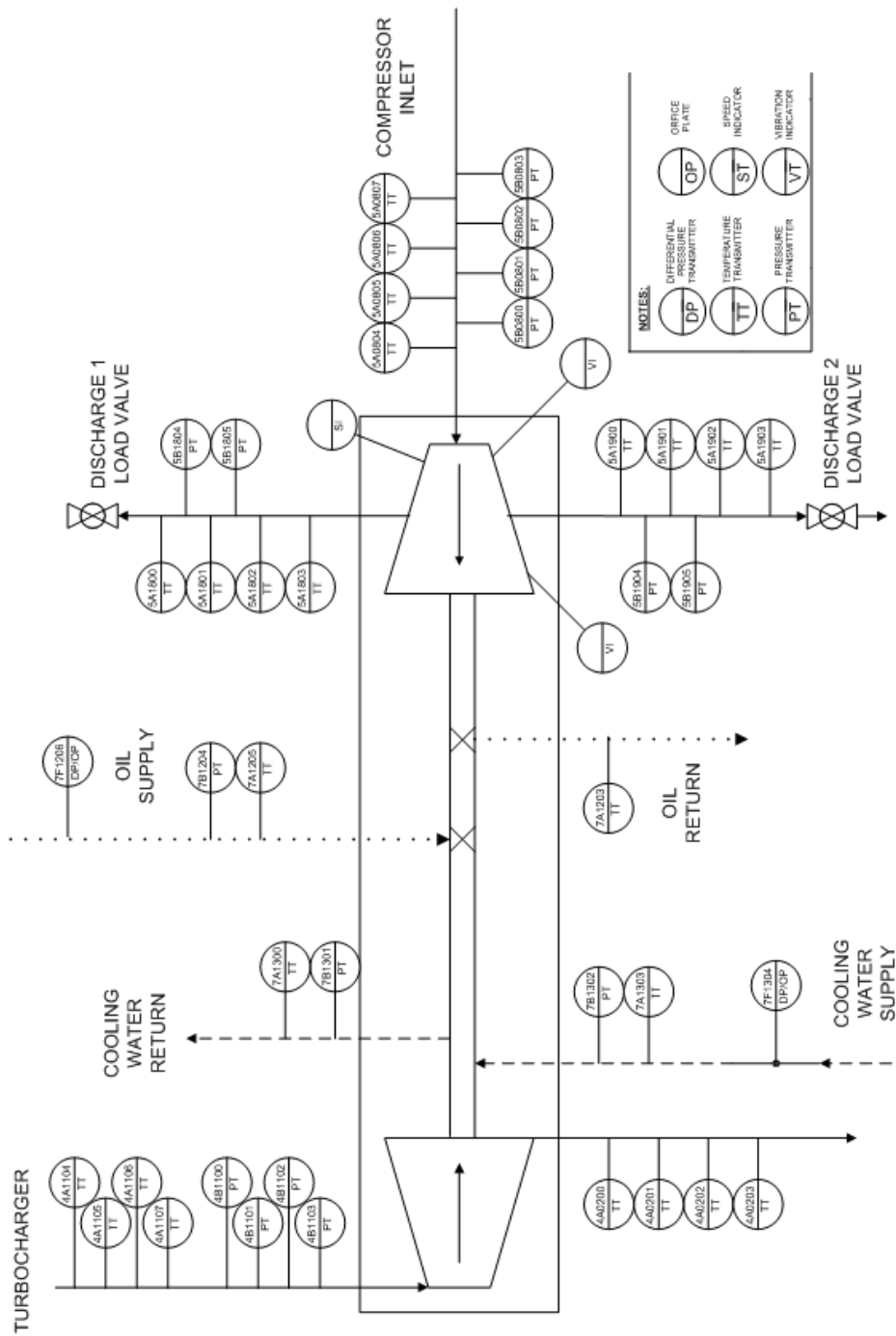
Figure 3.2: Turbocharger Test Cell Process and Instrumentation Diagram

3.5 Performance Measurement Data

The complete performance profile of a turbocharger is determined from temperature and pressure instruments, and the related thermodynamic and fluid mechanic properties. A PLC is programmed to compute flow and performance calculations of the operating turbocharger and record the performance data for test reporting. In accordance with the Test Standard for Testing Large-Bore Engine Turbochargers *(Chapman et al. 2005),* Table 3.1 details the measurements required to quantify turbocharger performance. This is also a table form of the P&ID detailed in Figure 3.2.

Table 3.1: Test Cell Turbocharger Performance Data

No.	Description	No.	Description
1	Barometric Pressure	8	Turbine Inlet Pressure
2	Ambient Temperature	9	Turbine Inlet Temperature
3	Relative Humidity	10	Turbine Discharge Pressure
4	Turbo RPM	11	Turbine Discharge Temperature
5	Compressor Inlet Pressure	12	Turbine Mass Flow Rate (fuel + air)
6	Compressor Inlet Temperature	13	Cooling Water Pressure & Temperature
7	Compressor Dis. Pressure	14	Cooling Water Flow Rate
8	Compressor Dis. Temperature	15	Lube Oil Pressure & Temperature
9	Compressor Mass Flow Rate	16	Lube Oil Flow Rate

CHAPTER 4: Turbocharger Specification

4.1 Specified Engine Design Point

As discussed in Section 2.1.3, the turbocharger is designed to provide airflow to the engine for exhaust gas scavenging, and to balance the air and exhaust manifold pressures necessary to achieve the specific trapped mass and deliver the required airflow per the site condition. This defines the turbocharger design specification, termed the design point. The design point details the site ambient conditions and inlet air condition to define: density, viscosity, isobaric specific heat, specific gas constant and the ratio of specific heats. This also details the mass flow and discharge pressure from the compressor to meet the required engine airflow and manifold pressure at the design point. The specified condition herein refers to the design point. This details the gas condition to the compressor inlet utilized for generating the compressor map(s) at specified conditions. The design point of the compressor of the turbocharger tested is detailed in Table 4.1.

Table 4.1: Turbocharger Design Point Condition

Measurement	Specified Condition
Inlet Temperature [°F]	59.0
Barometric Pressure [psia]	14.70
Relative Humidity [%]	0
Compressor Mass Flow [lb/sec]	12.680
Discharge Pressure [psia]	25.18

4.2 Compressor Design Point

As discussed in Section 2.3, site density controls the amount of delivered mass flow of the intake volume flow to the compressor. The design point of Table 4.1 must be converted from mass flow to inlet volumetric flow via the conservation of mass (Equation 2.2) to define the design point in terms of the compressor operation.

The ambient condition of the test center will not likely equal the ambient condition as defined in the specification. To develop the required infrastructure to preheat or cool the inlet airflow to the turbocharger to meet site conditions is cost prohibitive. Because the centrifugal compressor is a compressible work (head) machine, the site head required for the design point is calculated through the compressible work Equation (2.27). The head equation includes the site temperature, specific gas constant, and ratio of specific heats, repeated here for reference:

$$Head_{isentropic} = \mu_{s,c} = \frac{\dot{W}_{cv}}{\dot{m}} = \left(\frac{\kappa}{\kappa - 1} \right) R_g T_1 \left[\left(\frac{p_2}{p_1} \right)^{\frac{\kappa - 1}{\kappa}} - 1 \right] \tag{2.27}$$

With the specified gas condition defined in Table 4.1, the required compressible work is equated via the isentropic definition to utilize the ratio of specific heats exponent for the gas mixture, κ. The polytropic exponent of Equation (2.8) is defined by the inlet and outlet pressure and temperatures of the compressor. In a testing environment where the compressor performance is to be defined and the efficiency is yet unknown, the polytropic head cannot be calculated accurately prior to testing to define the design point. The results of the calculations to define the design point and the reference equation numbers herein detailing the specified condition are listed in Table 4.2.

Table 4.2: Compressor Design Point Calculation for Test

Description	Variable	Value	Eq. No.
Saturated Vapor Pressure [psia]	p_{sat}	0.2471	(2.50)
Relative Vapor Pressure [psia]	p_{vapor}	0	(2.45)
Mole Fraction	y_v	0%	(2.44)
Molecular Weight	MW_{mix}	28.97	(2.46)
Specific Gas Constant [ft·lbf/lbm·R]	R_g	53.34	(2.43)
Isobaric Specific Heat [ft·lbf/lbm·R]	$c_{p,mix}$	186.523	(2.52)
Ratio of Specific Heats	κ	1.401	(2.53)
Density [lb/ft³]	ρ_{inlet}	0.07651	(2.11)
Isentropic Discharge Temperature [°F]	T_2	145.38	(2.26)
Reduced Pressure [-]	p_r	0.05	(2.60)
Reduced Temperature [-]	T_r	2.25	(2.61)
Compressibility [-]	Z	1.0	(Figure 2.12)
Inlet Volume Flow [ft³/min]*	$\dot{V}$	9,944	(2.2)
Isentropic Head [ft·lbf/lbm]*	$\mu_{s,c}$	16,098	(2.27)
* Design point verification inlet volume flow and isentropic head			

4.3 Turbocharger Build Data

There are key dimensions of the turbocharger required to define the flow and head coefficients (Equations 2.79 and 2.84). To correct the performance data from test to specified conditions requires an evaluation of the machine Mach and Reynolds numbers (Equations 2.92 and 2.94). There are two physical characteristics for the performance and correction procedure; the impeller exit blade height, b_2, and the impeller tip diameter, D_2, to define the impeller tip speed u_2. Table 4.3 details the characteristic data required of the turbocharger for the correction method.

Table 4.3: Turbocharger Build Information

Symbol	Description	Value
b_2	Impeller Exit Blade Height	1.079 in
D_2	Impeller Diameter at Outlet Tip	1.500 ft

CHAPTER 5: Test Cell Data

5.1 Compressor Test Data

The turbocharger was tested and performance mapped in the test center. The compressor was tested at three operating speeds to collect the raw performance data detailed in Table 5.1 and Table 5.2. The performance map is established by operating the turbocharger at a set operating speed, controlled by balancing turbine power to compressor flow. Discharge load valves control the discharge pressure to establish compressible work (see Figure 3.1). At least four operating points are collected along a controlled turbocharger speed line for each speed curve. Table 3.1 in Section 3.5 details the data collected for each operating point.

Table 5.1: Test Cell Data (1 of 2)

Test Point Number	Point 1	Point 2	Point 3	Point 4	Point 5	Point 6	Point 7
Ambient Press (psia)	14.4	14.41	14.4	14.4	14.39	14.38	14.38
Ambient Temp (F)	59.33	57.38	58.01	58.28	61.29	63.73	64.58
Relative Humidity (%)	99.88	99.98	99.99	99.97	97.51	93.27	86.72
Turbocharger Speed (RPM)	8043	8007	8068	8040	9900	9901	9974
Compressor Inlet Press (psia)	14.03	14.07	14.08	14.1	13.93	13.94	13.96
Compressor Inlet Temp (F)	57.65	55.83	56.36	56.88	58.83	60.7	60.87
Compressor Outlet Prss-2 (psig)	3.77	3.92	4.13	4.26	6	6.23	6.55
Compressor Outlet Temp-2 (F)	107.58	107.55	108.22	110.62	133.48	136.79	139.17
Turbine Inlet Press (psig)	3.36	3.16	3.02	2.73	5.26	5	4.8
Turbine Inlet Temp (F)	761.08	819.34	914.46	1058.12	762.43	834.37	917.43
Turbine Outlet Press (psig)	-1.49	-1.49	-1.49	-1.49	-1.49	-1.49	-1.49
Turbine Outlet Temp (F)	643.08	703.61	790.38	915.78	637.59	703.23	777.14
Lube Oil Inlet Press (psig)	14.22	14.7	14.86	14.47	17.62	17.64	19.19
Lube Oil Inlet Temp (F)	148.8	146.87	144.05	148.02	148.1	146.66	147.58
Lube Oil Oulet Temp (F)	148.07	146.08	144.22	148.91	149.59	148.65	150.13
Water Inlet Press (psig)	32.28	32.4	32.52	32.72	32.36	32.35	32.42
Water Inlet Temp (F)	148.13	151.32	152.66	154.77	152.32	152.16	153.37
Water Outlet Press (psig)	29.19	29.2	29.33	29.6	29.29	29.33	29.48
Water Outlet Temp (F)	156.99	160.83	163.78	168.47	162.5	163.61	166.55
Compressor Airflow (lb/sec)	7.494	6.995	6.745	5.954	9.603	8.976	8.662
Lube Oil (lb/sec)	0.26	0.26	0.26	0.27	0.3	0.29	0.32
Cooling Water (lb/sec)	8.23	8.28	8.22	8.25	8.19	8.26	8.26
Compressor Flow (ACFM)	6082	5645	5448	4810	7830	7338	7081
Turbine Flow (ACFM)	0	0	0	0	0	0	0
Methane Flow (ACFM)	28	32	35	39	36	40	43
Lube Oil (GPM)	2.14	2.19	2.15	2.25	2.48	2.42	2.67
Cooling Water (GPM)	60.42	60.79	60.38	60.61	60.14	60.65	60.7
Pressure Ratio	1.295	1.303	1.316	1.323	1.464	1.478	1.499
Diff. Pressure (inHg)	0.83	1.55	2.26	3.12	1.51	2.5	3.56

Table 5.2: Test Cell Data (2 of 2)

Test Point Number	Point 8	Point 9	Point 10	Point 11	Point 12	Point 13	Point 14
Ambient Press (psia)	14.37	14.35	14.35	14.35	14.34	14.34	14.35
Ambient Temp (F)	64.44	67.54	67.67	67.58	69.67	70.68	71.79
Relative Humidity (%)	90.14	89.78	87.95	88.25	84.52	79.36	71.23
Turbocharger Speed (RPM)	9888	11852	11982	12017	11915	12026	12138
Compressor Inlet Press (psia)	13.99	13.73	13.74	13.73	13.76	13.79	13.83
Compressor Inlet Temp (F)	61.55	64.63	64.79	64.75	66.34	66.95	67.26
Compressor Outlet Prss-2 (psig)	6.61	8.84	9.03	9.08	9.22	9.72	10.24
Compressor Outlet Temp-2 (F)	139.97	171.01	173.92	175.01	176.32	179.82	183.78
Turbine Inlet Press (psig)	4.42	7.73	7.92	7.98	7.58	7.43	7.21
Turbine Inlet Temp (F)	1024.24	806.15	813.23	815.18	864.05	920.93	1003.36
Turbine Outlet Press (psig)	-1.49	-1.49	-1.49	-1.49	-1.49	-1.49	-1.49
Turbine Outlet Temp (F)	871.21	657.77	661.04	661.78	705.21	755.53	828.27
Lube Oil Inlet Press (psig)	18.79	25.34	24.89	24.85	25.19	25.31	25.12
Lube Oil Inlet Temp (F)	150.2	145.68	149.25	146.83	151.85	147.6	147.66
Lube Oil Oulet Temp (F)	152.54	150.48	153.49	151.61	157.6	154.26	154.94
Water Inlet Press (psig)	32.4	32.15	31.99	31.91	31.87	31.87	31.97
Water Inlet Temp (F)	154.85	152.68	153.21	153.56	153.28	154.63	155.4
Water Outlet Press (psig)	29.75	29.25	29.32	29.58	29.93	30.16	30.74
Water Outlet Temp (F)	169.83	165.08	166.31	166.48	167.33	169.75	172.26
Compressor Airflow (lb/sec)	7.91	11.692	11.808	11.912	11.287	10.921	10.578
Lube Oil (lb/sec)	0.33	0.38	0.39	0.39	0.41	0.4	0.41
Cooling Water (lb/sec)	8.23	8.22	8.19	8.19	8.16	8.22	8.25
Compressor Flow (ACFM)	6472	9690	9783	9859	9370	9072	8777
Turbine Flow (ACFM)	0	0	0	0	0	0	0
Methane Flow (ACFM)	47	49	49	48	50	54	58
Lube Oil (GPM)	2.74	3.16	3.24	3.22	3.47	3.37	3.39
Cooling Water (GPM)	60.46	60.38	60.15	60.16	59.93	60.43	60.6
Pressure Ratio	1.5	1.689	1.702	1.706	1.712	1.745	1.778
Diff. Pressure (inHg)	4.46	2.26	2.26	2.24	3.34	4.66	6.17

5.2 Base Compressor Performance Map

This data is plotted as the raw performance map in Figure 5.1, and includes the turbocharger design point. This plot presents the static polytropic head versus inlet volume flow as a starting point to detail the correction method. The tested nominal speeds detailed in Figure 5.1 are: 8,000 RPM, 9,900 RPM and 12,000 RPM. The actual operating speeds during testing varied within 1% of the nominal values. The following sections detail the method of correcting the test data to the specified condition.

Figure 5.1: Compressor Map Prior to Correction
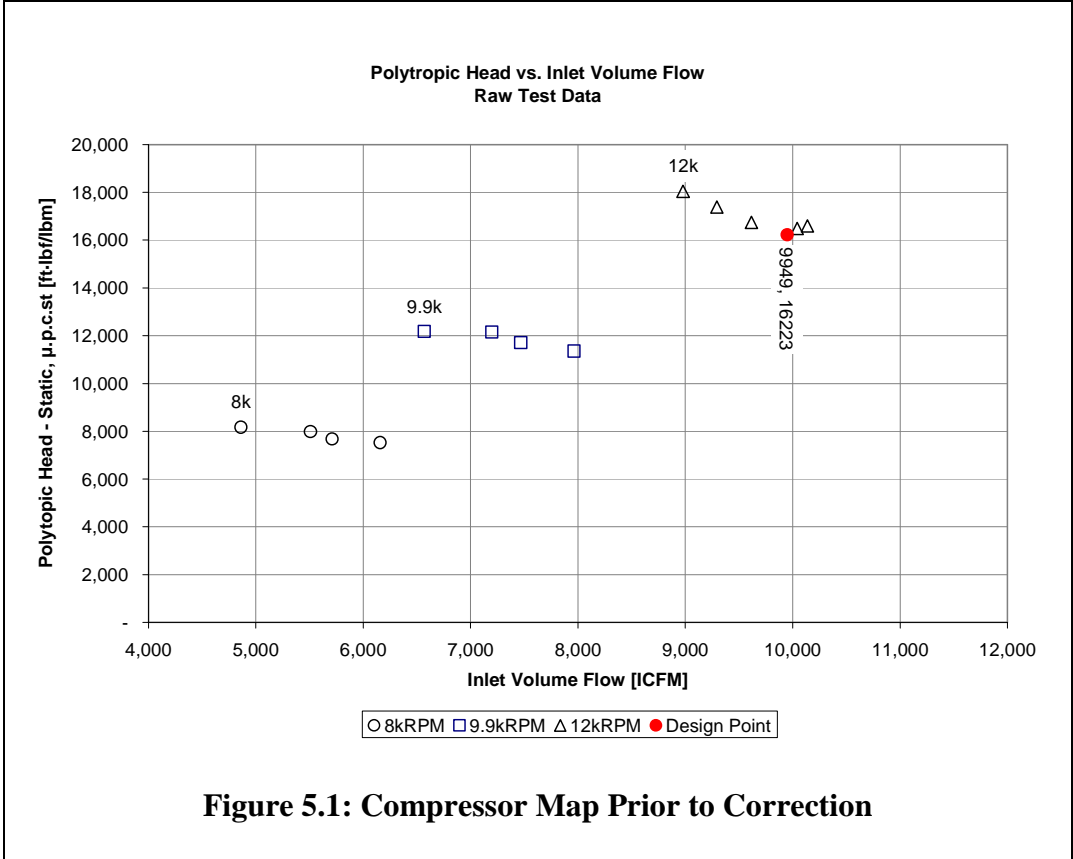
5.3 Compressor Discharge Piping Elbow Losses

Due to space considerations of the test stand configuration, there are piping elbows between the compressor outlet flange and the discharge pressure measuring station preceding the discharge load valve (see Figure 5.2). The pressure ratio (PR) defined in Equation (2.34) accounts for intake and discharge piping losses. A differential pressure transmitter is not installed in the test cell to measure losses through the elbows. To account for this pressure loss for the pressure ratio (PR in Figure 5.2), the Darcy Equation (2.42) is utilized. In the test cell, the compressor inlet piping does not change direction between the compressor inlet pressure measuring station and the compressor inlet, thus inlet losses for Equation (2.34) are negligible.
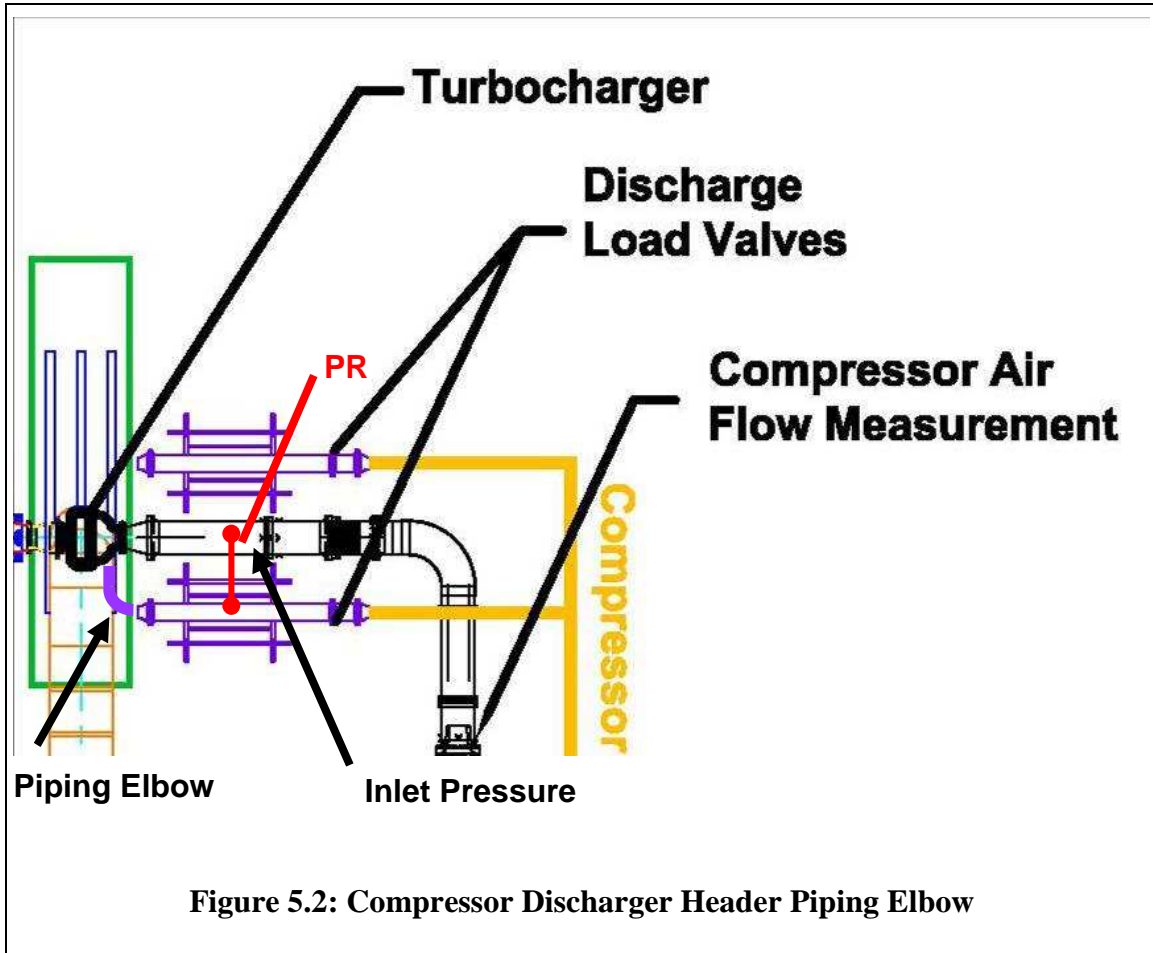
Figure 5.2: Compressor Discharger Header Piping Elbow

The Reynolds number is calculated from Equation (2.37) for the airflow through the compressor discharge header and outlet viscosity defined by the outlet temperature and Equation (2.55). Utilizing the Churchill Equation (2.41) the friction factor in the piping is calculated for the Darcy equation and pressure drop through the connection. Additionally the Darcy equation uses the equivalent pipe length to define the loss through the elbow connection. The equivalent pipe length (L_e in Eq. 2.42) for the 12" elbows in Figure 5.2 is 9 ft for use in the pressure loss calculation *(Lindeburg, 2001).*

The resulting pressure losses through the elbow are plotted versus inlet volume flow in Figure 5.3. The elbow pressure losses are added to the pressure ratio Equation (2.34) as $p_{dis.losses}$, for calculating compressor work.
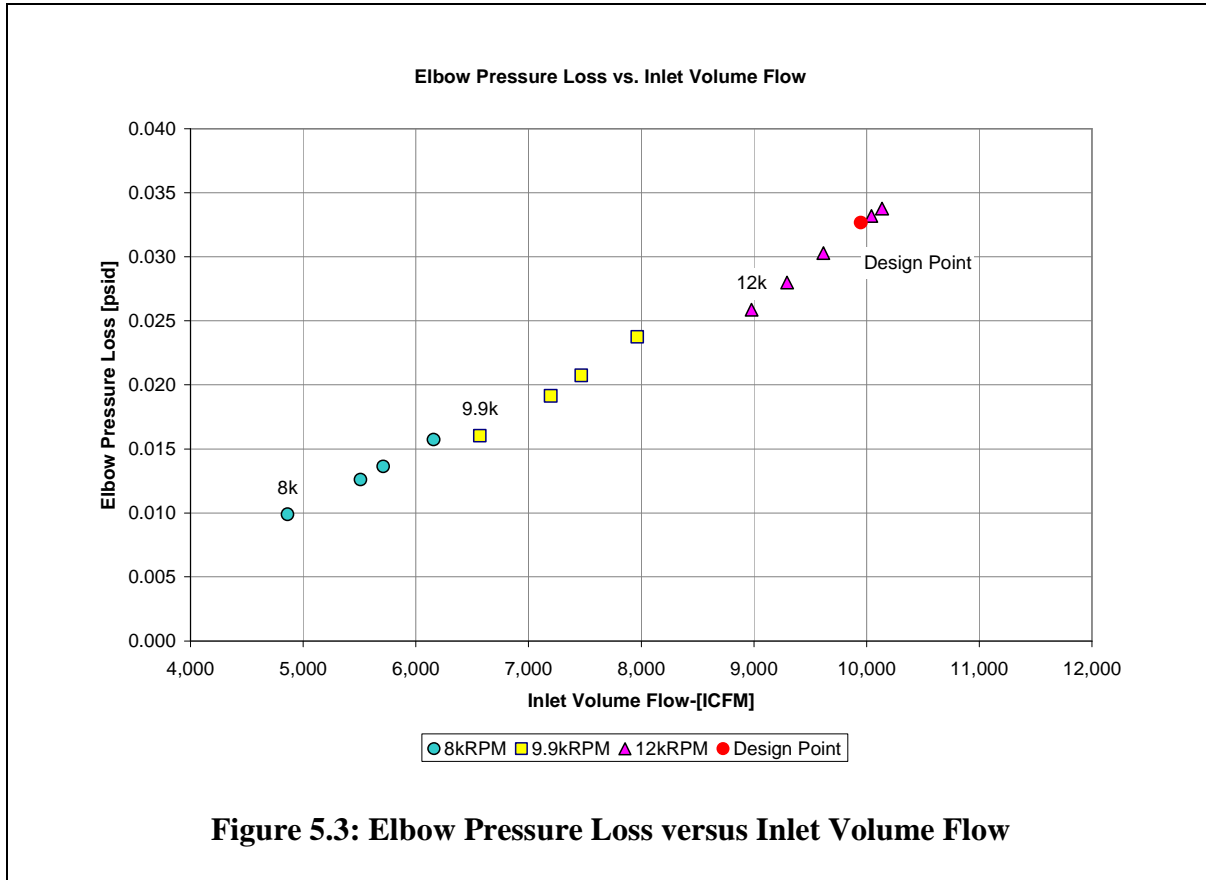

Figure 5.3: Elbow Pressure Loss versus Inlet Volume Flow

5.4 Total Tested Gas Condition

The pressure and temperature measurements collected during the test are static measurements. The total conditions for pressure and temperature are calculated from Equations (2.62) and (2.63) to include the dynamic condition of the fluid stream. The total pressure and temperature of the inlet and outlet, as well as the elbow losses of the discharge piping are included in the head and efficiency calculations. Figure 5.4 plots the total head and static head versus volume flow in the compressor map for comparison to evaluate the difference. The total head plotted for the

reference speeds is denoted as 8kRPM.t, 9.9kRPM.t, 12kRPM.t and Design Point.t, and includes

the elbow losses detailed in Figure 5.3. To determine the dynamic contribution to the polytropic

head, the difference in polytropic head between static and total conditions is calculated from

Equation (5.1) resulting in a maximum difference of 2.6% as detailed in the plot.

$$\text{Difference} = \frac{\mu_{p,c,total}}{\mu_{p,c,static}} - 1 \tag{5.1}$$
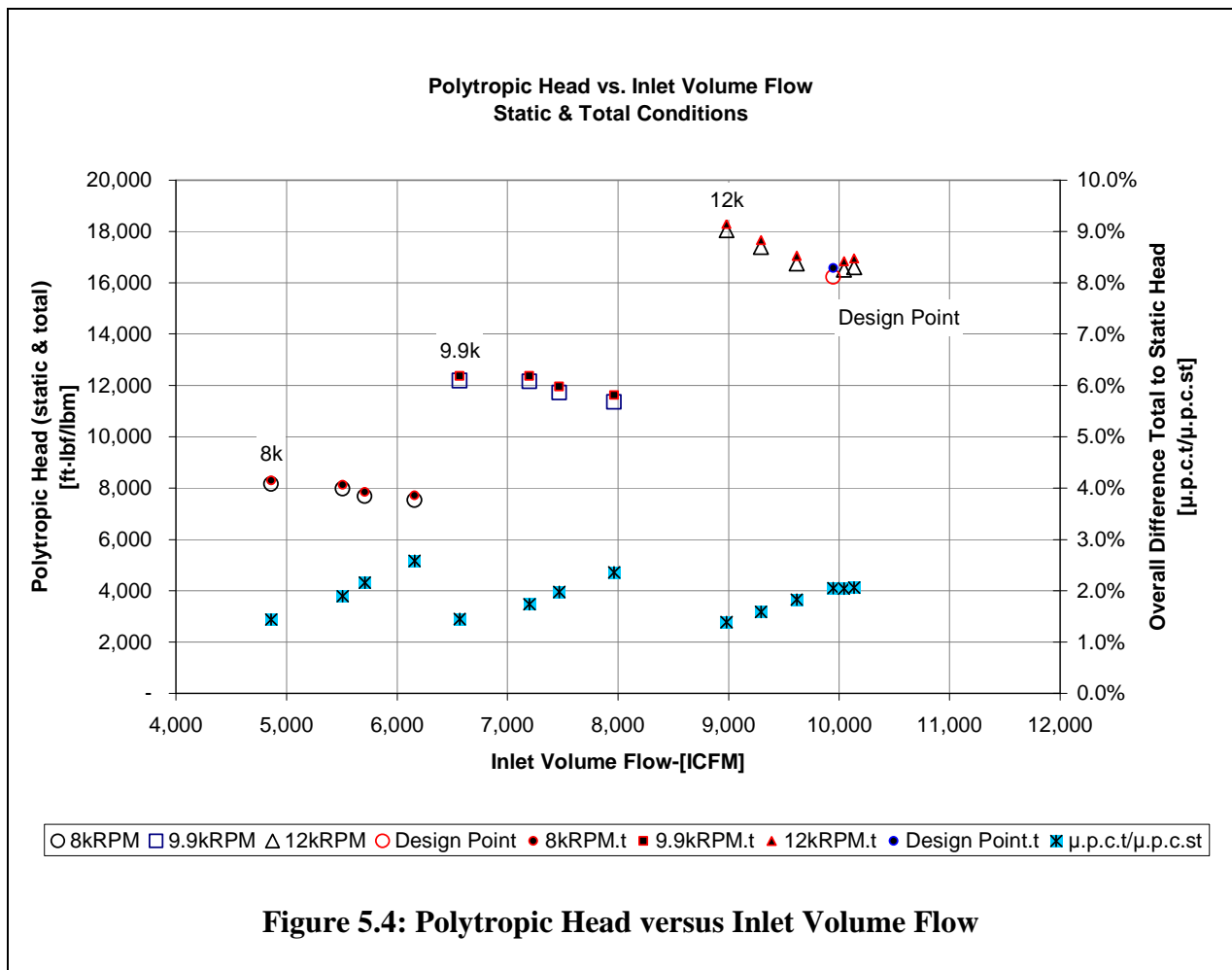

Figure 5.4: Polytropic Head versus Inlet Volume Flow

5.5 Dimensionless Coefficients

Using the equations for the flow and head coefficients, Equations (2.79 and 2.84), establishes a dimensionless compressor map (Figure 5.5). This dimensionless map is normalized total polytropic head and volume flow, with respect to speed, and the impeller diameter and geometry. The head coefficients for all tested operating speeds collapse to a single line, which represents the head and flow signature for this compressor.

The compressor polytropic efficiency is also plotted versus the flow coefficient. Efficiency is a function of the flow coefficient and the tip speed. The efficiency for the 8kRPM speed line is slightly below the efficiency of the remaining speeds of the tested turbo. Matching the flow and head coefficient between test and specified conditions to verify the specified operating point (Equation 2.78) ensures the operating efficiency of the compressor is established as expected to operate on engine at the specified condition. The highlighted region in Figure 5.5 details this match in the dimensionless compressor map. For the design point tested, the flow and head coefficients are: $\varphi=0.0396$, $\psi=0.616$; the complete list of dimensionless coefficients are detailed in Table 5.3.

Figure 5.5: Head Coefficient and Polytropic Efficiency versus Flow Coefficient
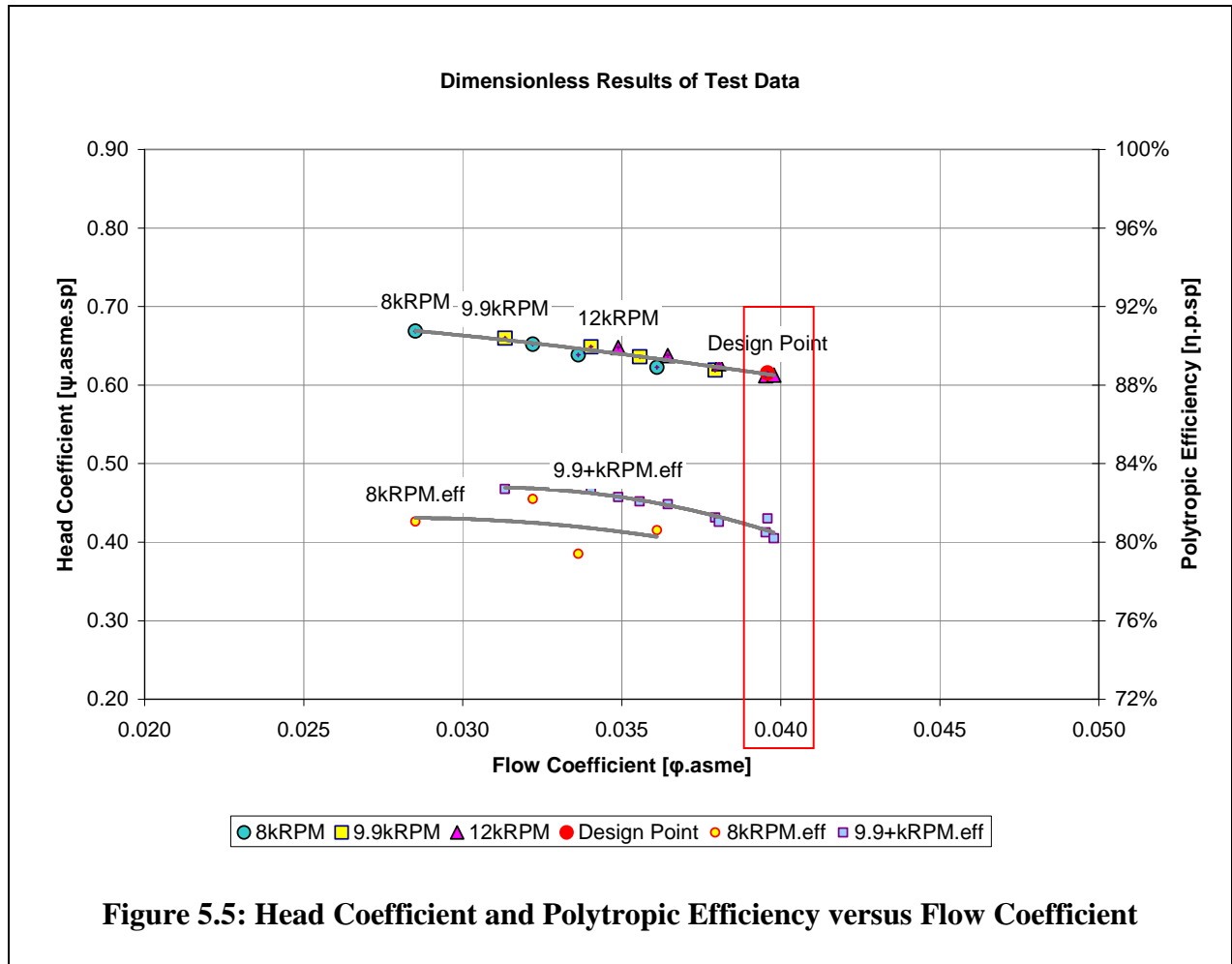
5.6 Corrected Compressor Map

The test data was corrected to the specified condition detailed in Table 4.1 with application of the Reynolds number correction method (Equations 2.95 thru 2.101). The resulting Reynolds number correction value, $Re_{m,corr}$, established a correction range of 0.0% to 0.1% for the test data head coefficient and polytropic efficiency. Therefore the Wiesner/PTC10 Reynolds number correction model has a low correction effect on the test cell collected head coefficient and polytropic efficiency for this turbocharger, between the test and specified condition.

By rearranging the flow and head coefficient of Equations (2.79) and (2.84), the inlet volume flow and polytropic head were calculated at the specified condition from Equations (5.2) and (5.3), normalized to 8,000 RPM, 9,900 RPM and 12,000 RPM. Table 5.3 provides a comparison of the test and corrected speed data. Figure 5.6 plots the corrected head versus volume flow compressor map.

$$\dot{V}_{sp} = 2\varphi_{sp}\, u_{2,sp} D_2^{\,2} \tag{5.2}$$

$$\mu_{p,sp} = \psi_{p,sp} u_{2,sp}^{\,2} \tag{5.3}$$

Table 5.3: Test Collected and Corrected Data

Condition			Test [min/max]			Specified		
Amb. Pressure	[psia]		13.844	14.10		14.70		
Amb. Temperature	[℉]		57.984	67.26		59.0		
Rel. Humidity	[%]		71.23	99.99		0		
	Flow Coefficient (te = sp)	Head Coefficient (sp)	Speed.te [RPM]	Volume Flow.te [ICFM]	Polytropic Head.te.t [ft·lbf/lbm]	Speed.sp [RPM]	Volume Flow.sp [ICFM]	Polytropic Head.sp.t [ft·lbf/lbm]
8kRPM	0.0361	0.623	8,043	6,158	7,719	8,000	6,125	7,640
8kRPM	0.0336	0.639	8,007	5,711	7,847	8,000	5,706	7,836
8kRPM	0.0322	0.652	8,068	5,509	8,137	8,000	5,463	8,002
8kRPM	0.0285	0.669	8,040	4,862	8,287	8,000	4,837	8,207
9kRPM	0.0379	0.619	9,900	7,965	11,628	9,900	7,965	11,633
9kRPM	0.0356	0.636	9,901	7,468	11,948	9,900	7,467	11,951
9kRPM	0.0340	0.649	9,974	7,198	12,368	9,900	7,145	12,190
9kRPM	0.0313	0.660	9,888	6,569	12,359	9,900	6,577	12,395
Des. Pt.	0.0396	0.616	11,852	9,949	16,565	11,846	9,944	16,561
12kRPM	0.0395	0.612	11,982	10,042	16,838	12,000	10,058	16,902
12kRPM	0.0398	0.613	12,017	10,137	16,946	12,000	10,123	16,912
12kRPM	0.0381	0.627	11,915	9,616	17,060	12,000	9,685	17,319
12kRPM	0.0364	0.638	12,026	9,294	17,673	12,000	9,274	17,609
12kRPM	0.0349	0.648	12,138	8,980	18,290	12,000	8,878	17,887

**Figure 5.6: Corrected Test Cell Compressor Map**
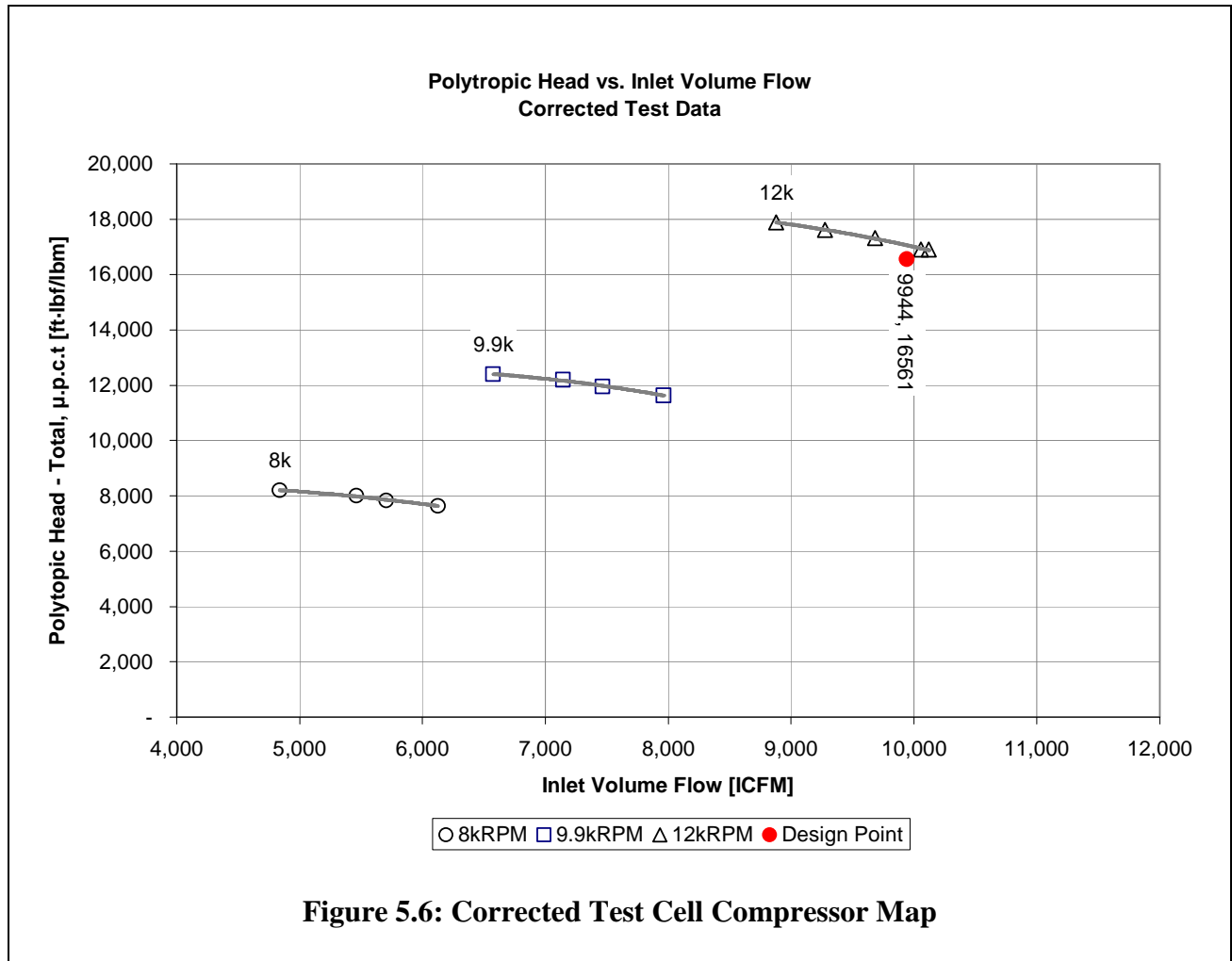
5.7 Test Cell Compressor Map at Specified Condition

The original turbocharger air specification detailed the design point in terms of mass flow and discharge pressure. The mass flow is calculated from the design point density in Table 4.2 and the normalized volume flow from Table 5.3 via the conservation of mass Equation (2.2). The discharge pressure is calculated by rearranging the polytropic head Equation (2.15) to define this in terms of pressure from the normalized and corrected polytropic head in Table 5.3 as follows:

$$p_{2,abs,t} = p_{1,abs} \left[\frac{\mu_{p,c,t}}{R_{sp} \cdot T_{inlet.sp}} \cdot \frac{\kappa_{sp} - 1}{\kappa_{sp} \eta_{p,c,t}} + 1 \right]^{\frac{\kappa_{sp} \eta_{p,c,t}}{\kappa_{sp} - 1}} \tag{5.4}$$

The resulting mass flow and discharge pressure forms the compressor map corrected to site conditions in Figure 5.7. This figure also details the design point from the tested conditions corrected to site conditions. For this turbocharger, the specified design point is 12.68 lb/sec at 25.18 psia. This turbocharger at site conditions will deliver the required mass flow with a slightly higher pressure of 25.31 psia considering total pressure conditions. Thus the turbocharger exceeds the required pressure for the design engine mass flow rate.

Figure 5.7: Compressor Map Corrected to Specified Conditions
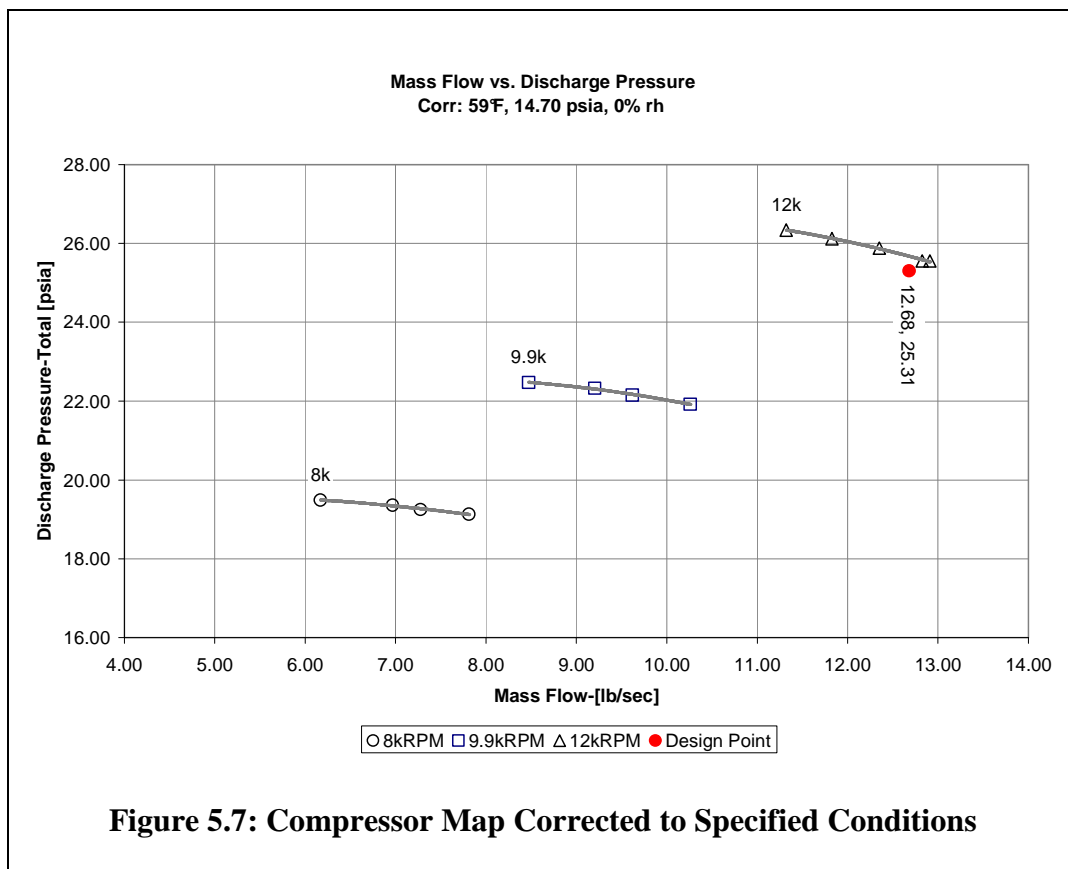
CHAPTER 6: Field Data

6.1 Field Installation

For the field installation, the turbocharger was instrumented to collect temperature and pressure of the inlet and outlet of the turbine and compressor while operating on engine following the recommendations presented in Section 2.5. Compressor mass flow, operating speed and local barometric pressure were collected as well. The compressor mass flow utilized a pitot tube to correlate the delivered mass flow to the engine air manifold. The on-board instrumentation was calibrated with performance measurements obtained from the test cell. A pictorial schematic of the instrumented turbocharger is detailed in Figure 6.1. A PLC connected to the instrumentation recorded measurements to a database thirty times throughout the operating day.

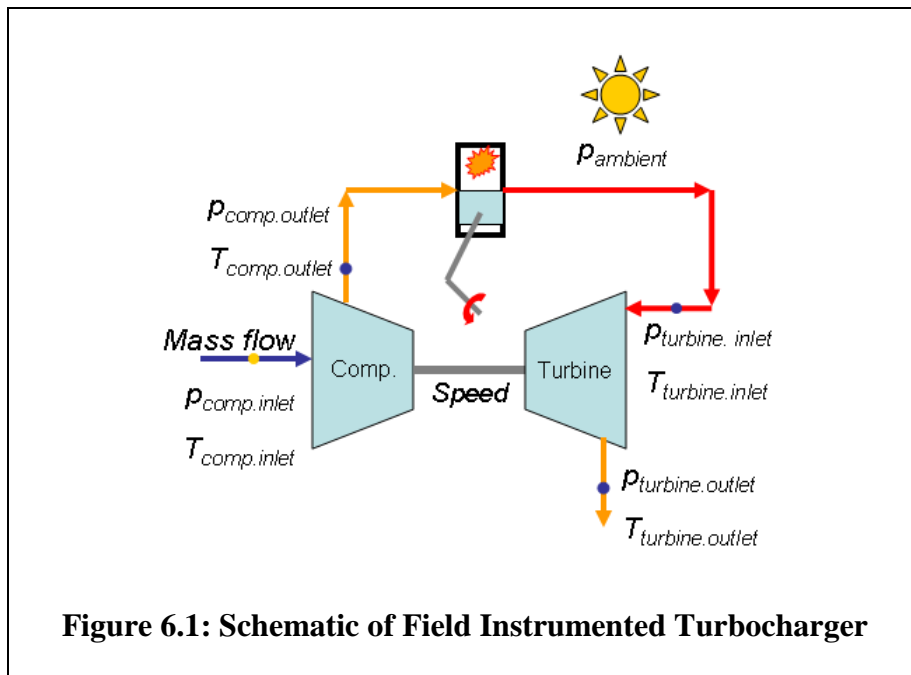**Figure 6.1: Schematic of Field Instrumented Turbocharger**

Figure 6.2 shows the field installed turbocharger with the applied instrumentation and instrument panel housing the instrument wiring, PLC and data recorder. The data utilized herein was recorded from July through mid September. During this period, the recorder collected over 1,500 data points of the turbocharger operating on-engine. Relative humidity was not part of the field data set. Inlet relative humidity obtained via historical weather data from www.weatherunderground.com was applied to the field data by matching the date and time recorded to the database to account for the inlet gas mixture and water vapor content.
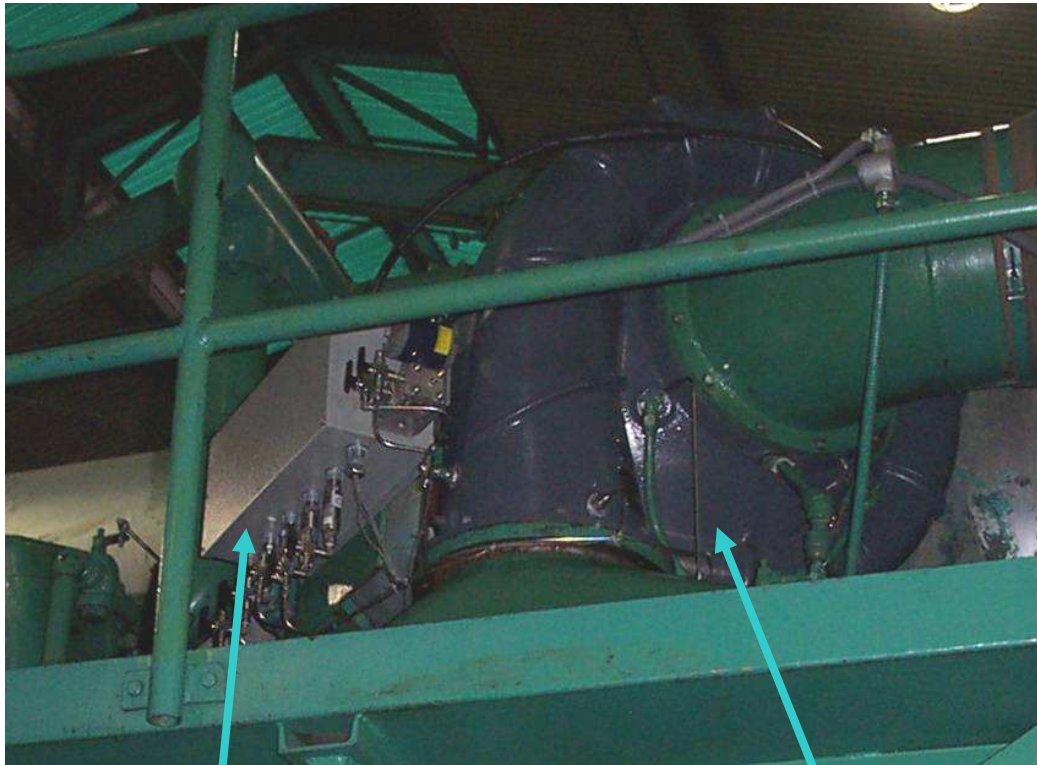
Instrument Panel   **Turbocharger**

**Figure 6.2: Instrumented Turbocharger Installation On-Engine**

6.2 Raw Field Data

The data recorded during these months provides significant variance of the ambient conditions compared to the data recorded from the test cell. Table 6.1 details the minimum, maximum and average ambient conditions for the data recorded during the field study. The field running condition also varies significantly in comparison to the specified condition for the turbocharger (see Table 4.1).

Table 6.1: Average Field Conditions

Measurement	Minimum	Maximum	Average
Ambient Temperature [°F]	58	117	84.9
Barometric Pressure [psia]	13.9	14.3	14.19
Relative Humidity	20	100	65
Speed [RPM]	8,337	10,326	9,339

The inlet volume flow and polytropic head were calculated from the field mass flow, pressure ratio and gas condition for each operating point in the field data set. Figure 6.3 plots the operating compressor map of the field data. The volume flow varied between 6,743 and 8,844 ICFM to the compressor, the polytropic head varied from 7,942 to 12,478 ft·lbf/lbm. These values are significantly lower than the design point specified for the turbocharger.

Figure 6.3: Raw Field Data, Head versus Volume Flow
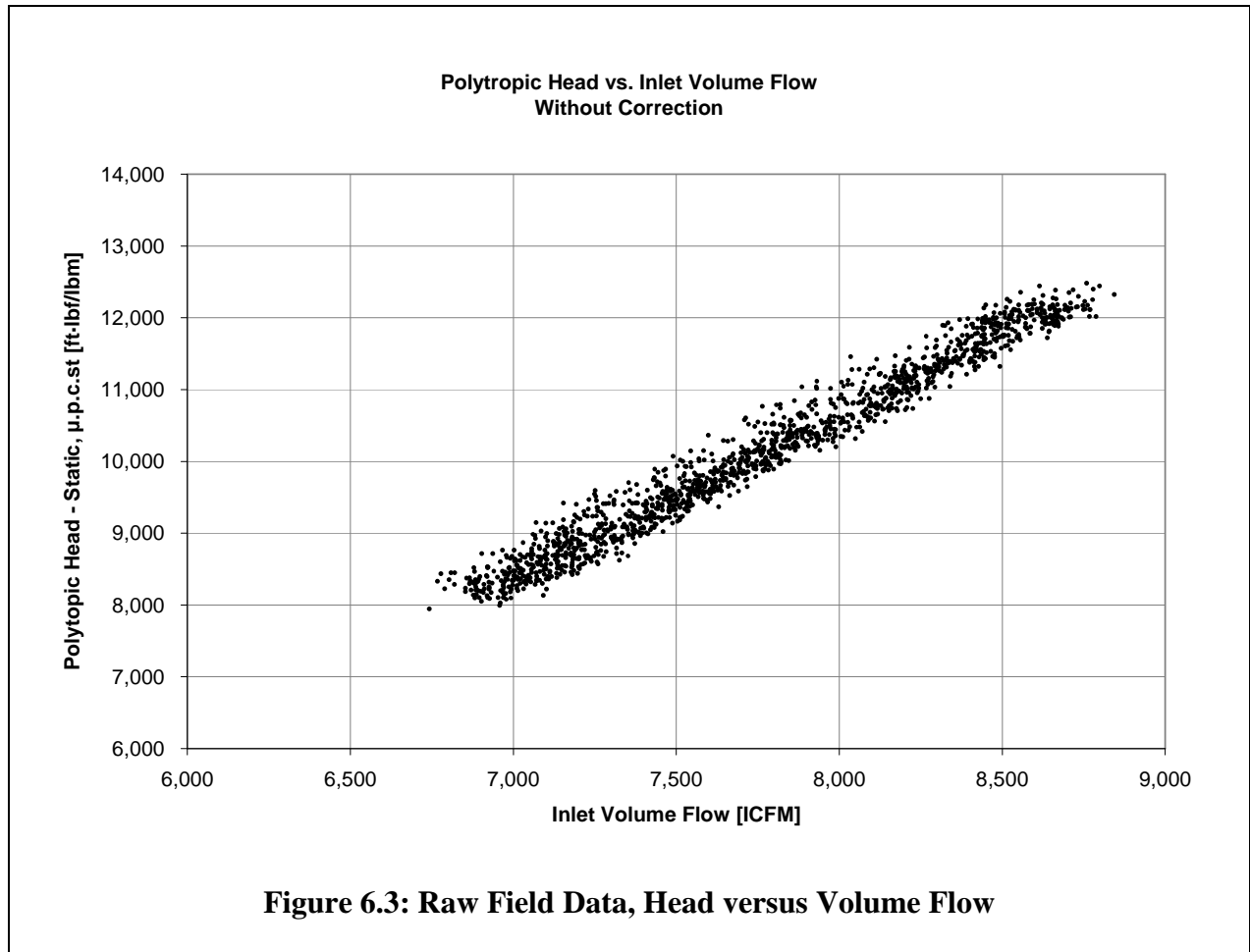
6.3 Compressor Inlet Pressure and Dimensionless Coefficients

Plotting the flow and head coefficients provides the best manner to evaluate the quality of the field data. From the field data there were two bands of head and flow coefficients (see Figure 6.5). Reviewing the data, the head coefficient is higher in July, the first month of operation. Upon inspection of the readings, the inlet pressure transmitter had a variance in comparison to the barometric pressure ranging from 0.19 to 0.25 psid during this time (see Figure 6.4). Plotting the difference between barometric pressure and compressor inlet pressure shows in late July there was a change to the inlet pressure of the compressor, highlighted in Figure 6.4.
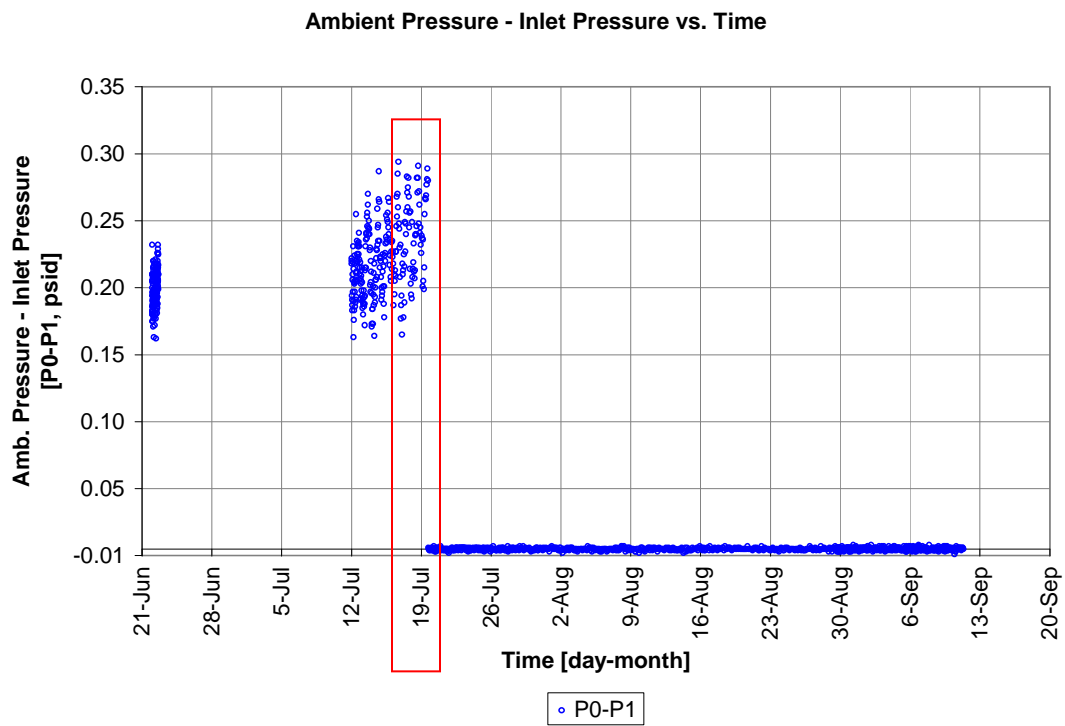
Figure 6.4: Difference Ambient Pressure to Compressor Inlet

Evaluating this finding in the dimensionless coefficients shows the same discrepancy as detailed in Figure 6.5 with the segregated coefficient groups.

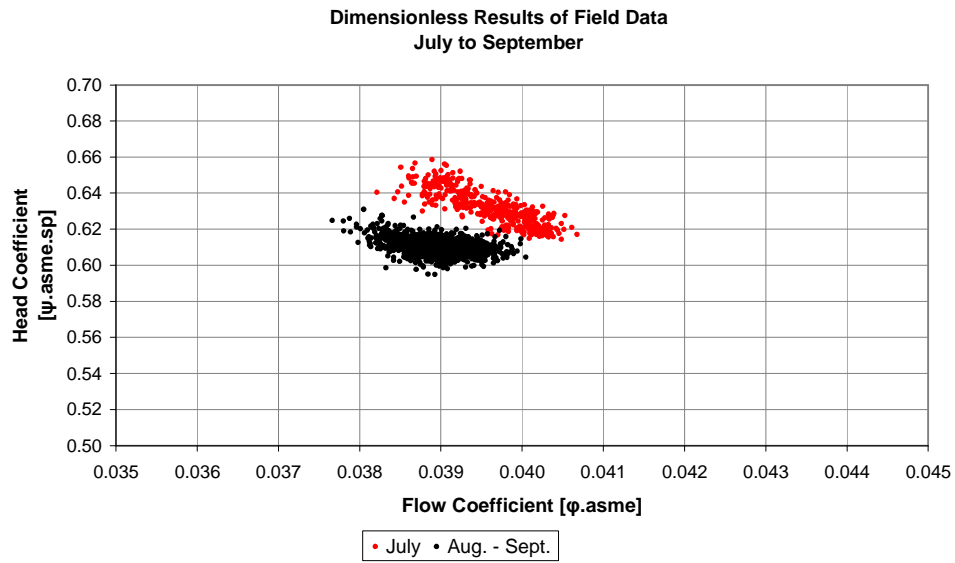**Dimensionless Results of Field Data**
July to September

Figure 6.5: Dimensionless Coefficients from Field Data

Inlet filter losses are a function of volume flow. However, there is no distinct pressure difference signature in the data as shown in Figure 6.6. The readings before and after July 19th will be treated separately in the analysis.

Figure 6.6: Inlet Filter Loss versus Volume Flow
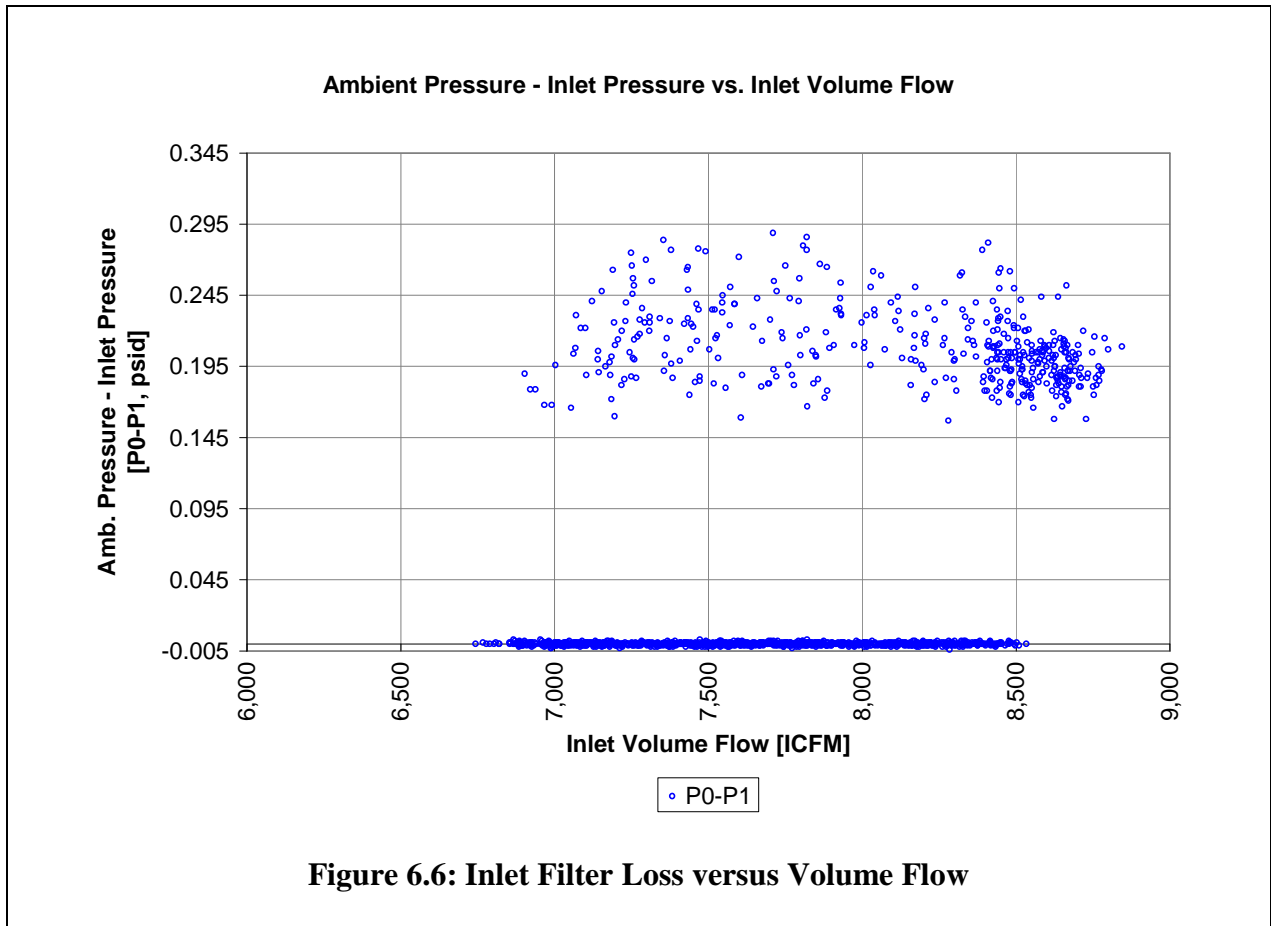
6.4 Correcting to Specified Conditions

The field data segregated for the time periods were corrected to the specified condition following the procedure in Section 5.7 - Test Cell Compressor Map at Specified Condition. To detail the speed in the large dataset from the field conditions, the following formula was applied to round-off trailing digits of the field recorded speed, and provides the specified speed for the correction procedure.

$$N_{sp} = \left[Integer\left(\frac{N_{field}}{100} \right) \right] \times 100 \qquad (6.1)$$

The field data corrected to the specified condition is plotted with respect to mass flow versus discharge pressure in Figure 6.7. The data from July details a slightly higher discharge pressure from the compressor. This plot details the operating line of the turbocharger on-engine. The field data and test cell data are compared in the next section to correlate the two and evaluate where the turbocharger is operating in comparison to the compressor map collected in the test cell.

Figure 6.7: Field Data Corrected to Specified Conditions
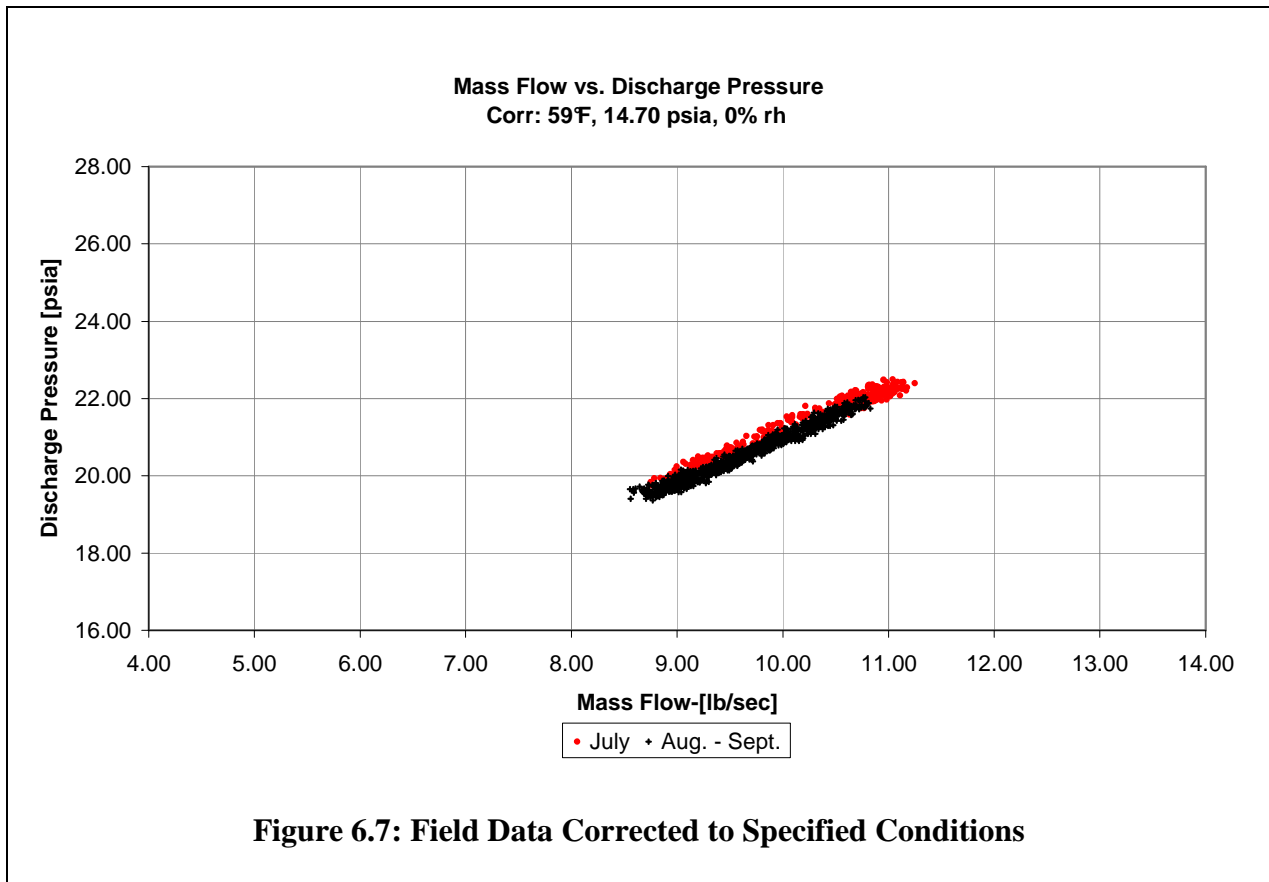
CHAPTER 7: Correlating Test and Field Data

The corrected data collected in the test cell provided the wide operating range of the compressor map between high flow and low flow or compressor surge for three different speed lines (Figure 5.7). This was collected in a precisely designed test apparatus to obtain the most accurate pressure, temperature and air or exhaust gas flow to the turbocharger. Conversely, the turbocharger operating on-engine as corrected to specified conditions follows one tightly formed line of mass flow and discharge pressure (Figure 6.7). This section details the comparison of the data sets, and differences between, finalizing with the verification steps of machine Mach and Reynolds numbers, and the ratio of densities (Equation 2.102). To begin, the data available between the two data sets are detailed in Table 7.1 for reference.

Table 7.1: Comparison of Test Cell and Field Data Available

| Test Cell Data	Field Operating Data
Date / Time	Date / Time
Barometric Pressure	Barometric Pressure
Compressor Inlet Pressure & Temperature	Compressor Inlet Pressure & Temperature
Compressor Dis. Pressure & Temperature	Compressor Dis. Pressure & Temperature
Compressor Mass Flow Rate	Compressor Mass Flow Rate
Turbine Inlet Pressure & Temperature	Turbine Inlet Pressure & Temperature
Turbine Discharge Pressure & Temperature	Turbine Discharge Pressure & Temperature
Turbo RPM	Turbo RPM
Turbine Mass Flow Rate (fuel + air)	None
Cooling Water Pressure & Temperature	None
Cooling Water Mass Flow Rate	None
Lube Oil Pressure & Temperature	None
Lube Oil Mass Flow Rate	None
Relative Humidity	None
Complete Energy Balance, Turbine & Compressor Performance	Compressor Performance

7.1 Dimensionless Coefficient Comparison

The turbocharger signature operating line formed by the dimensionless flow and head coefficients between the test and field data provides one method of comparing the data sets. Figure 7.1 presents the field and test cell dimensionless compressor map with the head coefficients corrected to specified conditions.

Figure 7.1: Plot of Compiled Dimensionless Coefficients
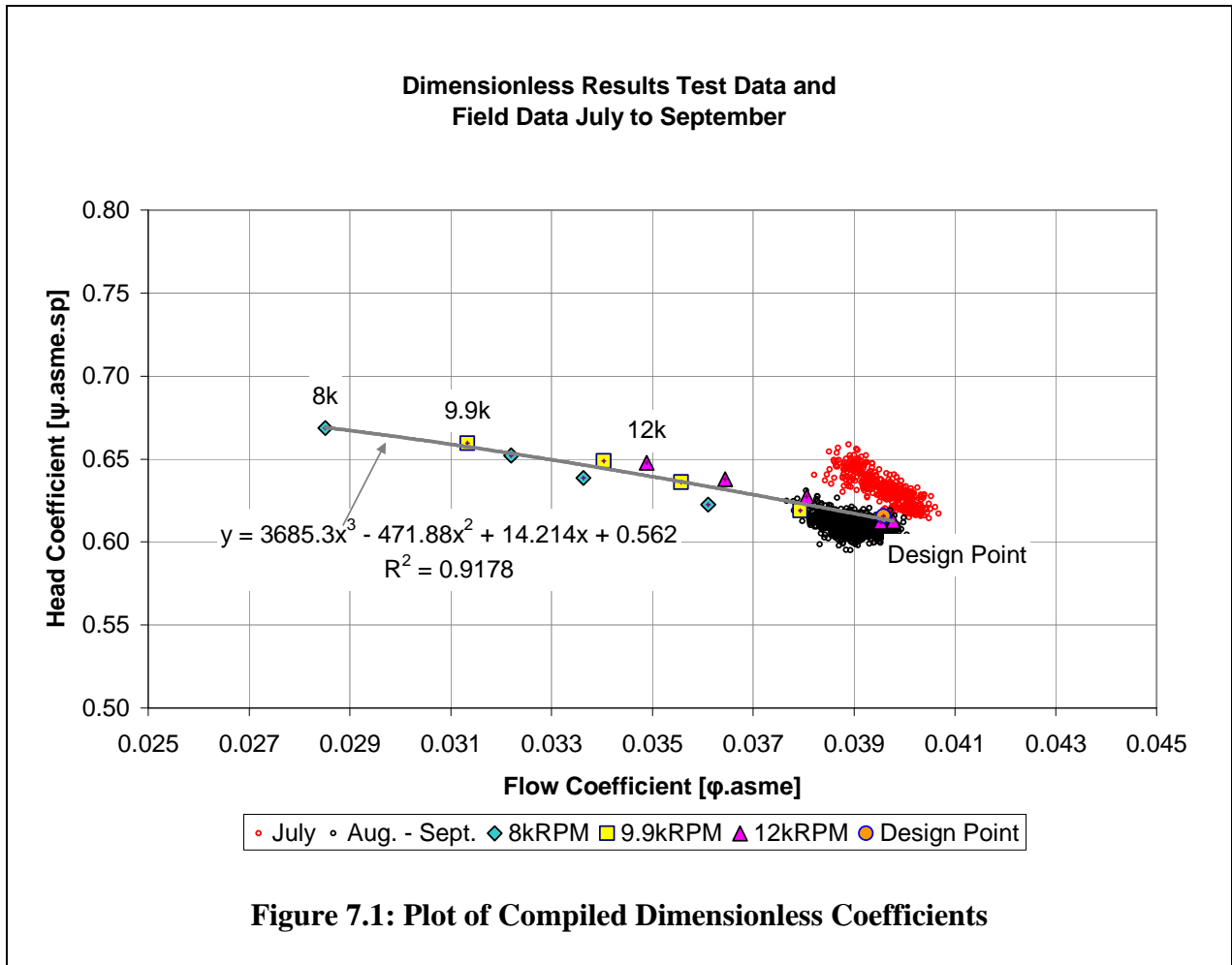
Comparing the flow and corrected head coefficients in Figure 7.1 for all data sets shows the following important points:

1. The test cell data forms a tight signature line within a range of -1.2% to +1.7% for all data points as compared to a cubic curve fit through the data set.

2. The July field data has a slightly higher head coefficient than this signature line as expected for higher inlet pressure losses; all data is within +5% of the signature line.

3. The field data head coefficient of Aug. and Sept. is within -3% of the signature line collected from the test cell.

4. The flow coefficient from the field data is within -5% to +3% of the design point flow coefficient.

5. The field data falls at the right most edge of the collected compressor map.

6. All head and flow coefficients are within ±5% of the signature line and specified design point. The turbocharger field data can be compared to the test cell data utilizing dimensionless coefficients noting the difference bands.

Figure 7.2: Polytropic Power Coefficient
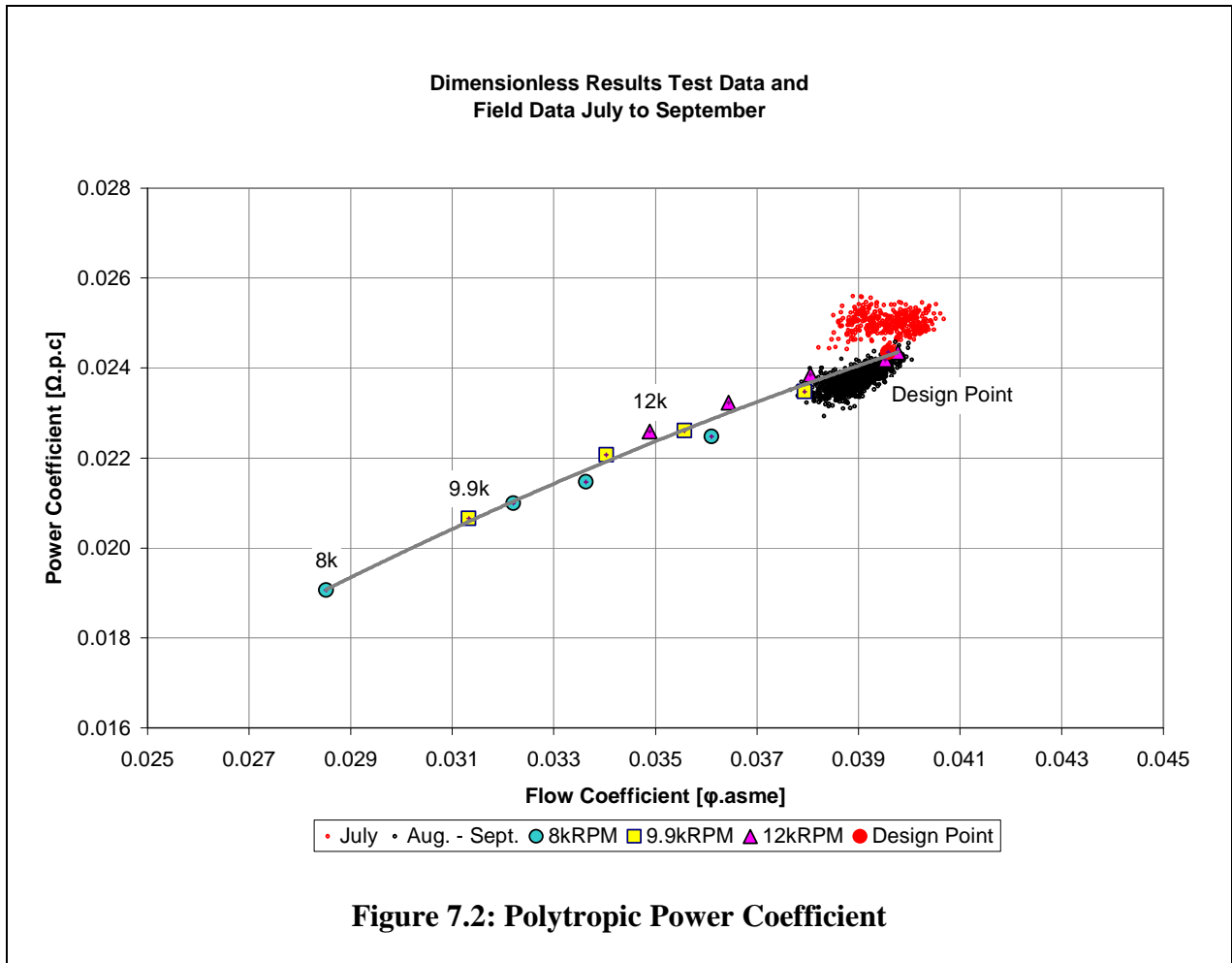
Comparing the polytropic power from Equation (2.90) of the test cell and field data sets establishes the power requirements of the compressor versus flow coefficient in Figure 7.2. This plot details the following important points:

1. The test cell data falls within -1.2% to 1.7% of the polynomial curve fit of the polytropic power curve.

2. The July field data has a slightly higher power coefficient line. The July data is within 0.6% to 6.2% of the polynomial curve fit from the test cell data.

3. The field data power coefficient of August and September is within -3.8% to 1.3% of the polynomial curve fit from the test cell data.

4. The data collected in August and September repeats the power signature collected in the test cell. Over 1,000 data points confirm this, therefore the earlier data collected in the July inaccurately provides the field operating performance of the compressor.

To further evaluate power, the actual power coefficient is calculated from Equation (2.91) to detail the compression power and contribution of compression efficiency. Figure 7.3 presents a distinct difference between the test and field data, with the two actual power coefficient curves between -3% to -5% different for all field data. As noted in Equation (2.91) the difference may be attributed to the compressor efficiency.
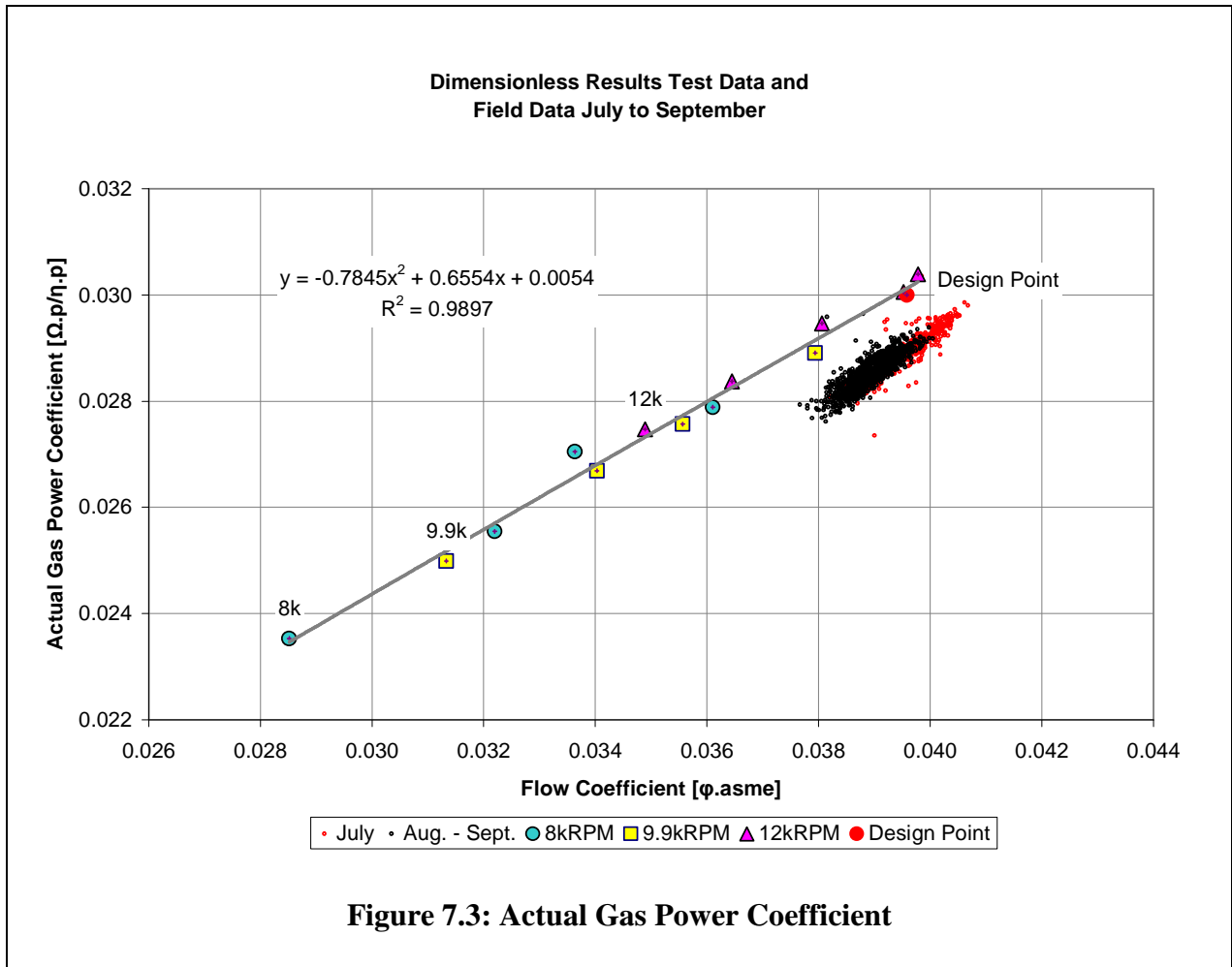
Figure 7.3: Actual Gas Power Coefficient

Figure 7.4 shows the field polytropic efficiency ranging from 0% to +6% when compared to the test cell data. This efficiency difference contributed to the difference in the actual power coefficient curves in Figure 7.3. This decreased the field actual gas power coefficient signature due to the efficiency in the denominator of the coefficient.
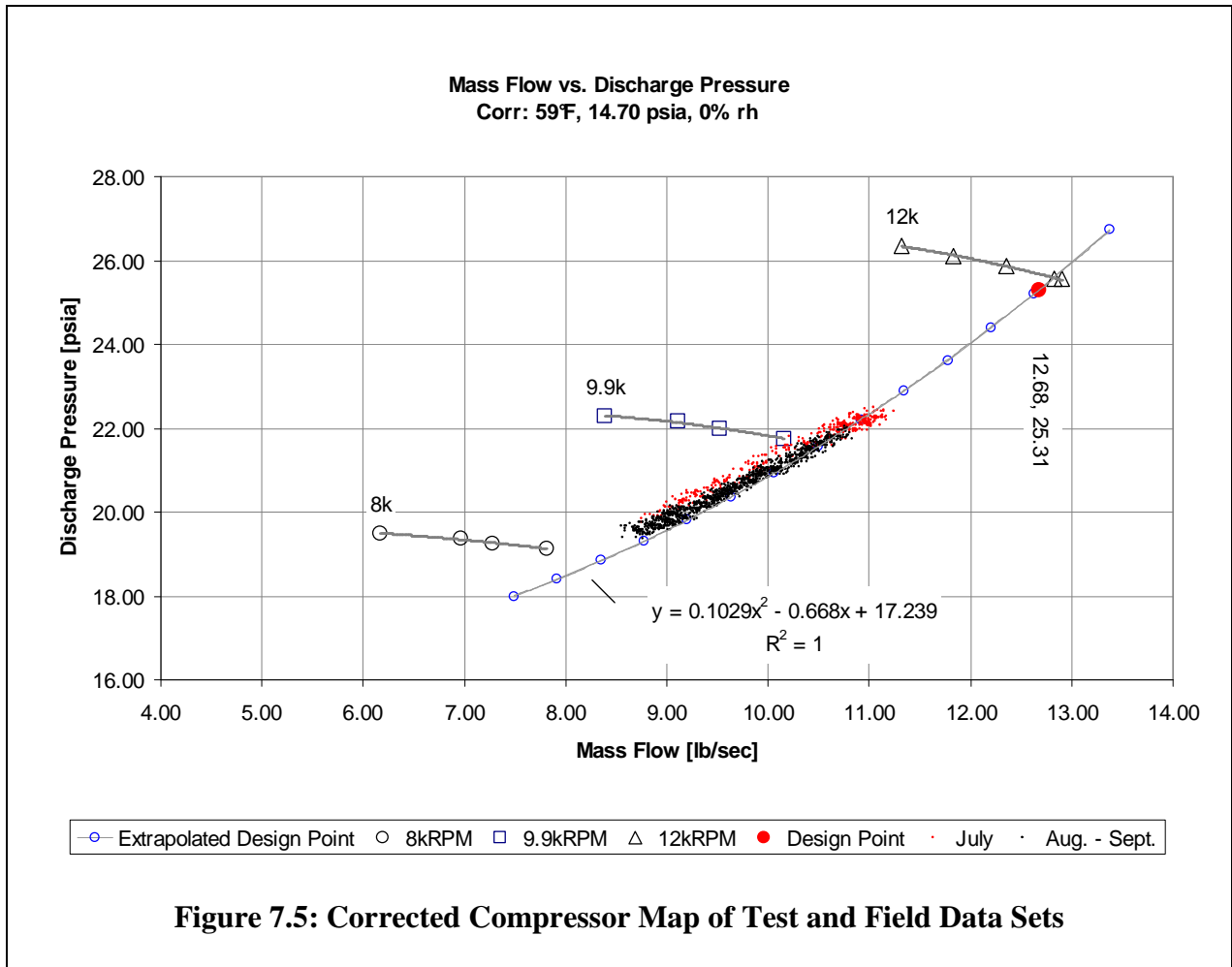
Figure 7.4: Polytropic Efficiency
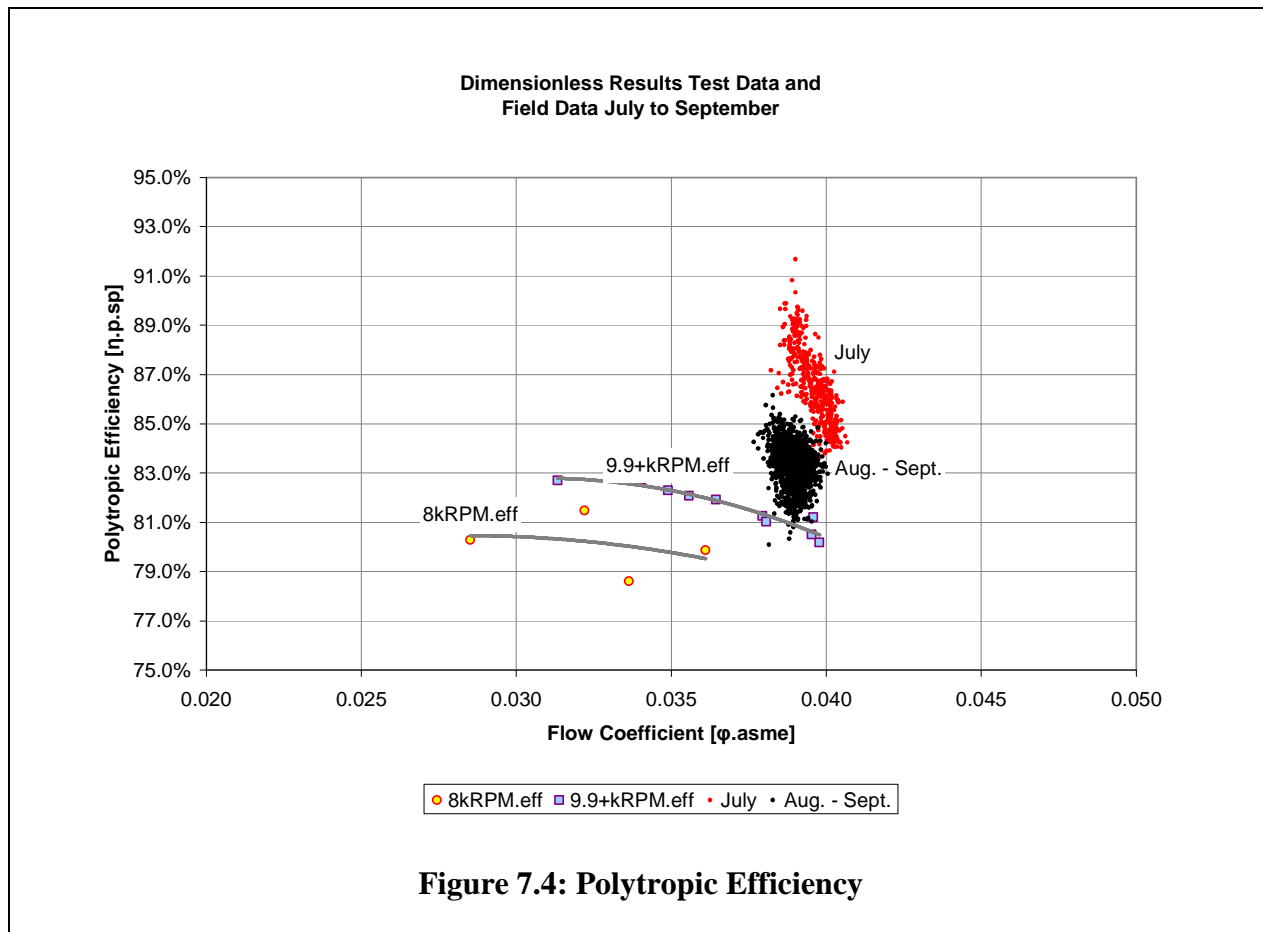
From Figure 7.1 and Figure 7.2, the head and power signature lines versus the flow coefficient provide comparative results between test and field data. These calculations are based on pressure measurements at the inlet and outlet flange locations of the compressor. The polytropic efficiency calculated through Equation (2.33) is a thermodynamic relation based on the gas composition for the ratio of specific heats, and temperature and pressure measurements. The difference in the efficiency of Figure 7.4 must be a difference in the temperature measurements between the test cell and field location. In the field installation, the effects of heat transfer from the compressor casing may influence the field temperature measurement and efficiency, and may be remedied with the application of insulation (see Figure 6.2). Further analysis of the temperature measurements are required to determine the root cause of the difference of the

efficiency calculations. This is required to resolve a comparison between data collected as a baseline from the test cell and utilized as a parameter to monitor the general health of the compressor operating on engine.

7.2 Compressor Map and Field Data Comparison

The test cell and field data compressor maps (Figure 5.7 and Figure 6.7) corrected to specified conditions are combined in Figure 7.5. The specified design point volume flow and head is significantly higher than the field operating data. Extrapolating the design point flow and head coefficients to the specified conditions (see Section 5.7) for various speeds between 7,000 RPM to 12,500 RPM creates an estimated operating line of the turbocharger, detailed in Figure 7.5 (Extrapolated Design Point). This line bisects the field data within 3% of the turbocharger operating line on-engine. The original design point for the turbocharger specification may have declared a discharge pressure much higher than collected in the field data; however the turbocharger operated within 3% of the point when expanded for various speeds. The engine may have operated significantly lower than full power as detailed by the lower field air manifold pressure.

Mass Flow vs. Discharge Pressure
Corr: 59°F, 14.70 psia, 0% rh

$y = 0.1029x^2 - 0.668x + 17.239$
$R^2 = 1$

12.68, 25.31

Extrapolated Design Point ○ 8kRPM □ 9.9kRPM △ 12kRPM ● Design Point · July · Aug. - Sept.

Figure 7.5: Corrected Compressor Map of Test and Field Data Sets

7.3 Verifying the Correction Method

The final step of comparing the correction method is to ensure the specified to test conditions falls within the bounds of the machine Mach and Reynolds number comparison (Figure 2.13 and Figure 2.14). This is to ensure the tip speed is in compliance with the established code and correction methodology. Additionally the density ratio between inlet and outlet for test and specified conditions must be considered. Each of the above are discussed in the following sections.

7.3.1 Machine Mach Number Verification

The difference of the test cell and field data machine Mach numbers (Equation 2.92) to the specified Mach number are plotted in Figure 7.6 to compare with limitations of the defined boundary. For this turbocharger, all corrected data falls well within the required bounds.

To further evaluate this, the range of speed correction with respect to the machine Mach number were checked to quantify the speed range to the limit boundaries. There were two ranges checked, the 8kRPM and 12kRPM tested speeds. For the lower operating speed (8kRPM), the data could be speed corrected between 5,500 to 9,400 RPM and maintain the reference limits. For the high operating speed (12kRPM), the data could be speed corrected between 10,800 to 12,400 RPM and maintain the reference limits. Although the flow and head coefficients of the collected data can be used to create virtually any operating speed line of the turbocharger compressor, the machine Mach number verification helps to limit this practice.
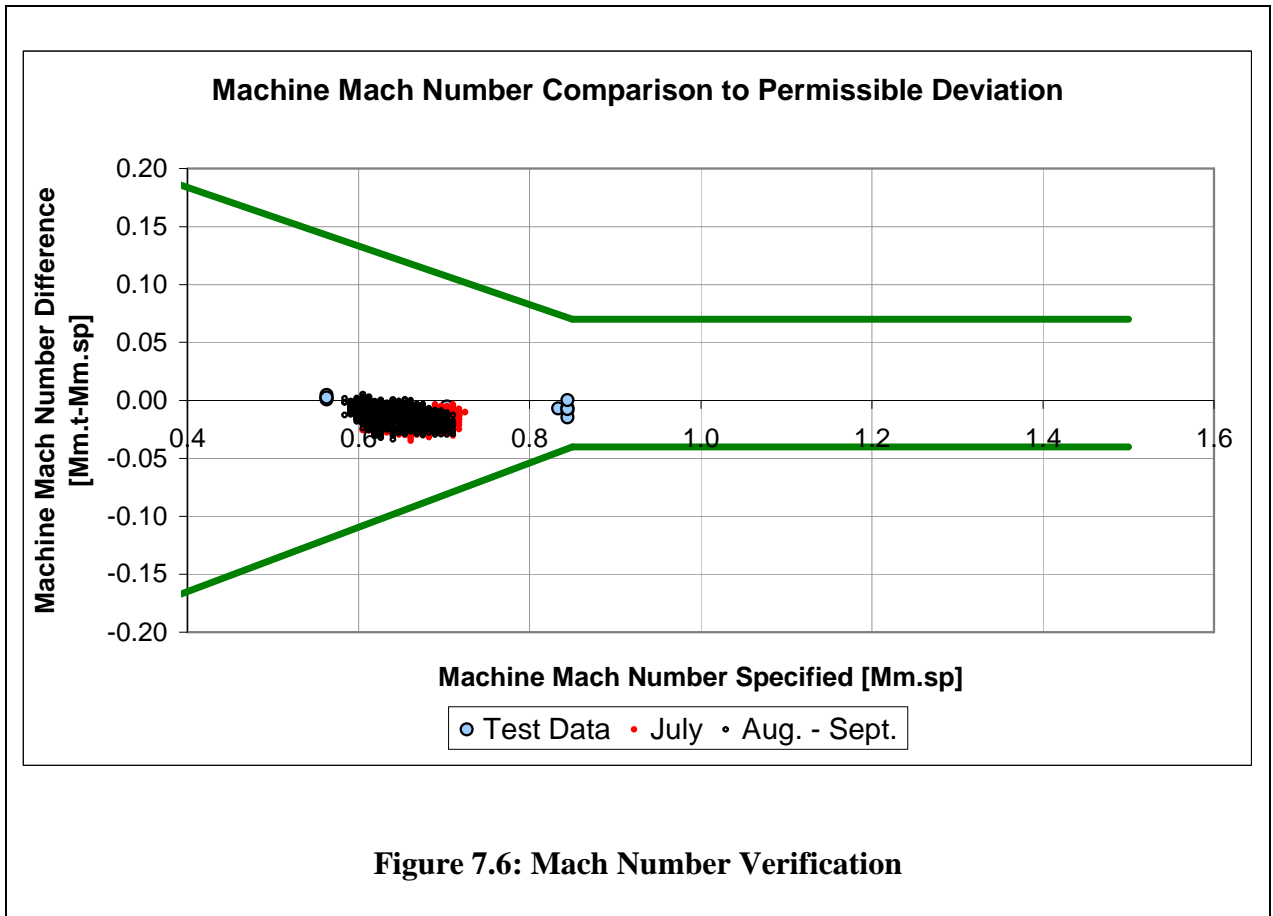
Figure 7.6: Mach Number Verification

7.3.2 Machine Reynolds Number Correction

The machine Reynolds number between test and specified conditions will likely not match, and is a secondary parameter of the methodology. The field and test cell data sets were corrected from the operating condition to the specified condition with the PTC10 Reynolds correction method (Equations 2.95 thru 2.101). Figure 7.7 presents the comparison between test and specified conditions, detailing all data falls within the boundary limits.

Figure 7.7: Reynolds Number Verification
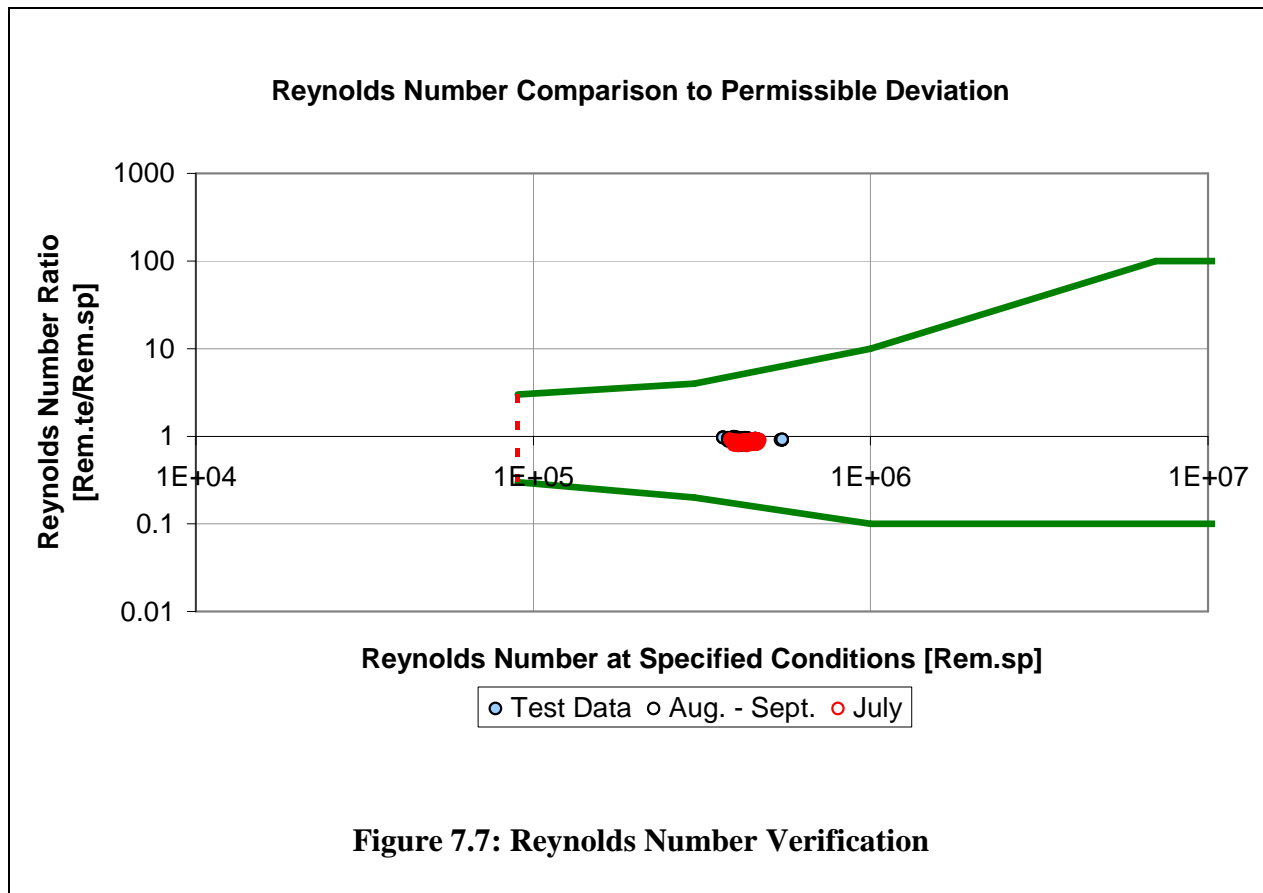
Similar boundary tests of the machine Mach number were checked against the machine Reynolds number methodology to test the speed range. The range of machine Reynolds Number to maintain the reference limits as detailed in Figure 7.7 are from 3,000 to 60,000 RPM for the specified speed and inlet gas viscosity.

To further evaluate the machine Reynolds number correction model, two tested data points with similar flow coefficients were checked for comparison. These were utilized to evaluate the correction model for speed and inlet viscosity to compare the resulting corrected polytropic efficiency. Table 7.2 details the comparison with the design point flow coefficient of 0.03958 and the point near the choke line for the 12kRPM speed line of 0.03952.

Table 7.2: Reynolds Number Evaluation

Flow Coefficient (te = sp)	Speed.te [RPM]	Poly.eff [%]	Speed.sp [RPM]	Poly Eff. Corr [%]	Diff. in Poly.Eff. [%]
0.03958	11852	81.16%	12000	81.23%	0.07%
0.03952	11982	80.45%	11852	80.50%	0.05%

The resulting difference in the polytropic corrected efficiency varies considerably compared to the difference in flow coefficients. From this comparison the reduced Wiesner model for correcting the head coefficient and efficiency to establish performance may be lacking the expected correction. Therefore a complete evaluation of this model is required before utilization.

Secondly, the Reynolds number correction method contains two constants. The constants detail that the data of the compressor shall be corrected in comparison to a specified surface roughness of $\varepsilon = 0.000125 \, in$ and specified machine Reynolds number of $Rem_{sp} = 4.8 \cdot 10^6 \times b_2$. This reduces the correction model to a comparison with the established constants.

7.3.3 Density Ratio

The density ratio was calculated for all data for the turbocharger. This results in a range of the density ratio from Equation (2.102) for all data sets between -0.3% to 2.5%. The density ratio as calculated for the population of data is within the limits of that specified by the performance code which is $\pm 4\%$.

7.4 Summary

This chapter utilized the systematic approach of establishing the compressor signature lines to overlay the test cell compressor map and field data. This provided a unique comparison of all data, independent of speed, to determine if a correlation existed. The dimensionless comparison provides a means of rapidly evaluating the field data with the specified design point of the turbocharger. The head and flow ranges of the signature lines between the test cell and field data overlay within ±5% as detailed in this section.

The test cell and field data were corrected to create the mass flow and discharge pressure compressor map at the specified condition. Plotting the two data sets together established that the specified design point mass flow and pressure condition was significantly higher than the comparative data from the turbocharger operating on engine. Of the possible reasons for this deviation, the engine may not have been operating at full load to achieve the specified design point during this dataset. If this is the case future data collected when operating with more engine demand could verify this hypothesis. Extrapolating the design point flow and head coefficient for a range of speeds created a flow and pressure line that bisected the field collected data. This supports the assumption of the engine operating at lower demand. Interestingly this extrapolated line from the design point may provide a means of testing the turbocharger operating flow and head range as expected on engine.

The machine Mach and Reynolds number limitations verified that all of the data were corrected within the guidance established in PTC10. From the two verification models, the machine Mach number is more stringent in limiting the correction range of the collected data for this case study with air as the working fluid. Rightly so as the pressure rise of the compressor depends on the tip

speed of the compressor. The boundary range limits the ability to correct into operating points of the compressor without test verification, preventing a method of falsified data. With test and specified gases that vary more significantly than air, the stringency of this limit may change.

The Reynolds number correction method for efficiency showed a minor influence when comparing data collected at the same flow coefficient and within 148 RPM. The expectation was the method would comparatively correct efficiency for speed and viscosity between closely collected speed data points for the same flow coefficient, however this was not the case. The compared corrected data exhibited a 0.07% difference in efficiency between the two collected data points. This minor difference is within the uncertainty of the pressure and temperature measurements of the efficiency equation. This forms the opinion that a detailed evaluation of the effects of this correction method should be verified on a number of different test turbochargers to further detail the application and use in the correction procedure.

CHAPTER 8: Conclusions

The work herein evaluated the background thermodynamics in pursuit of comparing data for a compressor operated in a precisely designed test cell to data collected from the same turbocharger operating on engine. The methodology utilized dimensionless coefficients and the concept of similitude to compare all collected data. Through the evaluation it was found the quality of the data sets compared well and within reasonable tolerance.

The complete evaluation process of the turbocharger requires measurements of only temperature, pressure, flow and speed. These measurements define the operation of the turbocharger through extensive thermodynamic calculations to establish gas conditions, stagnation conditions, compression processes, and a means for comparing test and specified conditions. The important takeaway from the evaluation process is the testing setup to establish ambient operating conditions to mimic that onsite is not required, thus greatly reducing the cost and setup of a test. Through this methodology ambient conditions that differ significantly between that of a test and as specified for the design can be accurately simulated to determine the turbocharger onsite performance.

The importance of this comparison to the operating engine is the fundamental evaluation of the design point specified to the actual operation on engine. Imagine a simple test with reduced operating points to only matching the specified design point. Through the methodology here, the single specified data point collected in the test cell is within a few percent of the inlet volume flow of the turbocharger operating on engine. If the evaluation process utilized a specified site mass flow match in place of the volume flow match utilized herein, it would place the design point significantly away from the real operating point and would be completely dependent on the

inlet density at test day. In the compressor map and dimensionless map, such a match establishes a different efficiency and may falsely prove turbocharger operation on engine. This establishes the importance of accounting for matching the site conditions correctly. Determining the field operation for the test accurately establishes the real on-engine efficiency of the turbocharger. The result will be found in the engine fuel consumption or turbocharger operating correctly given the accuracy of the specified point. In contrast, not following the method presented herein could miss an invalid compressor match during the verification process, nevertheless to be found in an engine operating with unstable combustion, missed environmental permits, or limited operating range due to a poorly established turbocharger.

References

American Society of Mechanical Engineers. *Performance Test Code on Compressors and Exhausters, PTC 10-1997.* New York: ASME, 1998. Print.

American Society of Mechanical Engineers. *Steam Tables. Thermodynamic and Transport Properties of Steam.* 6th ed. New York: ASME, 1993. Print.

Avallone, Eugene A., Theodore Baumeister III, and Ali M. Sadegh. *Mark's Standard Handbook for Mechanical Engineers.* 11th ed. New York: McGraw-Hill, 2007. Print.

Buckingham, Edgar. "On physically similar systems; Illustrations of the use of dimensional equations." *Physical Review* Vol. 4, (1914): 345-376. Print.

Bathie, William W. *Fundamentals of Gas Turbines.* 2nd ed. New York: Wiley 1995. Print.

Chen, Ning H. "An Explicit Equation for Friction factor in Pipe." *Industrial and Engineering Chemistry Fundamentals* Vol. 18, (1979): 296-297. Print.

Chapman, K. S., Keshavarz, A., Shultz, J., Sengupta, J., 2005, "Test Standard for Testing Large-Bore Engine Turbochargers," Gas Research Institute, Report No. GRI-05/0026, Des Plaines, IL.

Chapman, Kirby S. and Omar Mohsen. "Real Time Performance Measurement of an Elliot H-Series Turbocharger." *Proceedings from Gas Machinery Conference, 2000.* Gas Machinery Research Council, 2000. Print.

Churchill, Stuart W. "Friction-factor equations spans all fluid flow ranges." *Chemical Engineering* Vol. 91, (1977): 91-92. Print.

Daugherty, Robert L., Joseph Franzini. *Fluid Mechanics with Engineering Applications.* 7th ed. New York: McGraw-Hill, 1977. Print.

Dixon, S. L. *Fluid Mechanics and Thermodynamics of Turbomachinery.* 4th ed. Boston: Butterworth, 1998. Print.

Douglas, J. F., J. M. Gasiorek, and J. A.Swaffield. *Fluid Mechanics.* 2nd ed. Great Britain: Bath Press, 1985. Print.

Ehlers, Gary A. "Selection of Turbomachinery – Centrifugal Compressors." *Proceedings of the Twenty-Third Turbomachinery Symposium, September 13-15, 1994.* Texas A&M Univ., n.p. Turbomachinery Symposium, 1994. 151-62. Print.

Globe Turbocharger Specialties, Inc. *Globe 1215.* Web. 24 Nov. 2010. Available at: http://www.globeturbocharger.com/

Gresh, M. Theodore. *Compressor Performance: Aerodynamics for the User.* 2nd ed. Boston: Butterworth 2001. Print.

International Organization for Standardization. *Turbocompressors – Performance Test Code ISO 5389.* Switzerland: ISO, 2005. Print.

Ikoku, Chi U. *Natural Gas Production Engineering.* Malabar: Krieger, 1984. Print.

Japikse, David, Nicholas C. Baines. *Introduction to Turbomachinery.* Vermont: Concepts ETI, 1997. Print.

Langhaar, Henry L. *Dimensional Analysis and Theory of Models.* New York: Wiley, 1951. Print.

Lindeburg, Michael R. *Mechanical Engineering Reference Manual for the PE Exam.* 11th ed. Belmont: Professional Publications, 2001. Print.

Lüdtke, Klaus H. Process Centrifugal Compressors: Basics, Function, Operation, Design, Application. Berlin: Springer 2004. Print.

Moran, Michael J., Howard N. Shapiro. *Fundamentals of Thermodynamics.* 3rd ed. New York: Wiley, 1995. Print.

Munson, Bruce R., Donald F. Young, and Theodore H. Okiishi. *Fundamentals of Fluid Mechanics.* 4th ed. New Jersey: Wiley, 2002. Print.

Schlichting, Hermann and Klaus Gersten. *Boundary-Layer Theory.* 8th ed. Berlin: Springer, 2000. Print.

Shapiro, Ascher H. The Dynamics and Thermodynamics of Compressible Fluid Flow. 2 vols. New York: Ronald, 1953. Print.

Sillman, Sanford. "Overview: Troposphere ozone, smog and ozone-NOx-VOC sensitivity." Web. 20 Nov. 2010. Available at: http://www-personal.umich.edu/~sillman/ozone.htm

Simon, H. and A. Bülskämper. "On the Evaluation of Reynolds Number and Relative Surface Roughness Effects on Centrifugal Compressor Performance Based on Systematic Experimental Investigations." Transactions of the *ASME Journal of Engineering for Power*, paper no: 83-GT-118, (1983). Print.

Strub, R. A., L. Bonciani, C. J. Borer, M. V. Casey, S. L. Cole, B. B. Cook, J. Kotzur, H. Simon, M. A. Strite. "Influence of the Reynolds Number on the Performance of Centrifugal Compressors." Transactions of the *ASME Journal of Turbomachinery* Vol. 109, (1987): 541-544. Print.

Swamee, P. K. and A. K. Jain. "Explicit equation for pipe flow problems." *Journal of the Hydraulics Division* Vol. 102, (1976): 657-664. Print.

Tapley, Byron, D. *Eshbach's Handbook of Engineering Fundamentals.* 4th ed. New York: Wiley, 1990. Print.

Taylor, Edward S. *Dimensional Analysis for Engineers.* Glasgow: Oxford, 1974. Print.

von Mises, Richard. *Mathematical Theory of Compressible Fluid Flow.* New York: Dover, 2004. Print.

Wiesner, F. J. "A New Appraisal of Reynolds Number Effects on Centrifugal Compressor Performance." Transactions of the *ASME Journal of Engineering for Power* Vol. 101, (1979): 384-395. Print.

Zheng, Ming., Graham T. Reader, J. Gary Hawley. "Diesel engine exhaust gas recirculation - a review on advanced and novel concepts." *Energy Conversion and Management* Vol. 45, Issue 6, (2004): 883-900. Print.

Appendix A: Saturated Vapor Pressure Methods

This work utilized the saturated vapor pressure line as detailed by the K-function from the ASME Steam Tables *(ASME, 1993)* presented in Figure 2.11. Two alternatives to the K-function saturation line were evaluated for ambient air conditions between 32.018°F and 128°F in an effort to reduce the procedure to a more manageable and programmable method for utilization in a programmable logic controller or quick engineering calculation. These alternative relations have reduced complexity as compared to the K-function, with slightly reduced accuracy as well. The alternative calculations and reduced accuracy as compared to the steam tables are as follows:

Table A.1: Alternative Calculations for Saturated Vapor Pressure

| Equation		Error
$p_{sat}(psia) = \left[0.01231 + \left(\dfrac{T(°F) + 171.85}{273.18} \right)^{-8.2816} \right]$	(A.1)	0.18% -0.04%
$\beta_a = \dfrac{-7328.4}{T(°F) + 393.49}$ $p_{sat}(psia) = 2.67137 \cdot 10^6 \, e^{(\beta_a)}$	(A.2)	0.16% -0.02%
$\beta_a = (14.2805 - 5288.358/T(°K))$ $p_{sat}(bar) = e^{\beta_a}$ (Lüdtke, 2004)	(A.3)	-1.82% 0.41%

Appendix B: Turbocharger Operating Line

Table B.1: Design Testing Line Evaluation Procedure from the Design Point

| Step	Calculation	Required Data
1	Calculate Flow Coefficient $$\phi_t = \phi_{spt} = \frac{\dot{m}}{\rho_{inlet}} \frac{1}{2\pi N_{turbo} D_{wheel}{}^3}$$	Design Point Condition: - Ambient Temperature - Barometric Pressure - Relative Humidity - Design Point Speed - Impeller Diameter - Mass / Volume Flow Rate
2	Calculate Head Coefficient $$\psi_{dp} = \frac{\kappa}{\kappa-1} \cdot \frac{R_{air} T_{inlet}\left[\left(\dfrac{p_{out}}{p_{in}}\right)^{\frac{\kappa-1}{\kappa}} - 1\right]}{(\pi N_{turbo} D_{wheel})^2} = \psi_t \approx \psi_{sp}$$	Design Point Condition: - R-value Air - Ratio of Specific Heats - Inlet Pressure - Outlet Pressure - Barometric Pressure
3	Establish volume flow conditions for the design point line or engine load line, jj points in step 4.	
4	Calculate test speeds for volume flows $$N_{turbo,jj} = \dot{V}_{inlet,jj} \frac{1}{2\pi \phi_t D_{wheel}{}^3}$$	Volume flows from step 3
5	Calculate discharge pressure for test day condition $$p_{2,abs\,jj} = p_{inlet}\left[\frac{\psi_{dp}\left(\pi N_{turbo.jj} D_{wheel}\right)^2}{R_{sp} T_{inlet.te}} \cdot \frac{\kappa_{te}-1}{\kappa_{te}} + 1\right]^{\frac{\kappa_{te}}{\kappa_{te}-1}}$$	Test Day Condition: - R-value Air - Ratio of Specific Heats - Inlet Temperature - Speeds from Step 4

Appendix C: Overview of Correction Method

The following pseudo-code details the correction process from the measurements and dimensions of the compressor, corrected to the specified condition.

Figure C.1: Pseudo-code of Correction Method
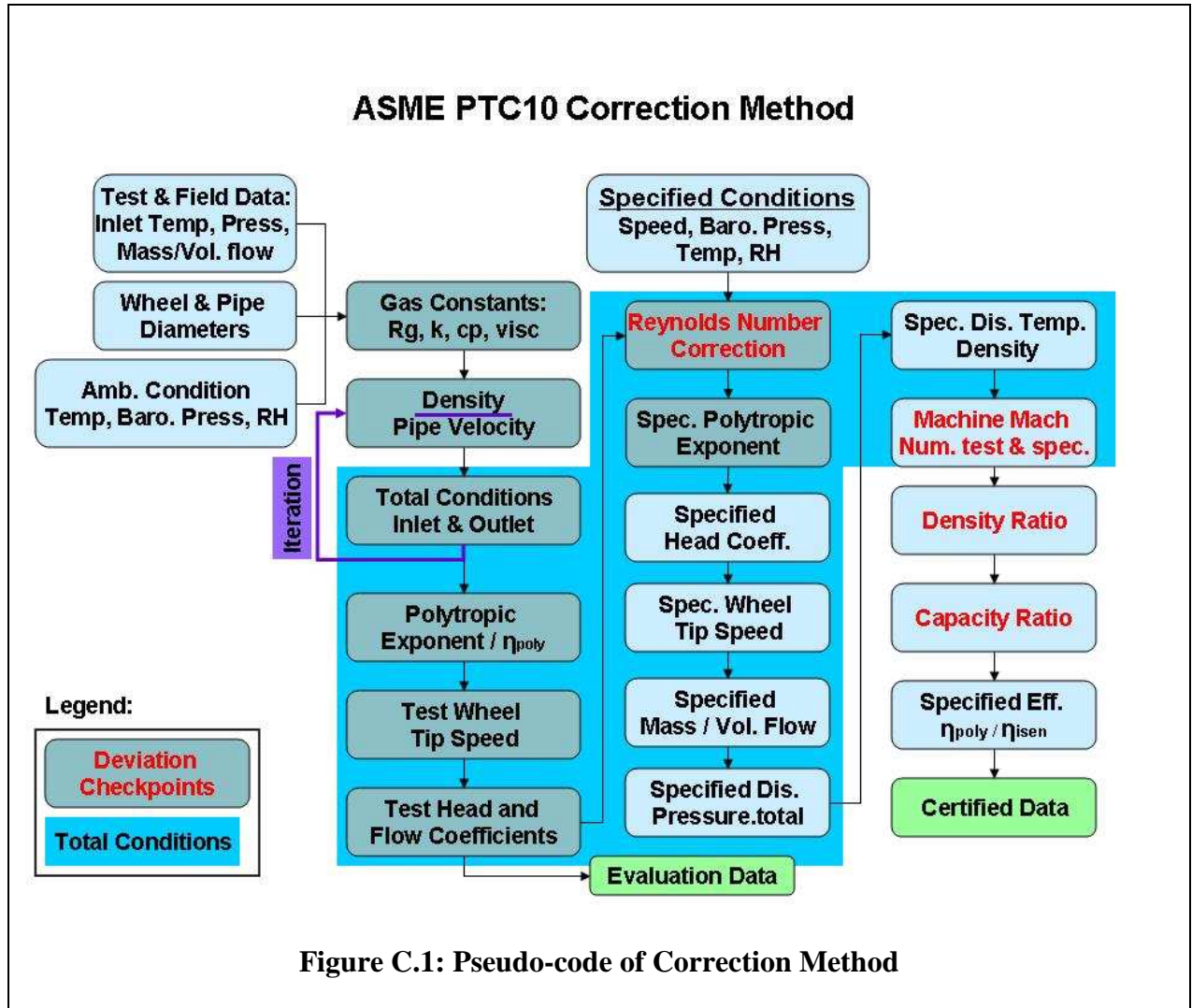
Appendix D: Conditions of Ambient Air

The following two plots detail the effects of relative humidity and temperature on the specific

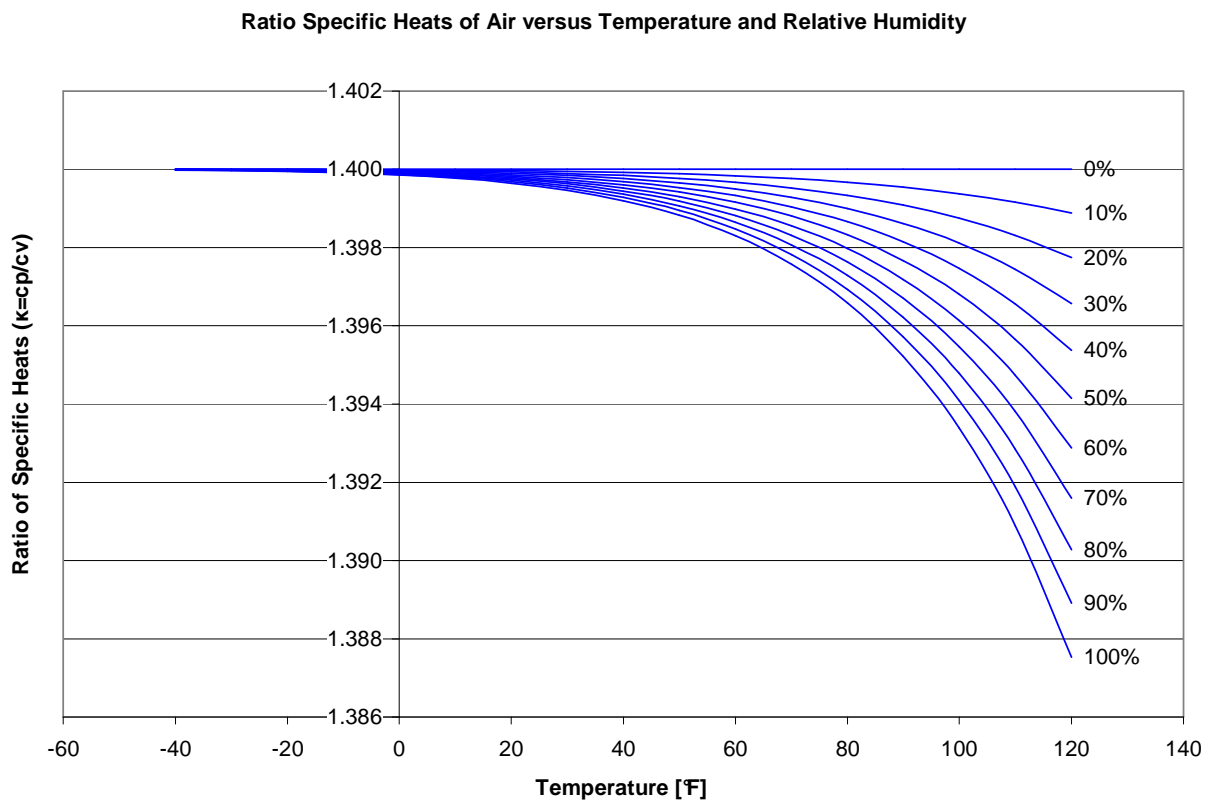gas constant and the ratio of specific heats.

Figure D.1: Specific Gas Constant of Air versus Temperature and Relative Humidity
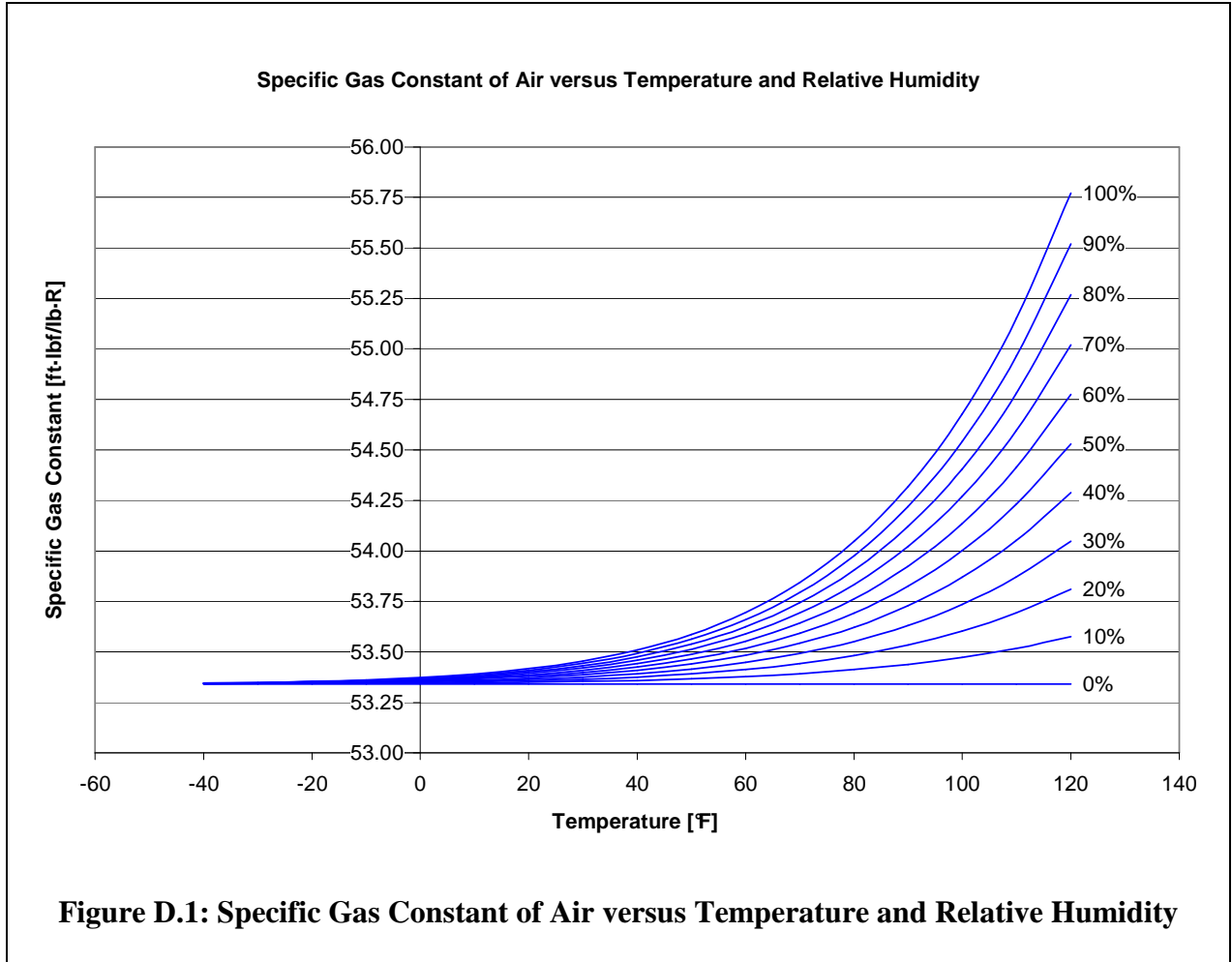
Figure D.2: Ratio of Specific Heats of Air versus Temperature and Relative Humidity

Appendix E: Instrument Uncertainty Analysis

Instrument uncertainty defines the quality of a recorded measurement in comparison to the absolute value obtainable with a 'perfect measurement system'. The uncertainty of a measurement is a function of the installation, instrument accuracy, instrument environmental effects, data acquisition system, and calculations resulting from the measurement or combination of measurements. A true uncertainty considers the uncertainty of a population of recordings to obtain a single averaged, recorded data point, and the uncertainty of the complete data measurement system. This analysis focuses on the measurement system uncertainty and considers the uncertainty of the population of data as an absolute recording. Therefore this considers the quality of the measurement independent of a population of recordings. The general calculation for uncertainty is as follows:

$$U_i = \sqrt{\left(x_1{}^2 + x_2{}^2 + x_3{}^2 + x_4{}^2 + x_5{}^2\right) N_{instruments}} \qquad \text{(E.1)}$$

where

x_1	Instrument full scale accuracy
x_2	Thermocouple cold junction
x_3	Accuracy of data acquisition conversion
x_4	Transmitter accuracy
x_5	Thermal environment compensation
$N_{instruments}$	Number of installed instruments

The percent uncertainty of the instrument from the above calculation is therefore:

$$\% \, U_i = \frac{U_i}{\text{Instrument Range}} \qquad \text{(E.2)}$$

Considering the equation for flow metering through a differential nozzle requires evaluation of the sensitivity of the variables of the flow equation. Therefore, the partial derivative of each variable is calculated to determine the contribution of each uncertainty to the flow calculation. The partial derivatives are summarized in the calculations detailed in Figure E.1.

$$`q_m = \frac{\pi}{4} \frac{C_d \varepsilon d^2}{\sqrt{1 - \beta^4}} \sqrt{2 \Delta P \rho_1} \qquad \text{(E.3)}$$

where

q_m Mass flow of differential device

d Nozzle bore diameter

$\beta = d \,/\, D$ Ratio of bore diameters, nozzle to pipe diameter

C_d Nozzle discharge coefficient

ε Gas expansion factor

Δp Differential pressure across measurement nozzle

ρ_{nozzle} Air density upstream of measurement nozzle

Table E.1: Instrument Uncertainty Summary

(See Figure E.1 for Detailed Calculation Procedure)

	Instrument	Number of Instruments	Range	Accuracy	Thermal Compensation	PLC Analog Conversion Accuracy	Thermal Compensation	Uncertainty
Test Cell	Opto Analog Accuracy					1.00E-03		
	Nozzle Inlet Temperature	4	250	0.10%	0.36	2.50E-01	0.75%	1.55%
	Nozzle Inlet Pressure	2	15	0.25%	0	1.50E-02	0	0.38%
	Nozzle Diff. Pressure	2	20	0.15%	0	2.00E-02	0	0.25%
	Compressor Inlet Temperature	4	120	0.10%	0.36	1.20E-01	0.75%	1.64%
	Compressor Inlet Pressure	4	30	0.25%	0	3.00E-02	0	0.54%
	Compressor Dis. Temperature	4	500	0.10%	0.36	5.00E-01	0.75%	1.53%
	Compressor Dis. Pressure	2	100	0.50%	0.00%	1.00E-01	0.03%	0.73%
Field Flow	Nozzle - See Calculation for Calculation Uncertainty					0.00E+00		**1.04%**
	Compressor Flow - dP	1	100	0.15%	0	1.00E-01	0.02%	0.18%
	Compressor Flow - Pitot	1	1	1%		0.00E+00		1.00%
	Compressor Flow	1	1			1.00E-03		**1.45%**

$1\mu A = 1 \times 10^{-6} A$ $1 mA = 1 \times 10^{-3} A$ $inH2O \equiv 62.316 \cdot \dfrac{lb}{ft^3} \cdot g \cdot 1 \cdot in$

$U_{opto} := \dfrac{16\mu A}{16 \cdot mA}$ $\phi_{throat} := 0.004 \cdot in$

Define the Uncertainty function for the instrument channels: **Individual Uncertainty Vector Legend**

$$U(x, N) := \sqrt{\sum_{i=0}^{rows(x)-1} \left[(x_i)^2\right] \cdot N}$$

$$\begin{pmatrix} accuracy\_full\_scale \\ thermocouple \\ PLC\_block \\ thermocouple\_transmitter \\ press\_thermal\_compensation \\ 0 \end{pmatrix}$$

Nozzle Inlet Temperature: **Nozzle Inlet Pressure:**

$nz_{sc.tp} := 250 \cdot R$ Scale range $nz_{sc.press} := 15 \cdot psi$ Scale range

$N_{nz.temp} := 4$ Number of instruments $N_{nz.press} := 2$ Number of instruments

$Nozzle_{temp} := \begin{pmatrix} 0.1\% \cdot nz_{sc.tp} \\ 0.2K \\ U_{opto} \cdot nz_{sc.tp} \\ 0.75\% \cdot nz_{sc.tp} \\ 0R \\ 0R \end{pmatrix}$ Individual Uncertainty $Nozzle_{press} := \begin{pmatrix} 0.25\% \cdot nz_{sc.press} \\ 0 \cdot psi \\ U_{opto} \cdot nz_{sc.press} \\ 0 \cdot psi \\ 0 psi \\ 0 psi \end{pmatrix}$ Individual Uncertainty

$U_{nozzle.temp} := U(Nozzle_{temp}, N_{nz.temp})$ $U_{nozzle.press} := U(Nozzle_{press}, N_{nz.press})$

$U_{nozzle.temp} = 3.883 \cdot R$ Uncertainty $U_{nozzle.press} = 0.057 \cdot psi$ Uncertainty

$pU_{nozzle.temp} := \dfrac{U_{nozzle.temp}}{nz_{sc.tp}}$ $pU_{nozzle.press} := \dfrac{U_{nozzle.press}}{nz_{sc.press}}$

$pU_{nozzle.temp} = 1.553 \cdot \%$ $pU_{nozzle.press} = 0.381 \cdot \%$

Individual Contributions   Individual Contributions

$Nozzle_{temp} = \begin{pmatrix} 0.25 \\ 0.36 \\ 0.25 \\ 1.875 \\ 0 \\ 0 \end{pmatrix} \cdot R$ $Nozzle_{press} = \begin{pmatrix} 0.038 \\ 0 \\ 0.015 \\ 0 \\ 0 \\ 0 \end{pmatrix} \cdot psi$

Figure E.1: Uncertainty Calculations

Nozzle Inlet dP:

$$Nozzle_{dp} := \begin{pmatrix} 0.15\% \cdot nz_{sc.dp} \\ 0 \cdot psi \\ U_{opto} \cdot nz_{sc.dp} \\ 0 \cdot psi \\ 0psi \\ 0psi \end{pmatrix}$$

Scale range
$$nz_{sc.dp} := 20 \cdot inH2O$$

Number of instruments
$$N_{nz.dp} := 2$$

Individual
Uncertainty

Individual Contributions

$$Nozzle_{dp} = \begin{pmatrix} 0.03 \\ 0 \\ 0.02 \\ 0 \\ 0 \\ 0 \end{pmatrix} \cdot inH2O$$

$$U_{nozzle.dp} := U\left(Nozzle_{dp}, N_{nz.dp}\right)$$

$$U_{nozzle.dp} = 0.051 \cdot inH2O \qquad \text{Uncertainty}$$

$$pU_{nozzle.dp} := \frac{U_{nozzle.dp}}{nz_{sc.dp}} \qquad pU_{nozzle.dp} = 0.255 \cdot \%$$

Compressor Inlet Temperature:

Scale range $\qquad CI_{sc.tp} := 140 \cdot R$

Number of instruments $\qquad N_{CI.temp} := 4$

$$CI_{temp} := \begin{pmatrix} 0.1\% \cdot CI_{sc.tp} \\ 0.2K \\ U_{opto} \cdot CI_{sc.tp} \\ 0.75\% \cdot CI_{sc.tp} \\ 0R \\ 0R \end{pmatrix}$$

Individual
Uncertainty

$$U_{CI.temp} := U\left(CI_{temp}, N_{CI.temp}\right)$$

$$U_{CI.temp} = 2.255 \cdot R \qquad \text{Uncertainty}$$

$$pU_{CI.temp} := \frac{U_{CI.temp}}{CI_{sc.tp}} \qquad pU_{CI.temp} = 1.611 \cdot \%$$

Individual Contributions

$$CI_{temp} = \begin{pmatrix} 0.14 \\ 0.36 \\ 0.14 \\ 1.05 \\ 0 \\ 0 \end{pmatrix} \cdot R$$

Compressor Inlet Pressure:

Scale range $\qquad CI_{sc.press} := 30 \cdot psi$

Number of instruments $\qquad N_{CI.press} := 4$

$$CI_{press} := \begin{pmatrix} 0.25\% \cdot CI_{sc.press} \\ 0 \cdot psi \\ U_{opto} \cdot CI_{sc.press} \\ 0 \cdot psi \\ 0psi \\ 0psi \end{pmatrix}$$

Individual
Uncertainty

$$U_{CI.press} := U\left(CI_{press}, N_{CI.press}\right)$$

$$U_{CI.press} = 0.162 \cdot psi \qquad \text{Uncertainty}$$

$$pU_{CI.press} := \frac{U_{CI.press}}{CI_{sc.press}} \qquad pU_{CI.press} = 0.539 \cdot \%$$

Individual Contributions

$$CI_{press} = \begin{pmatrix} 0.075 \\ 0 \\ 0.03 \\ 0 \\ 0 \\ 0 \end{pmatrix} \cdot psi$$

Compressor Discharge Temperature: **Compressor Discharge Pressure:**

Scale range $CD_{sc.tp} := 500 \cdot R$ Scale range $CD_{sc.press} := 100 \cdot psi$

Number of instruments $N_{CD.temp} := 4$ Number of instruments $N_{CD.press} := 2$

$$CD_{temp} := \begin{pmatrix} 0.1\% \cdot CD_{sc.tp} \\ 0.2K \\ U_{opto} \cdot CD_{sc.tp} \\ 0.75\% \cdot CD_{sc.tp} \\ 0R \\ 0R \end{pmatrix} \quad \begin{matrix} \text{Individual} \\ \text{Uncertainty} \end{matrix}$$

$$CD_{press} := \begin{pmatrix} 0.5\% \cdot CD_{sc.press} \\ 0 \cdot psi \\ U_{opto} \cdot CD_{sc.press} \\ 0 \cdot psi \\ 0.025\% \cdot \dfrac{psi}{R} \cdot 220R \\ 0psi \end{pmatrix} \quad \begin{matrix} \text{Individual} \\ \text{Uncertainty} \end{matrix}$$

$$U_{CD.temp} := U\big(CD_{temp}, N_{CD.temp}\big)$$

$$U_{CD.press} := U\big(CD_{press}, N_{CD.press}\big)$$

Uncertainty   Uncertainty

$$U_{CD.temp} = 7.666 \cdot R$$

$$U_{CD.press} = 0.725 \cdot psi$$

$$pU_{CD.temp} := \frac{U_{CD.temp}}{CD_{sc.tp}} \qquad pU_{CD.temp} = 1.533 \cdot \%$$

$$pU_{CD.press} := \frac{U_{CD.press}}{CD_{sc.press}} \qquad pU_{CD.press} = 0.725 \cdot \%$$

Individual Contributions   Individual Contributions

$$CD_{temp} = \begin{pmatrix} 0.5 \\ 0.36 \\ 0.5 \\ 3.75 \\ 0 \\ 0 \end{pmatrix} \cdot R$$

$$CD_{press} = \begin{pmatrix} 0.5 \\ 0 \\ 0.1 \\ 0 \\ 0.055 \\ 0 \end{pmatrix} \cdot psi$$

TTRF Compressor Flow Nozzle Uncertainty:

$$\beta := \frac{12.4432 \cdot in}{22.624 \cdot in} \qquad\qquad \beta = 0.55$$

Uncertainty Pipe and Nozzle Diameters:

$$pU_{D.pipe} := \frac{\sqrt{(0.24 \cdot in)^2 + 2 \cdot (0.082 \cdot in)^2}}{22.624 \cdot in} \qquad\qquad pU_{d.nozzle} := \frac{\phi_{throat}}{12.4432 \cdot in}$$

$$pU_{D.pipe} = 1.178 \cdot \% \qquad\qquad\qquad pU_{d.nozzle} = 0.032 \cdot \%$$

Sensitivity Calculations:

$$X_{\rho} := \left[\frac{1}{2} \cdot \left(\frac{100}{525}\right) \cdot pU_{nozzle.temp}\right]^2 + \left(\frac{1}{2} \cdot pU_{nozzle.press}\right)^2 \qquad X_d := \left[\frac{2}{(1 - \beta^4)} \cdot pU_{d.nozzle}\right]^2$$

$$X_{dp} := \left(\frac{1}{2} \cdot pU_{nozzle.dp}\right)^2 \qquad\qquad\qquad X_C := (1 \cdot 0.6\%)^2$$

$$X_D := \left(\frac{-2\beta^4}{1 - \beta^4} \cdot pU_{D.pipe}\right)^2 \qquad\qquad X_{nozzle} := \sqrt{X_{\rho} + X_{dp} + X_D + X_d + X_C}$$

$$X_{nozzle} = 0.70 \cdot \%$$

Nozzle Uncertainty:

$$X_{\rho} = 5.814 \times 10^{-6} \qquad\qquad \sqrt{X_{\rho}} = 0.241 \cdot \%$$

$$X_{dp} = 1.625 \times 10^{-6} \qquad\qquad \sqrt{X_{dp}} = 0.127 \cdot \%$$

$$X_D = 5.633 \times 10^{-6} \qquad\qquad \sqrt{X_D} = 0.237 \cdot \%$$

$$X_d = 5.008 \times 10^{-7} \qquad\qquad \sqrt{X_d} = 0.071 \cdot \%$$

$$X_C = 3.6 \times 10^{-5} \qquad\qquad \sqrt{X_C} = 0.6 \cdot \%$$

Field Pitot Flow Meter Uncertainty:

Scale range $\qquad$ $flow_{sc.pt} := 100 \cdot inH2O$

Number of instruments $\qquad$ $N_{fl.pt} := 1$

Individual
Uncertainty

$$Pitot_{pt} := \begin{pmatrix} 0.15\% \cdot flow_{sc.pt} \\ 0 \cdot psi \\ U_{opto} \cdot flow_{sc.pt} \\ 0 \cdot psi \\ 0.015\% \cdot \dfrac{inH2O}{R} \cdot 220R \\ 0psi \end{pmatrix}$$

Uncertainty

$$U_{flow.pt} := U\left(Pitot_{pt}, N_{fl.pt}\right)$$

$$U_{flow.pt} = 0.183 \cdot inH2O$$

$$pU_{flow.pt} := \frac{U_{flow.pt}}{flow_{sc.pt}}$$

Field Flow Uncertainty:

$$X_{dp.field} := 1\% \qquad X_{pitot} := pU_{flow.pt} \qquad pU_{flow.pt} = 0.183 \cdot \%$$

$$X_{pitot.flow} := \sqrt{X_{nozzle}^2 + X_{dp.field}^2 + X_{pitot}^2} \qquad X_{pitot.flow} = 1.24 \cdot \%$$